Detection of *BRAF* mutations in Lentigo maligna melanoma using a highly sensitive method

By

Mag.rer.nat. Elke Stadelmeyer

A dissertation submitted in fulfillment of the requirements for the degree of

Doctor of Medical Science

At the

Medical University Graz

Doctoral School of General and Clinical Pathophysiology (PATHMED)

Supervised by

Ass.-Prof. Priv.-Doz. Mag. Dr.rer.nat. Nadia Dandachi (1st Supervisor)

Univ.-Prof. Dr.med.univ. Peter Wolf (2nd Supervisor)

Carried out at the

Division of Oncology

Department of Internal Medicine

Graz, May 2012

_____

Dissertation

Detektion von *BRAF* Mutationen in der Lentigo maligna melanoma mittels hoch sensitiver Methode

eingereicht von

Mag.rer.nat. Elke Stadelmeyer

zur Erlangung des akademischen Grades

Doktor der Medizinischen Wissenschaften

an der

Medizinischen Universität Graz

Doctoral School of General and Clinical Pathophysiology (PATHMED)

ausgeführt an der

Klinischen Abteilung für Onkologie

Universitätsklinik für Innere Medizin

unter der Anleitung von

Ass.-Prof. Priv.-Doz. Mag. Dr.rer.nat. Nadia Dandachi (1. Betreuerin)

Univ.-Prof. Dr.med.univ. Peter Wolf (2. Betreuer)

Graz, am 24. Mai 2012 _____

To Peter,
Mom, and Dad

Eidesstattliche Erklärung

Ich erkläre ehrenwörtlich, dass ich die vorliegende Arbeit selbstständig und ohne fremde Hilfe verfasst habe, andere als die angegebenen Quellen nicht verwendet habe und die den benutzten Quellen wörtlich oder inhaltlich entnommenen Stellen als solche kenntlich gemacht habe.

Graz, _____ _____

Contributions

The following persons contributed to the work:

Planning the project and supportive dialogs

Assistant Prof. Nadia Dandachi (Division of Oncology, Department of Internal Medicine).
Prof. Peter Wolf (Research Unit for Photodermatology, Department of Dermatology and Venereology).
Prof. Lorenzo Cerroni (Research Unit for Dermatopathology, Department of Dermatology and Venereology).
Dr. Ellen Heitzer (Institute of Human Genetics)

Sample selection and defining tumor area for manual dissection

Prof. Peter Wolf (Research Unit for Photodermatology, Department of Dermatology and Venereology).
Prof. Lorenzo Cerroni (Research Unit for Dermatopathology, Department of Dermatology and Venereology).

Help making sections and isolating DNA from FFPE tissue

Margit Resel (Division of Oncology, Department of Internal Medicine).

Hematoxylin Eosin staining

Gerlinde Mayer (Department of Dermatology and Venereology).

Acknowledgments

I owe a debt of gratitude to many people who have supported me over the last years. Foremost, I am indebted to my advisor Assistant Prof. Nadia Dandachi for her support and help. Her guidance helped me in time of research and writing this thesis.

Besides my advisor, I would also like to thank the other members of my thesis committee Prof. Peter Wolf and Dr. Nassim Ghaffari-Tabrizi for their time, interest, and helpful comments.

I am indebted to Prof. Hellmut Samonigg, head of division of Oncology, for his financial support and giving his approval to this study. My thanks go also to Dr. Marcus Otte for his time and inspiring discussions, Prof. Lorenzo Cerroni for providing me first insights into microscopy, Dr. Frank Narz for helping me with the pyrograms, Gerlinde Mayer for preparing HE stains, and Dr. Ellen Heitzer for her valuable tips.

This thesis would not have been possible unless the help of my colleagues in the lab. Thank you Margit, Jasmin, Elisabeth, Daniela, and Bettina, for the fun we had, the continuous support, and your friendship.

Finally, I owe my deepest gratitude to my parents Brigitte and Helmut and my brother Peter for their love, encouragement, and unconditional support. Words simply cannot describe how thankful I am.

List of Contents

List of Figures

List of Tables

Abbreviations

AKT	v-akt murine thymoma viral oncogene homolog
ALM	acral lentiginous melanoma
AS	allele specific
bp	base pair
BRAF	v-raf murine sarcoma viral oncogene homolog B1
BRAF V600E	gene carrying the mutation
BRAF ^{V600E}	protein carrying the mutation
BSA	bovine serum albumin
COLD	coamplification at lower denaturation temperature
CSD skin	chronically sun damaged skin
DMSO	dimethyl sulfoxide
DNA	deoxyribonucleic acid
dNTP	deoxyribonucleotide triphosphate
E	glutamic acid
EGFR	epidermal growth factor receptor
FBS	fetal bovine serum
FFPE	formalin fixed-paraffin embedded
GAPDH	glyceraldehyde-3-phosphate dehydrogenase
gDNA	genomic DNA
hr.	hour
HRMA	high resolution melting analysis
K	lysine
KIT	v-kit Hardy-Zuckerman 4 feline sarcoma viral oncogene homolog
LINE	long interspersed nuclear elements
LM	lentigo maligna
LMM	lentigo maligna melanoma
LOD	limit of detection
LS	learning set
MAPK	mitogen-activated protein kinase
min.	minute
MM	malignant melanoma
MS	model system
mt	mutated
NM	nodular melanoma
NRAS	neuroblastoma RAS viral (v-ras) oncogene homolog
PAK	pigmented actinic keratosis
PBS	phosphate buffered saline
PCR	polymerase chain reaction
PPi	pyrophosphate
PTEN	phosphatase and tensin homolog
rpm	revolutions per minute
RT	room temperature
sec.	second
SL	solar lentigo
SNP	single nucleotide polymorphisms
SSM	superficial spreading melanoma
TBE	tris base, boric acid, ethylenediaminetetraacetic acid
TE	tris-EDTA (Ethylenediaminetetraacetic acid)
TS	training set
V	valine
WHO	World Health Organization
woD	without manual dissection
wt	wild type

Abstract

Better understanding of tumor progression at the molecular level has led to development of promising therapies for the treatment of otherwise poorly responsive malignant tumors. Compared to other subtypes of malignant melanoma (MM), lentigo maligna melanoma (LMM) is characterized by slow progression from a melanoma *in situ* to an invasive form. The structure of LMM tumors, with their solitary units or small nests of atypical melanocytes, has hampered molecular characterization and necessitates sensitive methods for mutation analysis. While *BRAF* mutation has been shown to be an early event in the development of MM, it has not been explored in LMM in adequately large sample sizes. Therefore, the objective of this study was to determine the occurrence of mutations in codon 600 of the *BRAF* gene in a large cohort of LMM patient samples. In order to analyze low tumor cell portions within LMM lesions, a highly sensitive PCR method was established for the detection of the *BRAF* V600E, as well as the *BRAF* V600K mutation. We found that in our hands allele specific PCR was more sensitive than other methods to detect low abundance mutations. We investigated the prevalence of *BRAF* mutations in a total of 61 LMM lesions. These lesions were prescreened for suitable DNA quality and manually dissected for the presence of at least 5% tumor cells within the tissue samples to be subjected to PCR analysis. In addition, from 39 of these LMM lesions DNA from normal tumor-adjacent tissue could be extracted and investigated for control purposes.

Unexpectedly, the *BRAF* V600K mutation was predominant in our set of LMM lesions and found exclusively in the DNA from tumor area in 16% (10/61) of the samples analyzed. In comparison, the *BRAF* V600E mutation was detected in only 5% (3/61) of the DNA samples from tumor area. Moreover, an additional 5% (2/39) of tumor adjacent normal skin carried a *BRAF* V600E mutation as well. However, it needs to be noted that in one of those cases the tumor adjacent skin contained a melanocytic nevus, a condition commonly associated with *BRAF* V600E mutation.

Taken together, the relatively low portion of LMM lesions mutated at the *BRAF* gene indicates that *BRAF* mutation plays a role at maximum in a subset of LMM lesions. At this time point due to limited follow-up no conclusion can be drawn, if there is any correlation between the presence of a *BRAF* mutation in a LMM *in situ* and the probability of tumor progression. However, the knowledge of the predominant existence of the *BRAF* V600K mutation in a subset of LMM lesions may contribute to a better understanding of the underlying mechanisms in melanoma development.

Zusammenfassung

Besseres Verständnis der Tumorentstehung auf molekularer Ebene hat zur Entwicklung von vielversprechenden Therapien für die Behandlung von bis dato schlecht therapierbaren malignen Tumoren geführt. Im Vergleich zu anderen Subtypen des malignen Melanoms (MM), ist die Lentigo maligna melanoma (LMM) gekennzeichnet durch die langsame Progression eines Melanom *in situ* zu einer invasiven Form. Die Struktur der LMM, mit einzelnen, oder in kleinen Nestern vorliegenden, atypischen Melanozyten, erschwert die molekulare Charakterisierung und erfordert sensitive Methoden zur Mutationsanalyse. Obwohl gezeigt werden konnte, dass die *BRAF* Mutation ein frühes Ereignis in der Entwicklung des MM ist, wurde sie bisher nicht in größeren Probensätzen von LMM untersucht. Deshalb war das Ziel dieser Studie die Bestimmung der Häufigkeit von Mutationen im Codon 600 des *BRAF* Gens in einem großen Satz an LMM Proben. Um den geringen Anteil an Tumorzellen in den LMM Läsionen zu analysieren, wurde ein hoch-empfindliches PCR-Verfahren zum Nachweis der *BRAF* V600E, sowie der *BRAF* V600K Mutation etabliert. In unseren Händen war die Allel-spezifische PCR bei der Detektion von Mutationen geringen Ausmaßes sensitiver als andere getestete Methoden. Das Vorkommen von *BRAF* Mutationen wurde in 61 LMM Läsionen untersucht. Diese Läsionen wurden auf adäquate DNA Qualität geprüft und manuell disseziert um einen Mindestanteil von 5% Tumorzellen in der zu analysierenden Gewebeprobe sicher zu stellen. Zur Kontrolle wurde zusätzlich von 39 dieser LMM Läsionen DNA von Tumor umgebender normaler Haut isoliert und untersucht.

Unerwarteter Weise war in unserem Probensatz an LMM Läsionen die *BRAF* V600K Mutation die vorherrschende Mutation, welche in 16% (10/61) der untersuchten Proben, ausschließlich in der DNA des Tumorbereichs gefunden wurde. Im Vergleich dazu, wurde die *BRAF* V600E Mutation in nur 5% (3/61) der DNA-Proben des Tumorbereichs nachgewiesen. Des Weiteren trugen 5% (2/39) der DNA-Proben der Tumor umgebenden normalen Haut eine *BRAF* V600E Mutation. Dabei ist zu beachten, dass sich in einem der beiden Fälle ein melanozytärer Nävus (welche häufig eine *BRAF* V600E Mutation tragen) in der Tumor umgebenden Haut befand.

In Summe deutet der eher geringe Anteil an LMM Läsionen, welcher eine Mutation im *BRAF* Gen trägt, darauf hin, dass die *BRAF* Mutation wenn, dann nur in einem Teil der LMM Läsionen eine Rolle spielt. Auf Grund des kurzen Follow-ups kann zu diesem Zeitpunkt kein Rückschluss auf einen Zusammenhang zwischen dem Vorhandensein einer *BRAF* Mutation in einer LMM *in situ* und der Wahrscheinlichkeit der Tumorprogression gezogen werden. Jedoch könnte das Wissen, über das vorwiegende Vorliegen der *BRAF* V600K Mutation in einem Teil der LMM Läsionen, zu einem besseren Verständnis der Mechanismen der Melanom-Entstehung beitragen.

1 Background

1.1 Melanoma

Malignant melanoma (MM) accounts for approximately 4% of skin cancer cases, but for 80% of all skin cancer deaths, which makes it the most aggressive form of skin cancer. According to the World Health Organization (WHO), the incidence of melanoma is increasing faster than that of any other type of cancer worldwide. In Austria, in the year 2009 more than 1200 people have been diagnosed with MM and the incidence and mortality have been rising over the last decades in the Western world, including Austria (Figure 1; data from (Statistik Austria 2011)).

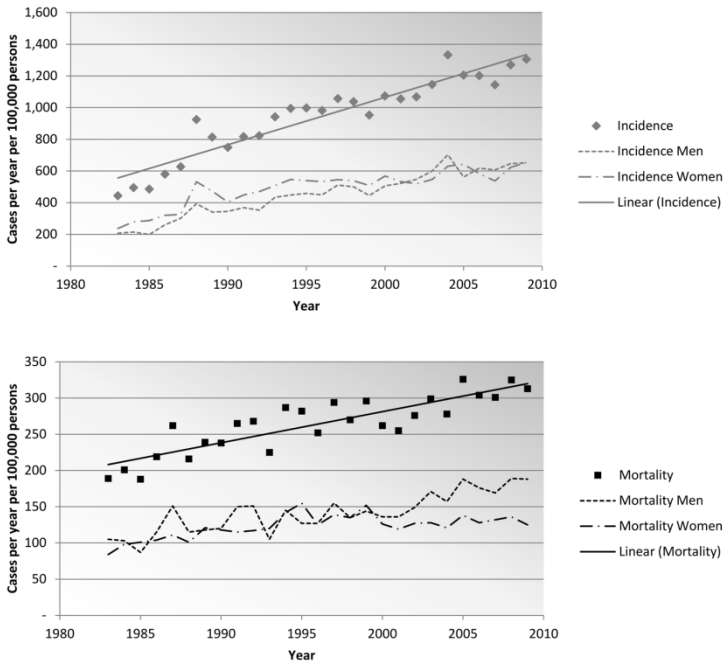

Figure 1: Incidence and mortality of malignant melanoma in Austria.
For the MM the incidence, as well as mortality has been rising over the last 3 decades in Austria (data from (Statistik Austria 2011)).

To improve overall survival early diagnosis of MM is essential since only 14% of patients with metastatic melanoma survive for five years (Miller, Mihm 2006), while there is a good chance of recovery for the patients if the primary lesion is detected and treated at an early stage.

One of the first attempts to classify MM was established in the 1970s by Clark (Clark 1979). This classification is mainly based on morphologic changes. The current WHO classification is based on this model and distinguishes four main types of melanoma: superficial spreading melanoma (SSM), lentigo maligna melanoma (LMM), nodular melanoma (NM), and acral lentiginous melanoma (ALM) (Viros et al. 2008) which comprise 70%, 4-15%, 10-15%, and <5% of invasive melanomas, respectively (McKenna et al. 2006). Although meanwhile other classification systems have been introduced taking into account clinicopathological features (Curtin et al. 2005), efforts

are directed towards defining another, new classification system, not only based on histomorphologic features, but also taking into account mutation status and the intensity of sun exposure (Broekaert et al. 2010). The demand for a new classification system not only displays the complexity and heterogeneity of melanoma, but also reflects the difficulty to discriminate malignant from benign lesions.

1.1.1 Lentigo Maligna Melanoma

The term lentigo maligna (LM) is often not uniformly used. While some authors define LM as a precursor to melanoma, (Clark, Mihm 1969), others classify LM as a malignant melanoma *in situ* (Cohen 1995) or suggest the term LM to be abandoned and generally use melanoma *in situ*, instead (summarized in (Swetter et al. 2005, Reed, Shea 2011)).

In its initial phase LM is characterized by a prolonged two-dimensional centrifugal growth pattern that is confined to the dermal-epidermal junction. Over the time LM may progress to an invasive melanoma. This type of lesion predominantly occurs on chronically sun-exposed (CSD) areas of the skin of elderly people and its diagnosis is often complicated due to the fact, that it can resemble pigmented actinic keratosis (PAK) or solar lentigo (SL) clinically and histopathologically (McKenna et al. 2006, Cohen 1995).

1.1.2 Melanoma Development

The evolution of a MM is thought to be a multi-step process. One of the first models for melanoma development has been published by Clark et al. (Clark et al. 1984). It formed the basis for subsequent progression models (reviewed in (Miller, Mihm 2006)). What they have in common is the hypothesis that multiple genetic and epigenetic alterations are necessary for the development of MM. A summary of molecular alterations that have been found at different stages of melanoma progression is given in Figure 2. Mutations in the *BRAF* gene are thought to be an early and frequent event in melanoma development and progression.

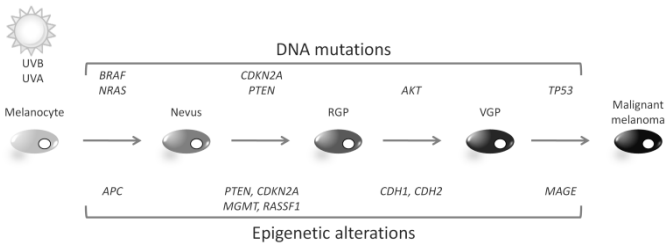

Figure 2: Model of melanoma progression.

The model is based on a series of histopathologic changes that come along with DNA mutations on the one hand and epigenetic alterations on the other hand. UV radiation is known to cause skin damages and increases the risk for melanoma development. Information summarized in Figure 2 is reviewed in, e.g., (Miller, Mihm 2006, Takata, Murata & Saida 2009, Zaidi, Day & Merlino 2008).

1.2 BRAF

BRAF (v-raf murine sarcoma viral oncogene homolog B1) belongs to the oncogenes and was first described by Rapp et al. and Moelling et al. (Rapp et al. 1983, Moelling et al. 1984). The *BRAF* gene encodes a serine/threonine-protein kinase which plays a role in the MAPK pathway. The BRAF protein belongs, alongside ARAF and RAF1, to the raf/mil family. Their function is the transduction of regulatory signals from RAS to MEK.

1.2.1 MAPK Pathway

Classically, the MAPK pathway consists of RAS, RAF, MEK and ERK (Figure 3). It relays signals from the cell surface to the nucleus. Normally, the signaling cascade is activated by the binding of a ligand (such as mitogens or hormones) to the receptor tyrosine kinase (RTK) located on the plasma membrane. This leads to a dimerization of the RTK and triggers the activation of RAS (RAS-GTP), which in turn recruits RAF from the cytosol to the membrane forming a complex und thus activating RAF. Activated RAF itself phosphorylates mitogen-activated protein kinase (MAPK) kinase (MEK), which subsequently activates MAPK/extracellular signal-regulated kinase (ERK) by phosphorylation (Avruch et al. 2001, Sebolt-Leopold, Herrera 2004, Inamdar, Madhunapantula & Robertson 2010). Activated ERK regulates several transcription factors like C-myc, Elk-1, c-Jun influencing essential cell cycle processes such as cell proliferation, differentiation, survival, and oncogenesis.

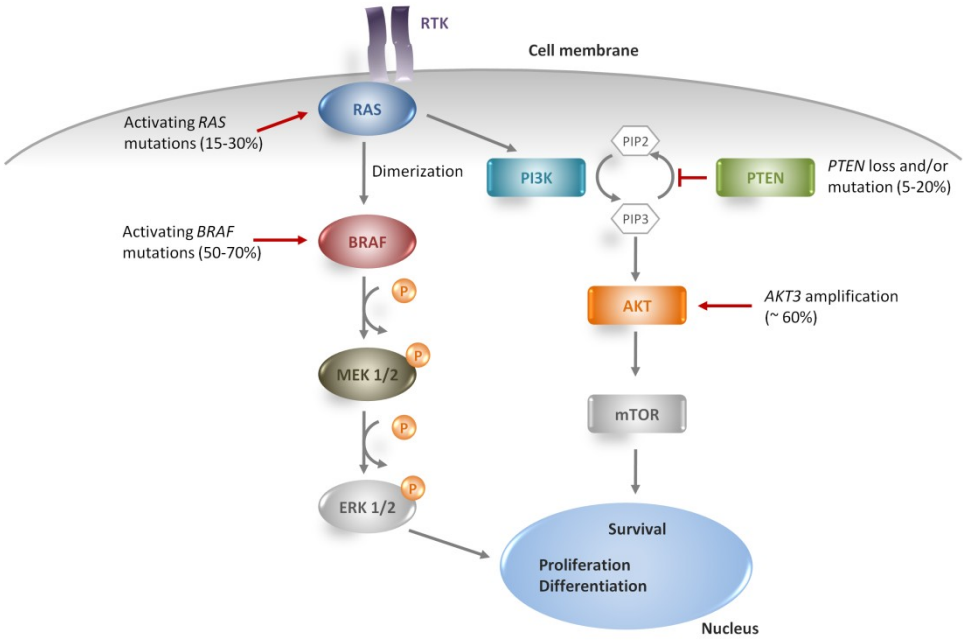

Figure 3: MAPK-pathway.

Simplified illustration of the signaling cascade in MAPK pathway and mutations found in melanoma. Indicated frequencies of the alterations found in MM are reviewed in, e.g., (Chudnovsky, Khavari & Adams 2005, Gray-Schopfer, Wellbrock & Marais 2007).

Although all three members of the RAF family are able to bind to RAS and phosphorylate MEK, BRAF seems to be the most efficient activator of MEK (Galabova-Kovacs et al. 2006).

The wild type BRAF protein ($BRAF^{wt}$) needs S446 phosphorylation leading to a conformational change – a prerequisite to be able to bind to RAS-GTP and form a complex and thus becoming activated. Mutated BRAF ($BRAF^{V600E}$) is independent of any interaction with RAS-GTP, implying that this mutation circumvents the need for RAS mediated phosphorylation. This would equal a constitutive activation of BRAF, thus leading to increased MEK phosphorylation and downstream pathway activation (Brummer et al. 2006).

Dysregulation of the MAPK pathway, frequently caused by activating mutations of *BRAF* or *RAS* can be found in several types of human cancer including melanoma, colorectal cancer, and papillary thyroid carcinoma (Sebolt-Leopold, Herrera 2004, Davies et al. 2002).

1.2.2 *BRAF* Mutation

The human *BRAF* gene is located on the negative strand of chromosome 7. Its 18 exons are coding for a protein of 766 amino acids (AA) length.

```
Score =  178 bits (96),  Expect = 1e-45
 Identities = 112/120 (93%), Gaps = 0/120 (0%)
 Strand=Plus/Plus

Query  176372  ATATATTTCTTCATGAAGACCTCACAGTAAAAAT AGGTGATTTTGGTCTAGCTACAGTGA  176431
               ||||| ||||||||||||||||||||||  |||||||||||||||||||||| |||||||
Sbjct  1981    ATATAGTTCTTCATGAAGACCTCACAGTGGAAATAGGTGATTTTGGTCTAGCCACAGTGA  2040

Query  176432  AATCTCGATGGAGTGGGTCCCATCAGTTTGAACAGTTGTCTGGATCCATTTTGTGGATGG  176491
               ||||| ||||||||||||||||||||||||||||||||||||||||  ||||||| ||||
Sbjct  2041    AATCTTGATGGAGTGGGTCCCATCAGTTTGAACAGTTGTCTGGATCTTTTTTGTGTATGG  2100
```

Figure 4: BLAST[1] result for sequence alignment of *BRAF* with *BRAFP1*.

Figure 4 shows the high sequence homology between *BRAF* (Query: NG_007873.1) and *BRAFP1* (Sbjct: NG_003108.2) adjacent to codon 600. Nucleotide 1799 (responsible for *BRAF* V600E mutation when T is exchanged with A) is marked with a black background color. SNP rs55939351 is bold written and underlined.

The *BRAF* V600E mutation results from a T to A transversion of nucleotide 1799 in exon 15, codon 600 (GTG ⇨ GAG) of the gene and causes a substitution of valine (V) by glutamic acid (E) (V600E). In close proximity to codon 600 a single nucleotide polymorphism (SNP, rs55939351) is located (NG_007873.1:g.176405T>A). Additionally, a pseudogene (*BRAFP1*), which is located on chromosome X, has been identified for this gene. Over a stretch of 120 nucleotides around codon 600 the *BRAF* gene shows 93% homology to *BRAFP1*. A circumstance that complicates primer design since the analysis should record mutations in the actual protein coding gene only and not the pseudogene. The detailed sequence of the area around codon 600 of the *BRAF* gene is shown in Figure 4.

[1] http://blast.ncbi.nlm.nih.gov/

Although *BRAF* V600E is the most frequent mutation in melanoma, other mutations have been described for the *BRAF* gene, most of them located in or in close proximity to codon 600 (Arkenau, Kefford & Long 2011, Wan et al. 2004). A summary of nucleotide exchanges is given in Figure 5 and Table 1.

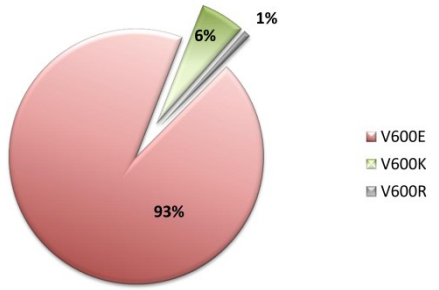

Figure 5: **Percentage distribution of *BRAF* mutation.**

The pie chart shows the percentages of activating *BRAF* V600 mutations found in melanoma. Besides *BRAF* V600E the *BRAF* V600K mutation is the second most frequent one detected in melanoma. Information from COSMIC database (Sanger Institute Catalogue Of Somatic Mutations In Cancer).

Table 1: ***BRAF* V600 mutations found in cancer**

Mutation	Sequence	Nucleotide change
BRAF V600 wt	5'TCTAGCTACAGTGAAATCTCGATGGAGTGG3'	wt sense strand
	3'AGATCGATGTCACTTTAGAGCTACCTCACC5'	wt opposite strand
p.V600E	5'TCTAGCTACAG**A**GAAATCTCGATGGAGTGG3'	1799 T>A
	3'AGATCGATGTC**T**CTTTAGAGCTACCTCACC5'	
p.V600G	5'TCTAGCTACAG**G**GAAATCTCGATGGAGTGG3'	1799 T>G
	3'AGATCGATGTC**C**CTTTAGAGCTACCTCACC5'	
p.V600A	5'TCTAGCTACAG**C**GAAATCTCGATGGAGTGG3'	1799 T>C
	3'AGATCGATGTC**G**CTTTAGAGCTACCTCACC5'	
p.V600D	5'TCTAGCTACAG**AT**AAATCTCGATGGAGTGG3'	1799_1800 TG>AT
	3'AGATCGATGTC**TA**TTTAGAGCTACCTCACC5'	
p.V600K	5'TCTAGCTACA**AA**GAAATCTCGATGGAGTGG3'	1798_1799 GT>AA
	3'AGATCGATGT**TT**CTTTAGAGCTACCTCACC5'	
p.V600R	5'TCTAGCTACA**AG**GAAATCTCGATGGAGTGG3'	1798_1799 GT>AG
	3'AGATCGATGT**TC**CTTTAGAGCTACCTCACC5'	
p.V600R*	5'TCTAGCTAC**GAG**GAAATCTCGATGGAGTGG3'	1797_1799 AGT>GAG
	3'AGATCGATG**CTC**CTTTAGAGCTACCTCACC5'	
p.V600M	5'TCTAGCTACA**A**TGAAATCTCGATGGAGTGG3'	1798 G>A
	3'AGATCGATGT**T**ACTTTAGAGCTACCTCACC5'	

Note: Codon 600 is indicated in yellow, mutations are indicated bold and underlined.

1.2.3 *BRAF* Mutations in Melanoma

One of the most common oncogenic events in melanoma is the exceeding activation of the MAPK pathway. The *BRAF* V600E mutation significantly increases the kinase activity thus leading to alterations in cell survival and proliferation (Davies et al. 2002). Up to 57% of primary melanoma

samples have been tested positive for this specific mutation (Goel et al. 2006), thus representing the most common mutation in MM besides less frequent ones like *NRAS*, *P16INK4a*, and *p53* mutations (reviewed in (Chudnovsky, Khavari & Adams 2005, Fecher et al. 2007)).

Although, profound knowledge exists about the incidence of the *BRAF* V600E mutation in MM in general, only little information is available about *BRAF* V600E and *BRAF* V600K mutation in LMM (Dandachi, Wolf 2010). A key limitation for the analysis of LMM is certainly the limited tumor cell count and the often small size of the lesions requiring sensitive methods for mutation analysis.

1.3 Mutation Analysis

Several methods are available for mutation analysis. In the following sections only those methods are described that were relevant for this study.

1.3.1 Sanger Sequencing

Sanger sequencing is accepted as the gold standard for mutation analysis. Its indisputable advantage is the fact that it provides sequence information, but it comes along with limited sensitivity only. Most authors specify a sensitivity of about 20% mt DNA in a background of wt DNA. In our hands using Sanger sequencing 12.5% mt DNA in background of wt DNA were often detectable, 25% mt DNA in a background of wt DNA were reliably detectable (Figure 6, (Pichler et al. 2009)).

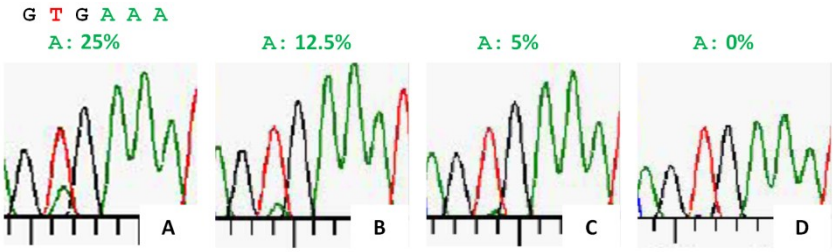

Figure 6: Sanger sequencing of *BRAF*.

Typical results from Sanger sequencing. Figure 6A depicts a sequencing chromatogram from cell line DNA carrying 25% *BRAF* V600E mutation (green peak on 2nd position) in a background of wt DNA (red peak on 2nd position). Figure 6B shows 12.5% mt *BRAF* DNA, the lowest percentage that can be identified in our system. Figure 6C and Figure 6D are chromatograms from 5% mt DNA and wt DNA.

Most of the studies done on MM analyzing *BRAF* V600 mutations used Sanger sequencing (Viros et al. 2008, Akslen et al. 2008). Taking into account that the tumor cell count in LMM samples may be lower than in other types of MM due to the morphology of the tumor Sanger sequencing could come to its limits of detection.

1.3.2 Coamplification at Lower Denaturation Temperature PCR

Coamplification at Lower Denaturation Temperature (COLD) PCR is a relative new and, until now, rarely described method (Li, Makrigiorgos 2009, Milbury, Li & Makrigiorgos 2009) which favors the amplification of small amounts mt DNA in a background of wt DNA in the template. It is characterized by an additional hybridization step and a selective denaturation which allows the preferential amplification of the hetero-duplexes. For a schematic overview of the method, see Figure 7. While this method has proven its advantages analyzing mutations with G>A or C>T exchanges, only few information is available on T>A exchanges. COLD PCR seemed to be the ideal method for analyzing samples carrying a mutation at very low levels. Using COLD PCR a 5- to 8-fold enrichment has been shown for T>A exchanges (Li et al. 2008).

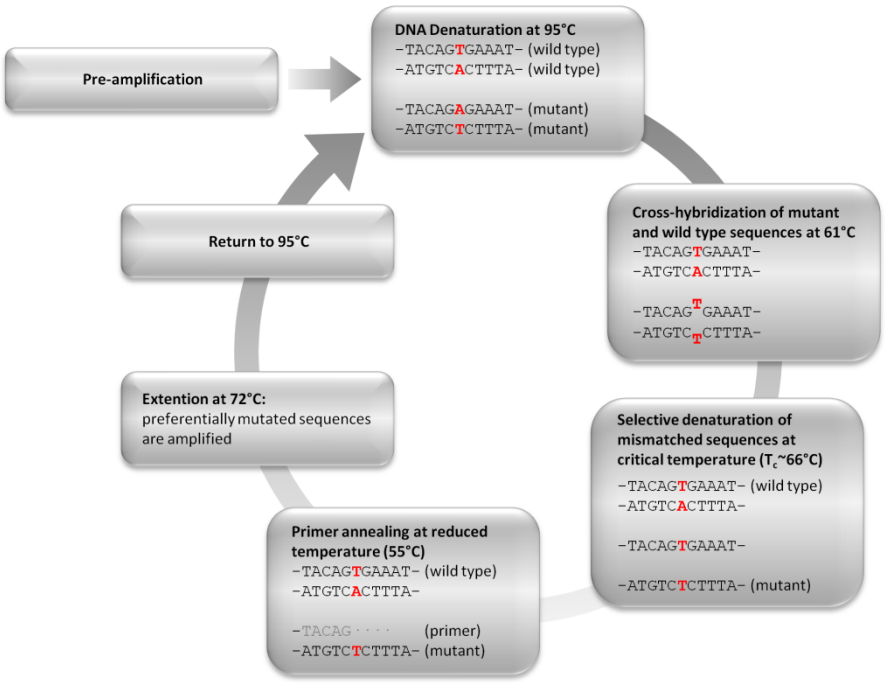

Figure 7: Principle of COLD PCR.

A number of regular PCR cycles enable the built-up of target amplicons. After that the program is switched to FULL COLD PCR: Following an initial denaturation step, the temperature is lowered to a degree where cross-hybridization between mt and wt sequences is possible. Since mutated sequences are in a minority, most mutant alleles end up in hetero-duplexes showing a lower T_m than fully matched structures (homo-duplexes). During the selective denaturation step at T_c hetero-duplexes are preferentially denatured over fully matched duplexes. Therefore, in the following primer annealing and extension steps mutated alleles are amplified in a preferred manner. Diagram based on the method published by Li and Makrigiorgos (Li, Makrigiorgos 2009).

1.3.3 High Resolution Melting Analysis PCR

In the last decade High Resolution Melting Analysis (HRMA) PCR has gained more and more importance in mutation analysis since it is an easily manageable, closed-tube method with a good sensitivity. The principle is comparable to standard real-time PCR using DNA intercalating dyes such as SYBR Green. The actual melting analysis, after PCR amplification, relies on highly saturating, DNA intercalating dyes like ResoLight, LCGreen Plus or EvaGreen. These dyes allow the discrimination of homo-duplexes and hetero-duplexes, caused even by a single nucleotide exchange, formed during PCR. Formation of hetero-duplexes results in a slightly different melting behavior of the PCR products which can be detected by HRMA (Figure 8). The sensitivity of the assay is primarily dependent on the type of nucleotide exchange (a G>A or C>T exchange normally results in a larger temperature shift than a T>A exchange) and the amplicon size (the longer the amplicon the smaller the effects of a single nucleotide mismatch).

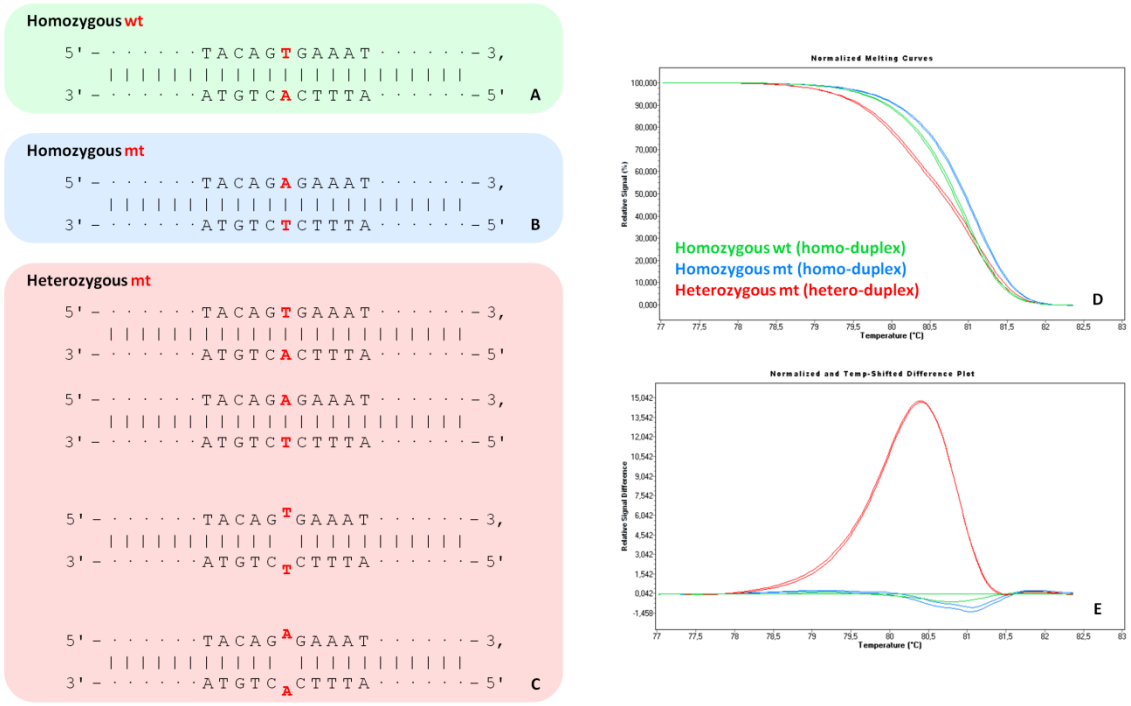

Figure 8: Principle of HRMA PCR.

During PCR different kinds of duplexes can be formed. Using wt DNA as template homo-duplexes are formed (Figure 8A). The same accounts for homozygous mt DNA, were homo-duplexes are formed, too (Figure 8B). When a heterozygous mt DNA is used as template, four different types of duplexes can be formed (Figure 8C): homo-duplexes as found in Figure 8A and B and hetero-duplexes formed from a wt amplicon and a mt amplicon containing a mismatch at the site of mutation. This mismatch leads to an altered melting behavior depict in Figure 8D and E. Very often the temperature-shifted difference plot is used for illustration (Figure 8E). (Principle is demonstrated on the example of *BRAF*.)

1.3.4 Allele Specific PCR

Allele Specific (AS) PCR is a well established method that makes use of mutation specific primers. In the ideal case mutation carrying DNA is amplified without any amplification of wt DNA. With the AS PCR it is possible to detect as few as 1% mt DNA in a background of wt DNA (Jarry et al. 2004). Besides its high sensitivity AS PCR has the disadvantage of being a rather rigid system since every mutation requires its own assay. In the case of the *BRAF* V600E mutation slight cross-reactivity with *BRAF* V600K is often detected since they share nucleotide exchange on nucleotide position 1799 (for details refer to Table 1). For the reliable detection of the *BRAF* V600K mutation a separate assay has to be utilized. Thus, AS PCR is not only a highly sensitive method, but also indirectly provides information on the sequence, by the efficiency of primer annealing and amplification. The principle of AS PSR is sketched in Figure 9.

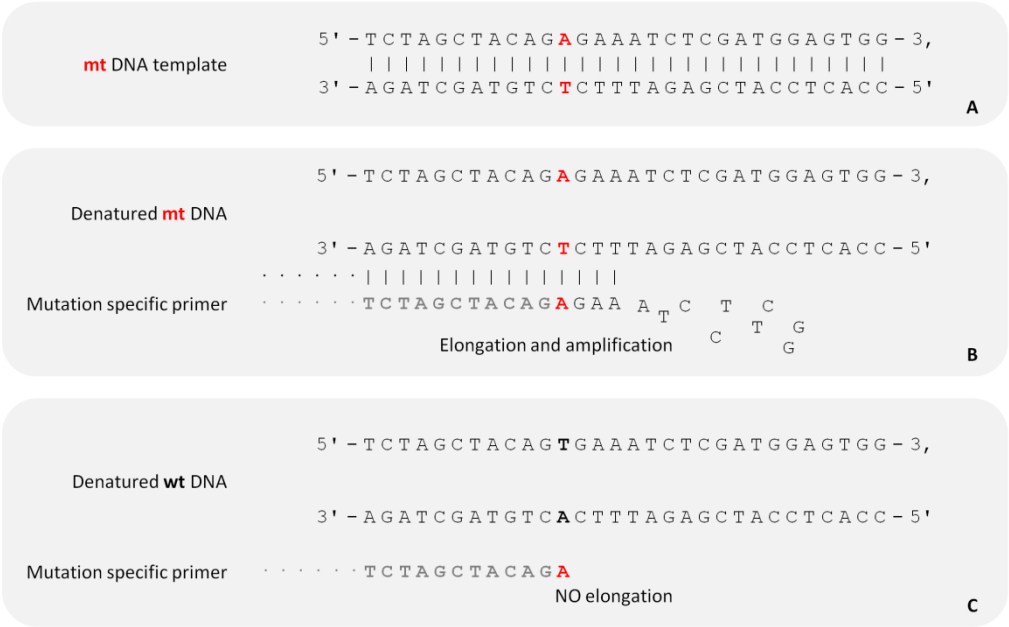

Figure 9: Principle of AS PCR.

Figure 9A depicts a part of the *BRAF* sequence which carries the *BRAF* V600E mutation (indicated in red). During AS PCR the template DNA is denatured to allow primer annealing. In the ideal case primer elongation occurs only when the primer perfectly matches the template sequence as shown in Figure 9B. The stringent conditions during AS PCR do not allow annealing and elongation of the mutation specific primer to the wt DNA (Figure 9C).

1.3.5 Pyrosequencing

Pyrosequencing was developed in the late 90s of the last century and is based on the 'sequence by synthesis' principle (Ronaghi, Uhlen & Nyren 1998). Its major advantage to Sanger sequencing is its higher sensitivity and speed. In contrast to AS PCR and HRMA PCR, sequence information is provided by pyrosequencing. The principle of pyrosequencing is schematically shown in Figure 10. The starting product for pyrosequencing is a PCR product where the primer of the strand which will be sequenced is biotinylated. With the help of the biotin-label this strand is isolated from the PCR reaction and mixed with sequencing primer. According to a dispensation order one

deoxyribonucleotide triphosphate (dNTP) at a time is added to the reaction. If the added dNTP is complementary to the single-stranded PCR amplicon, the sequencing primer is elongated releasing a pyrophosphate (PPi). This pyrophosphate in turn, reacts with APS and the enzyme Sulfurylase forming ATP. ATP in turn reacts with Luciferase converting luciferin to oxyluciferin and generates a light signal. Any dNTP, which has not been incorporated, is degraded by the enzyme Apyrase subsequently. The intensity of the generated light signal is proportional to the released pyrophosphate and thus allows quantification.

The software of the system allows the quantification of variable positions as found in the *BRAF* V600E mutation. More complex mutations, like the *BRAF* V600K mutation cannot be calculated automatically, but have to be evaluated by the investigator.

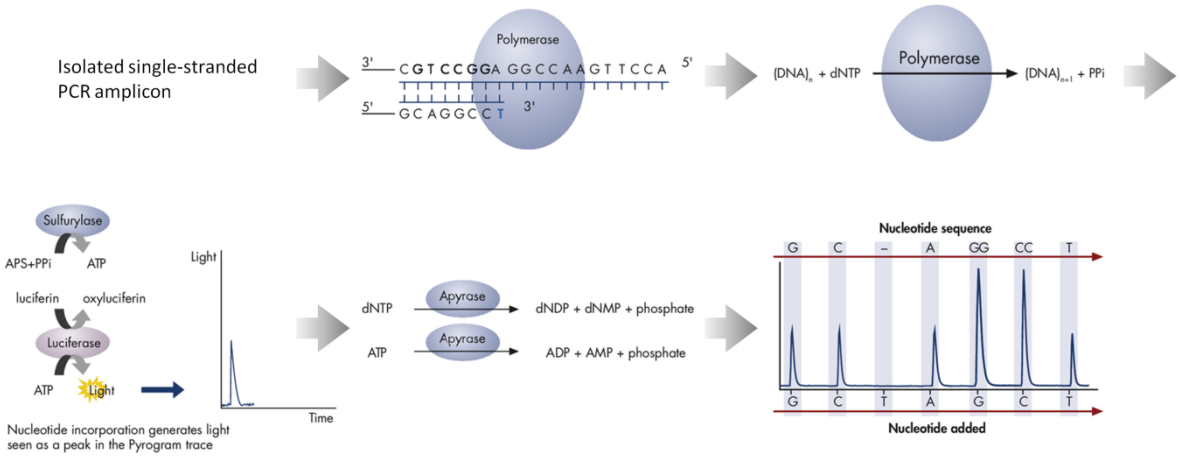

Figure 10: Principle of Pyrosequencing.

The isolated, single-stranded PCR amplicon is mixed with the sequencing primer and hybridized. One dNTP at a time is dispensed to the reaction. If the dNTP is complementary to the template strand it is elongated to the sequencing primer and a pyrophosphate is released. The pyrophosphate reacts with Sulfurylase and Luciferase resulting in the emission of a light signal proportional to the released PPi. Reprint of the figure is with permission from QIAGEN (© QIAGEN, all rights reserved).

The sensitivity of pyrosequencing is superior to the one of Sanger sequencing. For the *BRAF* V600E mutation sensitivities of up to 10% have been described (Jo et al. 2009, Spittle et al. 2007).

2 Rationale

An extensive review of the literature showed that although several publications have dealt with the *BRAF* mutation in melanoma, there is only little information about the frequency of this mutation in LMM. Most published data focused on metastatic melanoma (Alsina et al. 2003, Davies et al. 2009, Gorden et al. 2003, Kumar et al. 2003). When *BRAF* mutation was analyzed in DNA from primary melanomas, classification of the samples was not uniform since some authors used the sun exposure as criterion (CSD and nonCSD; e.g., (Fargnoli et al. 2008)) and some the current WHO classification system (NM, SSM, ALM, and LMM; e.g., (Viros et al. 2008, Akslen et al. 2008, Deichmann et al. 2004, Edlundh-Rose et al. 2006, Hacker et al. 2010, Poynter et al. 2006, Thomas et al. 2007). In addition, the method used for mutation analysis was very often Sanger sequencing. Taking into account the morphology of LMM, which is characterized by the diffuse presence of atypical melanocytes in the epidermis (individually or arranged in small nests), the necessity of a highly sensitive method for mutation analysis evolves. Furthermore, data published so far, often analyzed different subsets of MM, rendering the sample size of a single subset, for example, LMM relatively small. The largest sample set of LMM analyzed was described by the authors Viros et al. (Viros et al. 2008). They analyzed 302 cases of primary melanoma including 39 cases of LMM and used Sanger sequencing.

2.1 Aim of the Project

Given the fact, that LMM evolves differently than the other subtypes of MM (in contrast to the other subtypes, LMM is mostly found on CSD skin and shows a very slow progression (over decades, if any at all)) we wanted to gain more information on its mutational status. In addition, LMM can resemble solar lentigo (SL) or pigmented actinic keratosis (PAK). Thus, the existence of the *BRAF* V600E mutation in LMM could serve as an additional criterion for the differentiation of LMM, since no such mutation was found in SL and actinic keratosis, both studies using a highly sensitive method for mutation analysis (Hafner et al. 2009, Zaravinos et al. 2009). Therefore, we analyzed the *BRAF* V600 mutational status of a well characterized collective of malignant melanomas, lentigo maligna type using a highly sensitive, PCR based, method.

2.2 Structure of the Project

The milestones of the project reflect the major questions addressed in this study. First, there is the methodical emphasis, where a suitable method for the detection of low level mutations was established. The method had to fulfill several requirements: (1) high sensitivity due to low tumor cell count in the samples, (2) applicability on FFPE DNA, and (3) allowing an analysis from low amounts of gDNA. Second, the clinical aspect, since, to our knowledge, this is the first study,

examining a large sample-set of malignant melanomas, lentigo maligna type with a highly sensitive method. In addition, whenever applicable, DNA from the manually dissected tumor area was compared to DNA from the corresponding surrounding area. Third, the statistical evaluation of the results with respect to mutation frequency in DNA from tumor area vs. DNA from surrounding area and evaluation of the results from our study in context of the existing data from other studies.

Thus, the main objectives of the project can be summarized as follows:

1. Establishment, optimization and validation of 3 different PCR based assays for *BRAF* V600 mutational analysis.
2. Analysis of a well characterized, large sample set of malignant melanomas, lentigo maligna type.
3. Statistical evaluation and interpretation of the results in context of the existing literature.

In order to address these questions we set up a study design consisting of 5 work packages, illustrated in Figure 11.

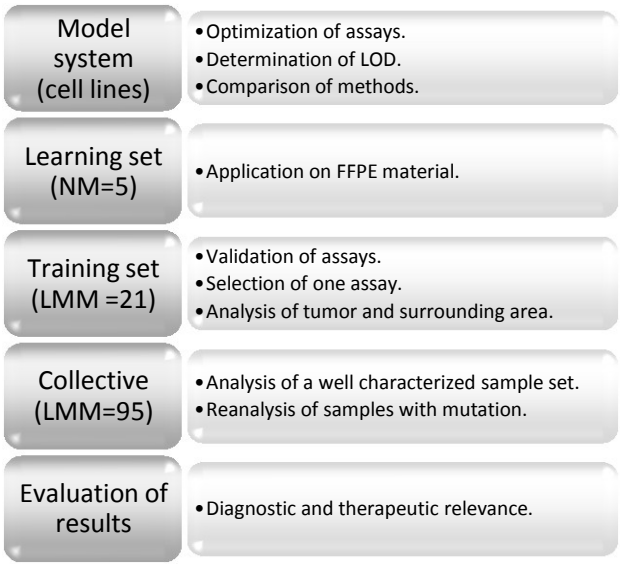

Figure 11: Work packages of the study.

The **model system**, consisting of cell lines, fulfilled requirements necessary for the establishment and optimization of our assays: It provided large amounts of high quality DNA with known mutational status. Thus, it allowed extensive testing and assured the same basic conditions for all the assays tested over the whole period of time. The **learning set** was used to prove the applicability of the assays on FFPE DNA. We chose tissue samples from NM because, on the average, tumor volume is larger in NM and the available data showed a higher frequency of the *BRAF* V600E mutation in NM than in LMM, thus increasing the probability to detect at least one mutated sample using this learning set. The **training set** posed the crucial test for the assays. Based on the results from this set, the most suitable assay for our sample set was chosen and we gained first information about the incidence of the *BRAF* V600 mutations in DNA from tumor area compared to DNA from surrounding area. All the aforementioned steps addressed the methodical emphasis. The clinical aspect was answered by the analysis of a large **collective** and followed by the **evaluation of the results** with respect to their potential diagnostic and therapeutic impact.

3 Methodology

3.1 Cell Lines

For the establishment, optimization of the assays as well as for the determination of the limits of detection (LOD) we used a model system of tumor cell lines.

3.1.1 Cell Culture

Melanoma cell lines SK-MEL-28, SK-MEL-30 and IGR-1 and colorectal adenocarcinoma cell line HT-29 were used in this model system. All cell lines were propagated as recommended by the distributor and indicated below.

SK-MEL-28 cell line (purchased from LGC Standards GmbH, Wesel, Germany) was propagated in MEM medium (PAA Laboratories GmbH, Pasching, Austria) supplemented with 10% FBS Gold (PAA), 1% NEAA (PAA), 1% sodium pyruvate (PAA) and 1% penicillin/streptomycin (PAA). This cell line harbors the *BRAF* V600E mutation homozygously and was used as a positive control.

SK-MEL-30 cell line (purchased from DSMZ, Braunschweig, Germany) was propagated in RPMI (Invitrogen, Lofer, Austria) supplemented with 10% FBS Gold (PAA) and 1% penicillin/streptomycin (PAA). SK-MEL-30 DNA was used as wild type control.

HT-29 cell line (purchased from LGC Standards GmbH LGC Standards GmbH, Wesel, Germany) was propagated in McCoy's 5a Medium (Biochrom AG, Berlin, Germany) supplemented with 10% FBS Gold (PAA) and 1% penicillin / streptomycin (PAA). HT-29 cell line is heterozygous for the *BRAF* V600E mutation.

IGR-1 cell line (purchased from DSMZ) was propagated in DMEM high glucose (Invitrogen) supplemented with 10% FBS Gold (PAA) and 1% penicillin/streptomycin (PAA). This cell line is heterozygous for the *BRAF* V600K mutation.

All cell lines were incubated at 37°C and 5% CO_2. For long term storage cells were frozen in culture medium supplemented with 5 to 10% DMSO in liquid nitrogen.

3.1.2 DNA Isolation and Quantification

DNA from cell lines was extracted with the Gentra Puregene Blood Kit (QIAGEN, Hilden, Germany) according to the instructions supplied by the manufacturer with following minor modifications:

Adherent cells were detached with 0.05% Trypsin with EDTA 4Na (Invitrogen, Lofer, Austria), washed twice with PBS (Apotheke LKH Graz) and frozen in aliquots of approx. 1×10^7 cells in 200 µl

PBS at -20°C. For DNA isolation cell suspensions were thawed, vortexed and lysed in the presence of RNase A. To precipitate the protein the solution was incubated on ice for 10 minutes and centrifuged at 3000 × *g* for 10 min. The DNA pellet was dried at 37°C for 5 min. and solubilized in 500 µl TE buffer (Apotheke LKH Graz).

DNA quantity of highly concentrated solutions was determined spectrophotometrically using a BioPhotometer (Eppendorf, Hamburg, Germany) in combination with a micro-cuvette (IMPLEN, Munich, Germany). For a more exact quantification and quantification of low concentrated DNA the Quanti-iT™ PicoGreen® dsDNA Reagent (this assay will be referred to as PicoGreen from now on; Invitrogen, Lofer, Austria) was used. A high range standard curve from λ-DNA ranging from 2.5 ng/µl to 0.004 ng/µl was prepared. The assay was done in a 96 well format (Fluotrac 600, Greiner Bio-One GmbH, Frickenhausen, Germany) with a final assay volume of 100 µl. Based on the results of the photometric measurement samples were diluted in TE buffer to a concentration within the standard curve. Samples were analyzed with a microplate reader (FLUOstar OPTIMA, BMG Labtech, Offenburg, Germany).

3.1.3 FFPE Cell Line DNA

To simulate FFPE modifications occurring during tissue archiving, cell culture cells were embedded in a mixture of citrated plasma and Thromborel S (human thromboplastin containing calcium; Siemens Healthcare Diagnostics Products GmbH, Marburg, Germany). Cells were harvested and washed with PBS twice. The resulting pellet was mixed with 100 µl plasma (blood samples taken from healthy volunteers) and 200 µl Thromborel S. The mixture was allowed to coagulate for 20 min. at RT. Afterwards the gel-like structure was transferred to an embedding cassette and fixed for 15 min. in formol (4% formol in PBS, Sigma-Aldrich Handels GmbH, Vienna, Austria). Further fixation procedure was carried out in a Histokinet (Tissue Tek VIP; Sakura, Alphen aan den Rijn, The Netherlands) with the following steps: 90% ethanol for 1 hr., 96% ethanol for 1 hr., 100% ethanol for 2 hrs., xylene for 2 hrs., and paraffin over night. On the next day, fixed samples were embedded in paraffin.

20 sections with 10 µm of each embedded cell line were used for DNA isolation. Isolation was done according to the protocol described in section 3.2.1. DNA from cell lines processed and isolated the way described here, will be referred to as FFPE cell line DNA.

3.2 Tissue Samples

Tissue samples were obtained from the Department of Dermatology and Venereology, Medical University of Graz. They were identified through an electronic search of the Histopathology

database of the Department of Dermatology and Venereology using 'lentigo maligna' as search criterion. The time period for the search was set from the year 2007 to 2009. Samples used in this study were melanoma tissue samples from patients diagnosed with lentigo maligna melanoma, mostly *in situ*, in two cases invasive. Patient characteristics are summarized in Table 7. This study has been approved by the ethical committee of the Medical University Graz (24-229 ex 11/12).

3.2.1 DNA Isolation, Clean-Up and Quantification

We tested different methods for DNA isolation: Methods using column technology, as well as ones using DNA precipitation. In our hands best results were obtained using the protocol described below.

DNA from FFPE tissue samples was isolated as follows. Ten to 15 sections (10 µm) of the tissue were mounted onto glass slides. To locate the tumor area and surrounding tissue for manual dissection in the learning set and the collective, a last section with 5 µm was prepared for a hematoxylin and eosin stain. The staining procedure was carried out at the Department of Dermatology and Venereology and the tumor area of the melanoma, lentigo maligna subtype was defined by Univ.Prof.Dr. Lorenzo Cerroni.

The tissue was manually dissected with a scalpel from the glass slides and chips were transferred into a microcentrifuge tube filled with 1 ml xylene (Merck KGaA, Darmstadt, Germany). The suspension was vortexed and centrifuged at RT at 16,000 × *g* for 10 min in a microcentrifuge. The supernatant was carefully removed and discarded. 1 ml xylene was added to the remaining pellet to completely remove residual paraffin. After centrifugation and removal of the supernatant rehydration of the pellet was achieved with descending concentrations of ethanol (Merck KGaA, Darmstadt, Germany). The rehydrated pellet was dried at 37°C for approximately 5 min. 200 µl lysis buffer ([4 M urea, 200 mM Tris, 20 mM NaCl, 200 mM EDTA, pH 7.4 (25°C)], Apotheke LKH Graz) was added to the pellet and the suspension was incubated for 30 min. at 98°C. Afterwards the sample was spun down and cooled to RT. 40 µl proteinase K (20 mg/ml; QIAGEN, Hilden, Germany) were mixed with the suspension and incubated over night at 57°C in a heat block. On the next day another 20 µl Proteinase K were added to the sample, vortexed and incubated at 57°C for at least 2 additional hours or until the tissue was completely lysed. The activity of the Proteinase K in the completely lysed sample was inactivated by heating the lysate to 98°C for 10 min. After the incubation the sample was centrifuged at 4°C at 16,000 × *g* for 20 min. The lysate was transferred into a new tube. The centrifugation step was repeated and the resulting lysate transferred into another tube. To precipitate the DNA 200 µl 2-propanol (Sigma-Aldrich Handels GmbH, Vienna, Austria) were mixed with the lysate and incubated at -20°C over night. On

the next day the solution was centrifuged at 4°C at 14,000 × *g* for 20 min., the supernatant discarded and the pellet washed with 70% ethanol. The air dried DNA pellet was dissolved in an appropriate volume (10 to 30 µl) of TE buffer (Apotheke LKH Graz) and stored at 4°C for short term or -20°C for long term storage.

In order to remove inhibiting melanin from tissue samples (personal communication with Prof. Becker, (Dorrie et al. 2006)), extracted genomic DNA was purified using Micro Bio-Spin 6 Columns, Tris buffered (Bio-Rad Laboratories Ges.m.b.H., Vienna, Austria) according to the instructions supplied by the manufacturer. After preparing the columns, the total volume of the samples (10 µl) was loaded onto the columns, centrifuged at RT at 1,000 × *g* for 4 min, and the volume of the DNA sample was determined. DNA from all tissue samples was quantified using the Quanti-iT™ PicoGreen® dsDNA Reagent (Invitrogen, Lofer, Austria) as described in section 3.1.2.

3.2.2 Quality Control

To determine DNA integrity, quality and amplifiability a LINE-assay designed by ORIDIS Biomarkers, Graz, Austria (personal communication with Marcus Otte, PhD) was used. The assay was adapted and optimized for the LightCycler® 480 Instrument (Roche Diagnostics GmbH) using white 96-well multiwell plates. The PCR reaction contained primer pairs either amplifying a 149 bp fragment of LINE or amplifying a 249 bp fragment. The PCR reaction with a final reaction volume of 20 µl contained 2x LightCycler® 480 SYBR Green I Master Mix (Roche Diagnostics GmbH, Vienna, Austria), additional 1.5 mM $MgCl_2$, 0.2 mg BSA (Fermentas GmbH, St. Leon-Rot, Germany), 0.1 µM of each primer, 200 pg gDNA and PCR-grade water. Cycling conditions were as follows: Initial denaturation step at 95°C for 10 min.; 40 cycles with denaturation at 95°C for 30 sec., annealing at 60°C for 30 sec. and extension at 72°C for 20 sec.; melting analysis with an initial denaturation step at 95°C for 1 min. and a temperature ramp from 65°C to 95°C with continuous fluorescence acquisitions (10 acquisitions per °C). Cycling ended with a final cooling step and hold at 40°C.

3.3 PCR Based Assays

PCR is a common and often used method for mutational analysis. Either for direct analysis of the resulting PCR product as in allele specific PCR or HRMA PCR, or as a preliminary amplification step as in sequence analysis. Irrespective which downstream method is going to be used, the PCR reaction set up and the cycling parameters have to be optimized. Since the optimization and validation of the assays was an essential part of this work in the section 'Methodology' the final settings are described only. Optimization process per se is described in the 'Findings' section.

All PCR runs included a no template control (NTC) to rule out contamination of the reagents with gDNA or earlier synthesized PCR products. All PCR products were checked for specificity on 2.5 % agarose gel as described in section 3.3.3. All concentrations are final concentrations unless otherwise indicated.

Unless indicated otherwise, all PCR assays were performed on a LightCycler 480 (Roche Diagnostics GmbH, Vienna, Austria; software release 1.5.0). Cp values were determined automatically by the software using the Second Derivative Maximum method.

3.3.1 Primers

For all PCR based methods a prudent design of primers is crucial. For the present study, primers were designed to amplify short fragments (up to 150 bp), to contain the *BRAF* V600E mutation site, to exclusively bind to the *BRAF* gene and not to the pseudogene and to exclude SNPs known at the time of assay design. Primers were designed using the 'Primer Designing Tool'[2] and their specific binding to the target sequence was checked by performing BLAST analyses. Primers for pyrosequencing were designed using PyroMark Assay Design Software 2.0 (QIAGEN, Hilden, Germany).

Table 2: Primers used for analyses.

	fwd (5'-3')	rev (5'-3')	Amplicon
Pre-Amplification			
BRAF_Pre [3]	AACAGGTGATTTTGGTCTAGCTAC	TAGTAACTCAGCAGCATCTCAGG	152 bp
HRMA PCR			
BRAF10	GATTTTGGTCTAGCTACAG	AGCCTCAATTCTTACCATC	96 bp
BRAF PM1	AGGTGATTTTGGTCTAGCTACAG	ATCAGTGGAAAAATAGCCTCAAT	114 bp
BRAF PM3	AACAGGTGATTTTGGTCTAGCTAC	ATCAGTGGAAAAATAGCCTCAAT	117 bp
AS PCR			
BRAF V [4]	AGGTGATTTTGGTCTAGCTACAGT	TAGTAACTCAGCAGCATCTCAGGGC	149 bp
BRAF E [4]	AGGTGATTTTGGTCTAGCTACAGA	TAGTAACTCAGCAGCATCTCAGGGC	149 bp
BRAF K	AGGTGATTTTGGTCTAGCTACAAA	TAGTAACTCAGCAGCATCTCAGGGC	149 bp
Pyrosequencing			
BRAF PM1	AGGTGATTTTGGTCTAGCTACAG	Bio-ATCAGTGGAAAAATAGCCTCAAT	114 bp
Sequencing S1	TGATTTTGGTCTAGCTACAG		
BRAF PM2	Bio-GCTTGCTCTGATAGGAAAATGA	CAAACTGATGGGACCCACTC	146 bp
Sequencing S2		CCACTCCATCGAGATT	
BRAF PM3	AACAGGTGATTTTGGTCTAGCTAC	Bio-ATCAGTGGAAAAATAGCCTCAAT	117 bp
Sequencing S3	GGTGATTTTGGTCTAGCTAC		

Primers were purchased from Eurofins MWG Operon (Ebersberg, Germany), dissolved in RNase/DNase free water to yield a stock concentration of 100 µM and stored in aliquots at -20°C.

[2] http://www.ncbi.nlm.nih.gov/tools/primer-blast/index.cgi?LINK_LOC=BlastAlnAd
[3] Reverse primer from (Willmore-Payne et al. 2005)
[4] Primers from (Jarry et al. 2004)

Unless otherwise indicated all primers were HPSF purified. Primers with a 5'-BIO modification were HPLC purified.

3.3.2 Dilution Series

To optimize the assays and to assess the LOD for the detection of the *BRAF* V600E mutation a series of DNA blends containing different amounts of mutated (mt) DNA (SK-MEL-28 DNA) in a background of wild type (wt) DNA (SK-MEL-30 DNA) was prepared. For the first experiments, percentages of mt DNA were: 100%, 50%, 20%, 4%, 0.8%, 0.16%, 0.0032%, and 0% in wt DNA with a final DNA concentration of 10 ng/µl.

From the time point of adapting the assays to the *BRAF* V600K mutation on: 100%, 50%, 25%, 10%, 5%, 2.5%, 1%, 0.5%, 0.1%, 0.05%, and 0% in wt DNA with a final DNA concentration of 10 ng/µl.

For the analysis of the *BRAF* V600K mutation a corresponding series of DNA blends containing IGR-1 DNA (heterozygous for the *BRAF* V600K mutation) and SK-MEL-30 DNA with the following percentages mt DNA 50%, 25%, 12.5%, 5%, 2.5%, 1.25%, 0.5%, 0.25%, 0.05%, 0.025%, and 0% was prepared.

For reasons of simplification percentages indicating mt DNA in a background of wt DNA will refer from now on to DNA content, irrespectively whether the mutation is homo- or heterozygous.

To ensure equivalency between mt and wt DNA of amplifiable *BRAF* molecules and to compensate eventually occurring gene amplifications in the cell lines used, a correction factor was determined. A HRMA PCR using the BRAF PM3 primers (for details please refer to Table 2) amplifying a serial dilution from 50 ng to 0.4 ng of the respective DNAs was done and the amount of DNA was normalized to wt DNA. For details, and results please refer to section 4.1.1.

3.3.3 Pre-Amplification

Since the FFPE tissue samples were rather small and the DNA yield showed to be a limiting factor, it was necessary to do a pre-amplification. 20 ng gDNA were amplified in a reaction consisting of 0.5 µM of each primer (BRAF_Pre, for details refer to Table 2), 1x Phusion HF Buffer, 0.2 mg BSA (Fermentas GmbH), 0.2 mM of each dNTPs (Finnzymes, Espoo, Finland), additional 3 mM $MgCl_2$ (final concentration 4.5 mM), 0.02 U/µl Phusion® Hot Start II DNA Polymerase (Finnzymes, Espoo, Finland). PCR grade water (Roche Diagnostics GmbH, Vienna, Austria) was added to a final volume of 25 µl. Cycling conditions were as follows: Initial denaturation at 98°C for 30 sec.; 30 cycles with denaturation at 98°C for 10 sec., annealing at 62°C for 20 sec. and extension at 72°C for 8 sec.; a

final extension at 72°C for 5 min. was performed before cooling the reaction to 4°C. PCR was done with a MyCycler Thermal Cycler (Bio-Rad Laboratories Ges.m.b.H., Wien, Austria) using 0.2 ml tubes.

The resulting pre-amplification products were checked on a 2.5% agarose gel Biozym, Hessisch Oldendorf, Germany) in 1 x TBE buffer (Apotheke LKH Graz), using 5 µl PCR product mixed with 6x DNA loading dye (Fermentas GmbH). DNA markers (GeneRuler™ Low Range DNA Ladder and 50 bp DNA Ladder, Fermentas GmbH) were used for sizing the PCR products. Ethidium bromide was used for DNA visualization. The gels were casted and run in a Wide Mini-Sub Cell GT Cell (Bio-Rad Laboratories Ges.m.b.H., Wien, Austria) for 30 min. at 100 Volts.

To eliminate residual nucleotides/oligonucleotides and enzymes from the pre-amplification reaction products were cleaned up using QIAquick PCR Purification Kit (QIAGEN, Hilden, Germany). Purified PCR products were eluted with 30 µl EB buffer (supplied in the kit) and quantified using the Quanti-iT™ PicoGreen® dsDNA Reagent (Invitrogen, Lofer, Austria) as described in section 3.1.2.

The amount of copies/ng was calculated with the equation (1).

$$\text{Copies/ng} = \frac{\text{Avogadro constant}}{\text{Molecular mass}} \times 10^9 \qquad (1)$$

The Avogadro constant is defined as $6.02214879 \times 10^{23}$. The molecular mass for this specific amplicon was calculated using OligoCalc (Kibbe 2007). The calculated value of copies/ng was 6.42×10^9. With this information and the results from the DNA quantification the copies/µl were calculated and dilution series were prepared with a final working concentration of 4×10^3 copies/µl. To increase the stability of the dilution series carrier RNA (QIAGEN, Hilden, Germany) was added to the RNase/DNase free water used as diluent to a final concentration of 10 ng/µl. 2×10^4 copies served as template for further analysis in HRMA PCR and AS PCR, 4×10^3 copies were used for pyrosequencing.

3.3.4 COLD PCR

COLD PCR is a relatively new method for mutational analysis and has been described to be very sensitive (Li et al. 2008). COLD PCR is a quite complex PCR system which needs to be empirically optimized for the target gene of interest, the instrumentation and the reagents used. The principle of COLD PCR is described in section 0. Since the optimization was an essential part of this work the results are presented in section 4.1.2. Therefore, in this section information on the basic parameters, i.e. reagents used and instrumentation is given only.

A total of 10 primer pairs were designed and run through the optimization process. The workflow of optimization is given in Figure 14. The cycling program for a full COLD PCR can be divided into 5 steps: (1) Initial denaturation at 95°C for 10 min., (2) pre-amplification with 10 cycles denaturation at 95°C for 10 sec., annealing with touchdown starting at 60°C down to 55°C with step size 0.5°C for 10 sec., extension at 72°C for 4 sec., (3) COLD with 35 cycles denaturation at 95°C for 15 sec., hybridization at 61°C for 8 min., critical denaturation at 66°C for 3 sec., annealing at 55°C for 10 sec. and extension at 72°C for 4 sec., followed by (4) HRMA with denaturation at 95°C for 1 min., 40°C for 1 min., temperature ramp from 70°C to 90°C with 25 acquisitions per °C and (5) a final cooling step and hold at 40°C.

Two different chemistries were tested for COLD PCR. First, we used a reaction mix comparable to that used for HRMA PCR: 1x LightCycler® 480 High Resolution Melting Master Mix (Roche Diagnostics GmbH, Vienna, Austria), varying concentrations of primer (from 0.05 µM to 0.3 µM, dependent on the primer) and varying amounts of $MgCl_2$ (from 1.5 mM to 3.0 mM, dependent on the primer).

Second, we tested a reaction mix containing 0.2 µM of each primer, 1x Phusion HF Buffer, 0.2 mM of each dNTPs (Finnzymes, Espoo, Finland), 0.02 U/µl Phusion® Hot Start II DNA Polymerase (Finnzymes, Espoo, Finland) and 1x LCGreen Plus+ (Idaho Technology Inc., Salt Lake City, UT, USA). Primer and $MgCl_2$ concentration varied.

For all COLD PCR reactions 50 ng gDNA were used in a final reaction volume of 20 µl.

3.3.5 High Resolution Melting Analysis PCR (HRMA PCR)

HRMA PCR is a convenient, closed tube method for mutation analysis. Starting point for HRMA PCR for this work was an assay described by our group (Pichler et al. 2009). In order to further increase the sensitivity of this assay a total of 12 different primer pairs were designed and tested. For the four most promising primer pairs amplification conditions were optimized on the LightCycler® 480 Instrument (Roche Diagnostics GmbH) using white 96-well multiwell plates. For reasons of comparability the same amounts of templates were used in HRMA PCR as described for AS PCR. The reaction mix consisted of 1x LightCycler® 480 High Resolution Melting Master Mix (Roche Diagnostics GmbH, Vienna, Austria), varying amounts of primer (from 0.15 µM to 0.3 µM, dependent on the primer) and varying amounts of $MgCl_2$ (from 2.5 mM to 4.0 mM, depending on the primer). The final reaction volume was adjusted to 20 µl. Optimal cycling conditions proved to be an initial denaturation step at 95°C for 10 min, followed by 50 cycles of denaturation at 95°C for 10 sec., annealing at 56°C for 10 sec. and extension at 72°C for 5 sec. The amplification was

followed by the melting analysis with high resolution data acquisition with an initial denaturation step at 95°C for 1 min., a cooling step at 40°C for 1 min. and a temperature ramp from 70°C to 90°C with continuous fluorescence acquisitions (25 acquisitions per °C) and a final cooling step and hold at 40°C.

3.3.6 Allele Specific PCR (AS PCR)

The AS PCR used in this work is based on the method described by Jarry et al. (Jarry et al. 2004) with following essential modifications. Either 50 ng gDNA or 2×10^4 copies (5 µl) from the pre-amplification reaction were analyzed in a reaction consisting of 1x LightCycler® 480 SYBR Green I Master Mix (Roche Diagnostics GmbH, Vienna, Austria), 0.25 µM of each primer (for detail refer to Table 2) and PCR grade water with a final volume of 20 µl. The amplification conditions were optimized for the LightCycler® 480 Instrument (Roche Diagnostics GmbH) using white 96-well multiwell plates. Cycling conditions were as follows: Initial denaturation at 95°C for 5 min.; 45 cycles with denaturation at 95°C for 10 sec., annealing at 68°C for 20 sec. and extension at 72°C for 15 sec.; melting analysis with initial denaturation at 95°C for 5 sec. and a temperature ramp from 65°C to 97°C with continuous fluorescence acquisitions (10 acquisitions per °C). Cycling ended with a final cooling step and hold at 40°C.

The calculation of the percentage mutated DNA in samples was based on standard curves for *BRAF* wt, *BRAF* V600E and *BRAF* V600K which were included on every PCR plate. Therefore, serial dilutions of pre-amplification products from SK-MEL-28 (100% *BRAF* V600E), IGR-1 (50% *BRAF* V600K), and SK-MEL-30 (wt) from 2×10^4 copies to 20 copies were prepared. The equivalency of amplifiable pre-amplification products between cell lines was checked with HRMA PCR. The mean Cp values of the samples analyzed were converted in copies based on the regression equations from the standard curves. Copy numbers detected by the assay (either wt alone or, if a mutation was detected, the sum of wt copies and mutated copies) served as 100% copies amplified. The percentage of mutated DNA was calculated thereof.

3.3.7 Pyrosequencing

For PCR amplification of the template DNA we used the PyroMark PCR Kit (QIAGEN, Hilden, Germany). 10 ng gDNA or 4×10^3 copies of pre-amplification product were amplified in a reaction mix containing 1x PyroMark PCR Master Mix, 1x CoralLoad Concentrate, 0.2 µM of each primer and PCR-grade water to give a final volume of 25 µl. The amplification was done with a MyCycler (Bio-Rad Laboratories Ges.m.b.H., Wien, Austria) using 0.2 ml tubes. Cycling protocol started with an initial denaturation at 95°C for 15 min. followed by 45 cycles of denaturation at 94°C for

30 sec., annealing at 60°C for 30 sec. and extension at 72°C for 30 sec. After a final extension at 72°C for 10 min. the reaction was cooled to 4°C.

2 µl PCR product were directly loaded onto a 2.5% agarose gel (for details refer to3.3.3) to check the specificity of the product.

The immobilizing of the PCR products was done using the PyroMark Q24 Vacuum Workstation (QIAGEN, Hilden, Germany). A reaction mix containing 3 µl streptavidin-coated Sepharose® beads (GE Healthcare, Vienna, Austria), 40 µl binding buffer and 27 µl Milli-Q water (Millipore, Billerica, MA, USA) was dispensed in a 96-well plate. 10 µl of the PCR product were added to each well and the reaction was agitated for 10 min. at 1400 rpm at RT using an orbital shaker (Thermomixer, Eppendorf, Hamburg, Germany) to bind the PCR product onto the beads.

25 µl sequencing primer (diluted to 0.3 µM with annealing buffer) were dispensed into each well of a PyroMark Q24 plate (QIAGEN).

After binding of the PCR product to the Sepharose® beads, beads were captured to the filter probes of the vacuum tool and sequentially flushed with 70% ethanol for 5 sec., denaturation solution for 5 sec. and 1x wash buffer for 10 sec. Afterwards beads were released into the primer solution in the PyroMark Q24 plate. The loaded Q24 plate was heated to 80°C in a plate holder for 2 min. and cooled to RT for at least 10 min. Meanwhile the Q24 Cartridge (QIAGEN) was filled with PyroMark Gold Q24 Reagents (QIAGEN). Sequencing was done with the PyroMark Q24 instrument (QIAGEN), assay design and further sequence analysis was done with the PyroMark Q24 software (QIAGEN).

A NTC was included in every run to rule out contamination during PCR. At the beginning every assay was tested for ‘unspecific sequencing’ by including a reaction containing PCR product and beads but no sequencing primer. This control tested whether loop formation of the PCR product is occurring during sequencing, allowing a sequencing reaction without the addition of a sequencing primer. In another control reaction the assays were tested for primer dimer formation of the sequencing primer resulting in ‘primer sequencing’. Therefore, a reaction containing sequencing primer and beads but no template was analyzed. All assays described in this work gave neither product in NTC, or in ‘unspecific sequencing’ controls, or in ‘primer sequencing’ controls.

Because we wanted to detect and quantify different mutations, analysis became quite complicated. Figure 12 shows pyrograms of 100% wt DNA, homozygously mutated *BRAF* V600E DNA and heterozygously mutated *BRAF* V600K DNA on the left hand side. On the right hand side the dispensation order, sequence to analyze and the sequence read per dispensation are depicted

for copies carrying the mutation only. This figure should demonstrate the different progress which is made per dispensation depending on the sequence. To quantify the mutations, reference peaks have to be determined. In our case the only reference peaks that can be used for quantification are dispensation 4 [G] and dispensation 10 [C]. In a first step the mean value for the peak height of the reference peaks is calculated. Then deviations from peak heights at the other dispensations are evaluated: A *BRAF* V600E mutation leads to a higher peak at dispensation 5 [A] and a lower peak at dispensation 6 [T]. A *BRAF* V600K mutation results, on the one hand, in higher peaks at dispensation 2 [A] and dispensation 5 [A]. The peak height at dispensation 8, on the other hand, becomes lower. The extent of peak variation allows the calculation of percentages mutated DNA contained in a sample. Each sample is calculated individually. Peak heights for [A] dispensations are corrected by the correction factor defined by the PyroMark software. Sometimes it is obvious that a mutation is at hand (i.e. peak height at dispensation 5 [A] is above background signal), but it cannot be defined whether it is a *BRAF* V600E or a *BRAF* V600K mutation. These results are indicated as 'uncertain'.

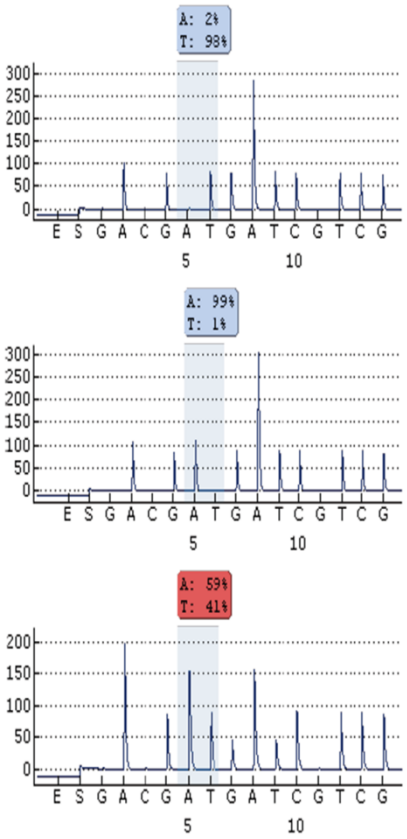

Dispensation order *BRAF* wt	GACGATGATCGTCG
Sequence to analyze	AG/_T/_GAAATCTCG
Sequence read per dispensation	AGTGAAATCTCG
Dispensation	24678 9

Dispensation order *BRAF* V600E	GACGATGATCGTCG
Sequence to analyze	AG/__/AGAAATCTCG
Sequence read per dispensation	AGAGAAATCTCG
Dispensation	24578 9

Dispensation order *BRAF* V600K	GACGATGATCGTCG
Sequence to analyze	A_/A_/AGAAATCTCG
Sequence read per dispensation	AAAGAAATCTCG
Dispensation	2 45 6

Figure 12: Examples for *BRAF* V600E and *BRAF* V600K mutation in Pyrosequencing.

On the left hand side pyrograms are showing wt DNA, homozygously mutated *BRAF* V600E DNA and heterozygously mutated *BRAF* V600K DNA. On the right hand side the sequences to analyze and the dispensations incorporated in the elongated sequence are indicated.

3.4 Statistics

The sensitivity of the assays was determined by calculating the Z-factor (Z) according to equation (2) (Zhang, Chung & Oldenburg 1999) where μ_S and μ_C denote for the means of the samples and negative control, respectively. The standard deviations (SD) for the samples and the control are denoted as σ_S and σ_C, respectively.

$$Z=1-\frac{(3\sigma_s+3\sigma_c)}{|\mu_s+\mu_c|} \quad (2)$$

A Z-factor <0 describes an assay where the sample cannot be distinguished from the negative control. Z-factors between 0 and 0.5 describe marginal assays, whereas excellent assays have Z-factors between 0.5 and 1. A Z-factor of 1 is ideal and describes an assay without any SD.

The frequencies of *BRAF* V600 mutations found in the tumor area and the surrounding area were compared using Fisher's exact test with an alpha α=0.5. *P* values ≤ 0.05 were considered statistically significant.

The MIQE Guidelines were followed whenever appropriate and feasible (Bustin et al. 2009).

4 Findings

4.1 Model System

The model system consisted of tumor cell line DNA and was used to establish and optimize the process of all assays. This model system has the advantages of providing high quality DNA with defined mutational status in large quantities.

To ensure constant conditions throughout the project, at the beginning DNA from cell lines was isolated in a sufficient extent for the whole study. DNA was not only quantified with the PicoGreen assay, but also with respect to its amplifiability by determining its equivalents.

4.1.1 Equivalents of DNA

Since minute amounts of mt DNA in a background of wt DNA were used in the serial blends, it was necessary to perform a thorough quantification of amplifiable DNA from cell lines. Therefore, DNA from cell lines was normalized to the wt cell line SK-MEL-30. Results for the IGR-1 cell line DNA are shown in Figure 13. The concentration of the serially diluted cell line DNA was plotted on the x-axis; the mean Cp values were plotted on the y-axis. The actual concentration of amplifiable IGR-1 DNA was calculated using the regression equation resulting from SK-MEL-30 DNA. Finally, a mean correction factor for IGR-1 DNA was determined. The same procedure was done for SK-MEL-28 DNA. After re-calculating DNA concentrations, another PCR with serially diluted DNA was done to control calculations. This procedure also takes into account copy number variations for the *BRAF* gene, which may occur in cell lines.

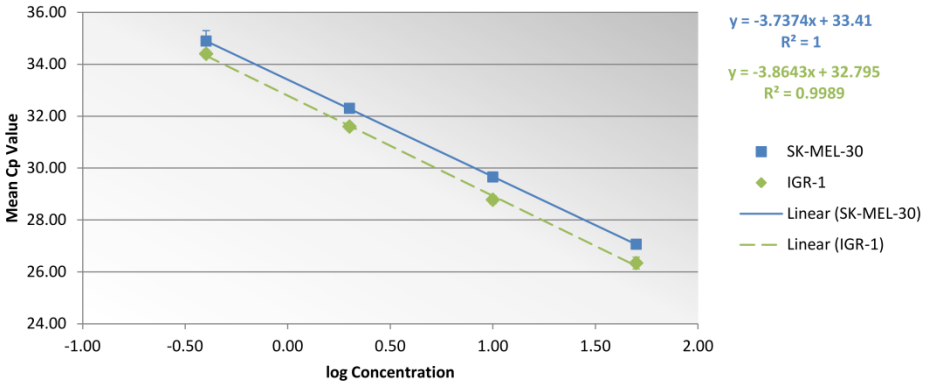

Figure continued on next page.

	SK-MEL-30				IGR-1			
Conc. est.	**Mean CP**	**ng calc.**	**Corr. factor**	**Mean Corr.**	**Mean CP**	**ng calc.**	**Corr. factor**	**Mean Corr.**
50.00	27.07	49.82	1.00	**1.000**	26.34	77.95	1.56	**1.543**
10.00	29.66	10.10	1.01		28.78	17.34	1.73	
2.00	32.30	1.98	0.99		31.60	3.05	1.53	
0.40	34.89	0.40	1.00		34.40	0.54	1.36	

Figure 13: **Determination of the correction factor for IGR-1.**

The correction factor for IGR-1 cell line is calculated by plotting the log concentration on the x-axis and the mean Cp values of the cell lines from HRMA PCR on the y-axis. The resulting regression equation from SK-MEL-30 DNA is used to determine the actual concentration of IGR-1 DNA (ng calc.). The mean of the correction factor is used correct the initially determined concentration. This procedure was repeated for any DNA used in the model system. Finally, equivalents were checked by another HRMA PCR.

4.1.2 Optimization of COLD PCR

COLD PCR is a complex PCR where hybridization and denaturation temperatures are critical factors which have to be determined empirically. We planned to use COLD PCR as an enrichment step for mutated DNA prior to HRM analysis. Therefore, in the context of our results, the term COLD PCR will be used for COLD PCR with subsequent HRMA. In the course of this project we developed a workflow for the optimization of COLD PCR which is shown in Figure 14.

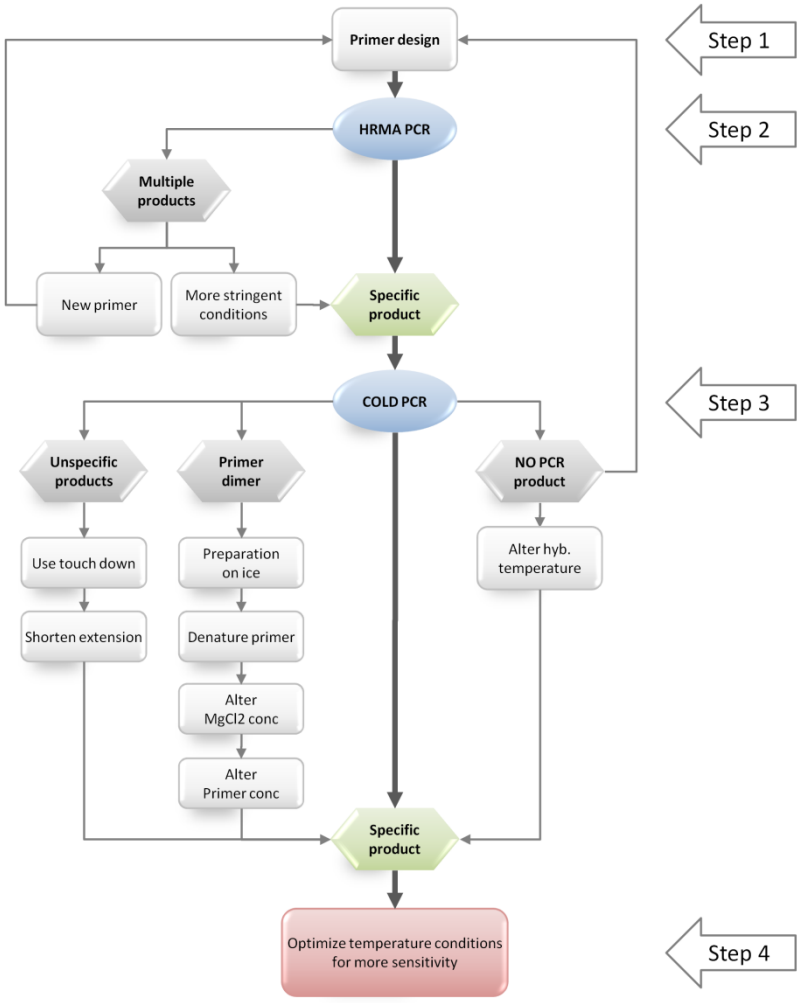

Figure 14: **Workflow for the optimization of COLD PCR.**

Ten primer pairs were designed, 8 of them were tested in HRMA PCR and 4 of them were used in COLD PCR. Only 2 primer pairs gave a specific product in COLD PCR and were further optimized with respect to $MgCl_2$ concentration and primer concentration.

For the detection of the *BRAF* V600E mutation a total of 10 primer pairs were designed for COLD PCR that specifically amplified a region of the *BRAF* gene covering the codon 600 (this step is referred to as 'Step 1' in Figure 14). The formation of a specific PCR product during conventional HRMA PCR is a prerequisite for the use of the primers in COLD PCR, since COLD PCR seems to favor the formation of primer dimers. This step is referred to as 'Step 2' in Figure 14. The specificity of the primers was checked with melting analysis after amplification and on an agarose gel. Eight primer pairs underwent optimization process for COLD PCR ('Step 3'). We started using the Roche chemistry. At the beginning none of the primers yielded a specific product after COLD PCR, only primer dimers could be detected. The addition of a denaturation-step of the primers prior to preparation of the master mix, keeping the reactions constantly on ice, and lowering the hybridization temperature, clearly improved the results as shown in Figure 15.

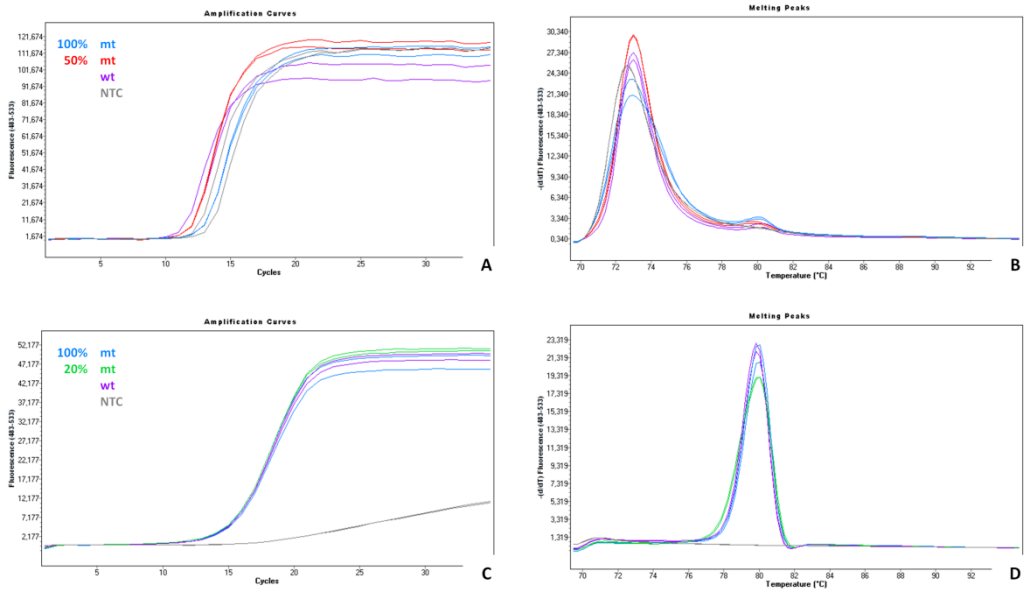

Figure 15: Primer dimer formation during COLD PCR.

Figure 15A and B depict the amplification curves and melting analysis of COLD PCR before optimizing set-up conditions. NTC and samples gave the same amount and type of product. Melting analysis shows the formation of mainly primer dimers (as confirmed on an agarose gel; data not shown) with a T_m of approx. 73°C. After optimizing set-up conditions and lowering the hybridization temperature, a specific PCR could be amplified using the same primers (as confirmed on an agarose gel; data not shown), as shown in Figure 15C and D.

Two primer pairs produced specific products during COLD PCR. For both pairs $MgCl_2$ concentration (ranging from 1.5 mM to 5 mM) and primer concentration (ranging from 0.05 µM to 0.3 µM) were optimized ('Step 4'). The primer pair internally named BRAF10 (for details see Table 2) gave the best results. To maximize the sensitivity of the system different hybridization temperatures, as well as critical denaturation temperatures were tested. In summary, 10 different temperature settings (with hybridization temperatures ranging from 48°C to 70°C and critical denaturation temperatures ranging from 52°C to 80°C) were tested. Unfortunately, the sensitivity of the assay could not be increased in comparison to conventional HRMA PCR.

To check whether the PCR cycling conditions or the chemicals are the reason why we were not able to improve sensitivity using COLD-PCR, we tried to reproduce the results published by Milbury et al. (Milbury, Li & Makrigiorgos 2009). Using identical primer sequences for detection of the *TP53* mutation, genomic DNA from the same cell line carrying the *TP53* mutation, and cycling conditions as similar as possible as described in the publication, we tried to reproduce their results with our chemicals and instrumentation. Again, as shown in Figure 16 we were not able to increase the sensitivity using COLD PCR in this assay.

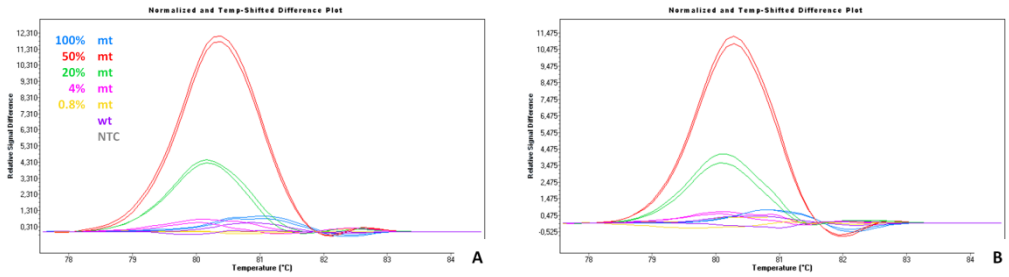

Figure 16: Comparison of difference plots from HRMA PCR and COLD PCR for *TP53* mutation.

Figure 16A shows a difference plot after HRMA PCR, Figure 16B a difference plot after COLD PCR. 4% mt DNA can hardly be discriminated from wt DNA in both graphs.

Since our results using the Roche chemistry for COLD PCR were nonsatisfying, a different chemistry (Phusion polymerase in combination with LC green; for details see section 3.3.4) was tested and optimized. The results of the optimization process are summarized in Figure 17. In our set-up, COLD PCR was more sensitive using the High Resolution Melting Master Mix (4% can be distinguished from wt), compared to using Phusion polymerase in combination with LCGreen Plus+ (wt and 4% mt DNA cannot be discriminated).

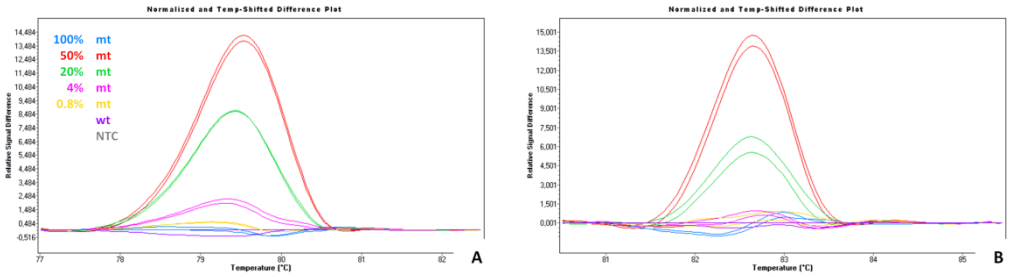

Figure 17: Comparison between two different chemistries for COLD-PCR.

Figure 17A shows a difference plot after COLD-PCR using the High Resolution Melting Master Mix (Roche). In this set-up a differentiation of samples containing 4% mt DNA from wt samples is possible. Figure 17B shows a difference plot using Phusion polymerase (Finnzymes) in combination with LCGreen Plus+ (Idaho Technologies). Here it is not possible to distinguish 4% from wt. Both set-ups underwent an extensive optimization process.

Although COLD PCR did not improve the sensitivity of HRMA PCR, we tested its applicability on FFPE cell line DNA. For this assay, FFPE and fresh cell line DNA revealed the same sensitivity (data not shown).

Unfortunately, despite extensive optimization of the assay, we were not able to increase the sensitivity of our HRMA PCR using COLD PCR for the detection of *BRAF* V600E mutation.

4.1.3 Sensitivity of AS PCR

The sensitivity of AS PCR for the detection of *BRAF* V600E mutation was determined using a series of DNA blends containing 100%, 50%, 25%, 10%, 5%, 2.5%, 1%, 0.1%, 0.05% and 0% mt DNA (SK-MEL-28) in a background of wt DNA (SK-MEL-30). Data is summarized in Figure 18 indicating a LOD of the assay of 0.1% mt DNA in a background of wt DNA giving a Z-factor of 0.69 (indicated by the gray arrow). Thus, AS PCR proved to be a very reliable and sensitive method.

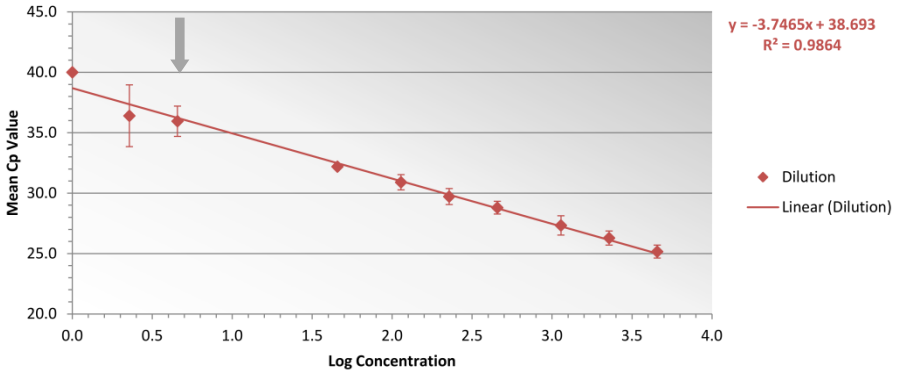

Figure 18: **LOD of the AS PCR for the *BRAF* V600E mutation.**

Using 15 ng gDNA with varying percentages of mt DNA, a LOD of 0.1% mt DNA in a background of wt DNA could be defined (indicated by the gray arrow). The calculated Z-factor for 0.1% is 0.69. (Results from two independent PCR runs with triplicates for each sample.)

4.1.4 Sensitivity of HRMA PCR

The sensitivity of HRMA PCR was determined using the same templates as for AS PCR. Based on the difference plot, 4% can be discriminated from wt as demonstrated in Figure 19. Summarizing the data for HRMA PCR this method has a moderate sensitivity, but allows the detection of any mutation found within the sequence of the amplicon regardless of the type of mutation (*BRAF* V600E or *BRAF* V600K).

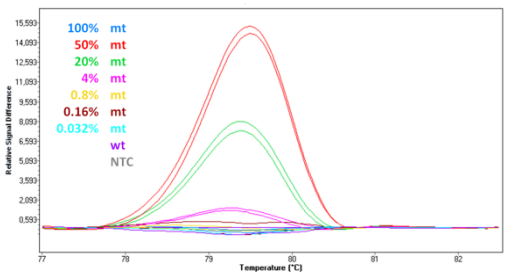

Figure 19: **LOD of the HRMA PCR with BRAF10 primer.**

Using the BRAF10 primer for HRMA PCR, 4% mt DNA in a background of wt DNA can be distinguished. If a Z-factor is calculated by taking the mean fluorescence values of the difference plot between 79.3 to 79.7°C (vertex in the difference plot) and their SD, a Z-factor of 0.2 results for 4%, which is rather moderate.

4.1.5 Establishing and Optimization of Pyrosequencing

For the detection of the *BRAF* V600E mutation two different pyrosequencing assays were designed, one forward (BRAF PM1) and one reverse (BRAF PM2) assay. The forward assay proved to be more sensitive than the reverse assay, which tended to give a higher background signal in wt samples (data not shown). Results for the BRAF PM1 assay are shown in Figure 20. The LOD for the BRAF PM1 assay is 4% with a Z-factor of 0.5. The indisputable advantage of pyrosequencing is the sequence information it provides. Thus, pyrosequencing is favored over HRMA PCR.

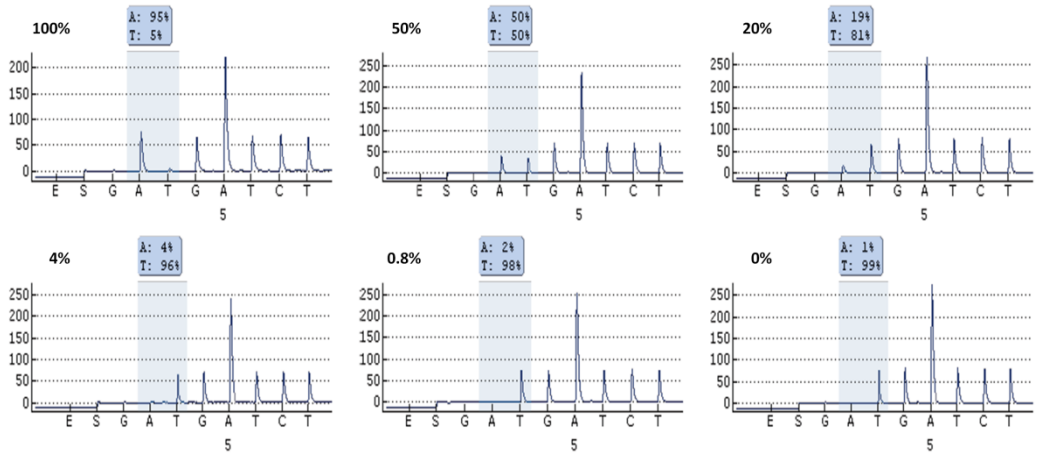

Figure 20: LOD of the PM1 Pyrosequencing assay.

Using the BRAF PM1 assay the LOD for the *BRAF* V600E mutation is 4% with a Z-factor of 0.5.

4.1.6 Summary – Model System

The comparison of the established and optimized assays (i.e. COLD PCR, AS PCR, HRMA PCR and pyrosequencing) showed that AS PCR is by far, the most sensitive method with a LOD of 0.1% for the *BRAF* V600E mutation. All other methods proved to have a comparable LOD of 4% with varying Z-factors. The sensitivity of HRMA PCR could not be improved by the use of COLD PCR despite extensive optimization work. Results of the MS are summarized in Table 3.

Table 3: Results of the MS.

	Sensitivity (Z-factor)	Advantages	Disadvantages
COLD PCR			
	4.0%		no improvement of sensitivity
AS PCR			
	0.1% (0.7)	very sensitive	assay specific for one mutation
HRMA PCR			
	4.0% (0.2)	any mutation within the amplicon sequence can be detected	
Pyrosequencing			
	4.0% (0.5)	information about the sequence	

4.2 Learning Set

The learning set consisted of 5 NM tissue samples and was used to test all established assays on FFPE tissue derived DNA. In comparison to LMM, NM are larger skin lesions. Therefore, the DNA yield was expected to be higher. In addition, the *BRAF* V600E mutation is described to be more frequent in NM than in LMM. Thus, the use of NM combined the advantages of larger DNA quantity and higher probability of the occurrence of the *BRAF* V600E mutation.

The actual mean DNA yield (ng ± SD) of the samples of the LS was 826 ± 454 (median 712 ng). The learning set (NM1 to NM5) was analyzed using the assays described in section 4.1. Very soon it became obvious, that NM4 carries a sequence alteration other than the *BRAF* V600E mutation. HRMA PCR with BRAF10 primer classified NM4 as wt, whereas AS PCR repeatedly detected a low level mutation (data not shown). Pyrosequencing using BRAF PM1 assay detected a T>A exchange of approx. 15% which seemed to be a *BRAF* V600E mutation, whereas pyrosequencing using BRAF PM2 assay (reverse assay) revealed the *BRAF* V600K mutation in NM4 (Figure 21). Results for NM5 were inconclusive and not always reproducible. Analysis of the amplifiability of the DNA with a multiplex GAPDH assay showed poor DNA quality of NM5 (for details refer to section 7.2.2), increasing the probability of the occurrence of PCR artifacts and errors during amplification. Therefore, we added the criterion of the minimal requirement of the DNA quality. Samples not fulfilling the requirement were excluded from further analysis.

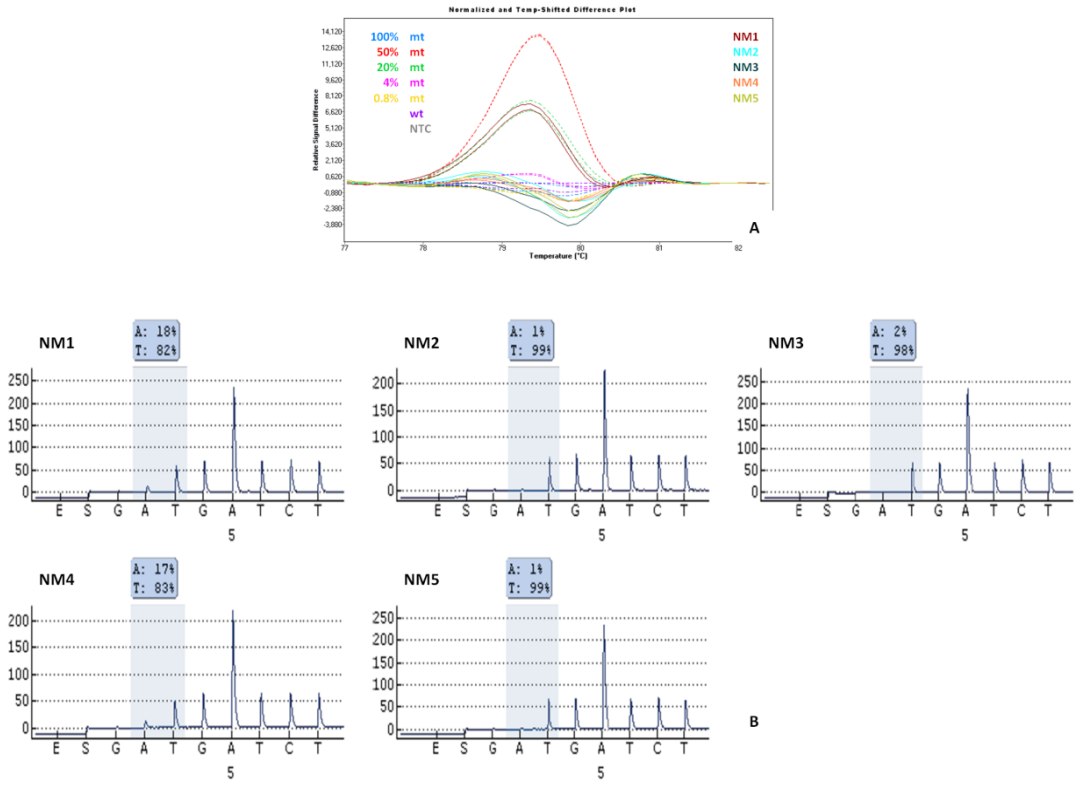

Figure continued on next page.

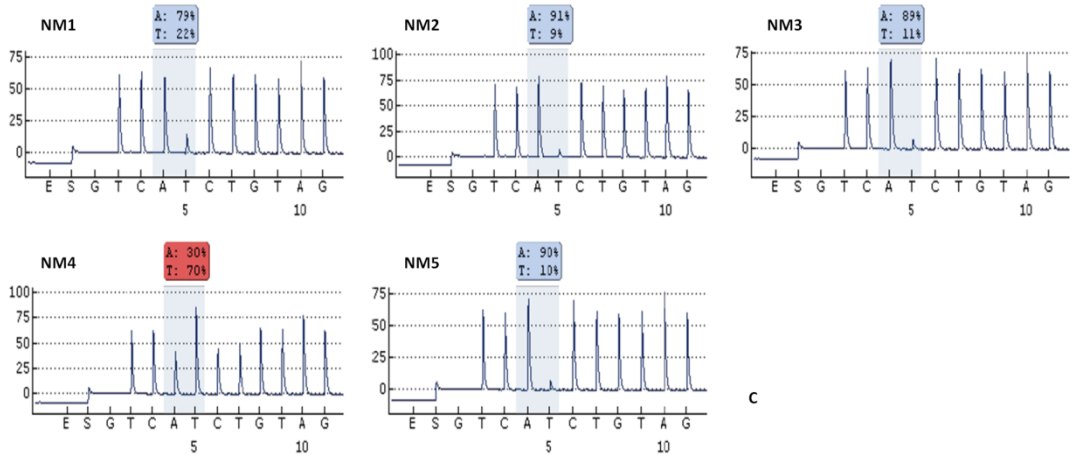

Figure 21: Analysis of the *BRAF* V600E mutation in the LS.

Figure 21A depicts the difference plot of HRMA PCR using the BRAF10 primer. Dotted lines indicate the serial dilution of cell line DNA blends. Solid lines in indicated colors define the samples. NM1 clearly shows an altered melting behavior compared to wt DNA. NM2 to NM5 are wt. The results for NM4 from HRMA PCR are not concordant to those of pyrosequencing. Figure 21B shows pyrosequencing results for the PM1 assay: NM1 and NM4 seem to carry the *BRAF* V600E mutation; NM1, NM2, and NM5 do not carry any mutation. The PM2 assay, for the first time, revealed the occurrence of the *BRAF* V600K mutation in NM4 (please note that PM2 is a reverse assay, therefore the sequence to analyze is complementary. For details refer to section 1.3.5).

The results from the LS showed the necessity to modify our assays to allow the simultaneous detection of the *BRAF* V600E as well as the V600K mutation. Primers for HRMA PCR and pyrosequencing were designed to amplify a region more up-stream of nucleotide 1799. For the AS PCR a new *BRAF* V600K mutation specific primer was designed. All assays were optimized using the MS again, adding a new cell line (i.e. IGR-1) carrying the *BRAF* V600K mutation. For results of the MS with the adapted HRMA assay refer to section 7.2.4. Results from pyrosequencing for the LS using the modified assays are summarized in Figure 22.

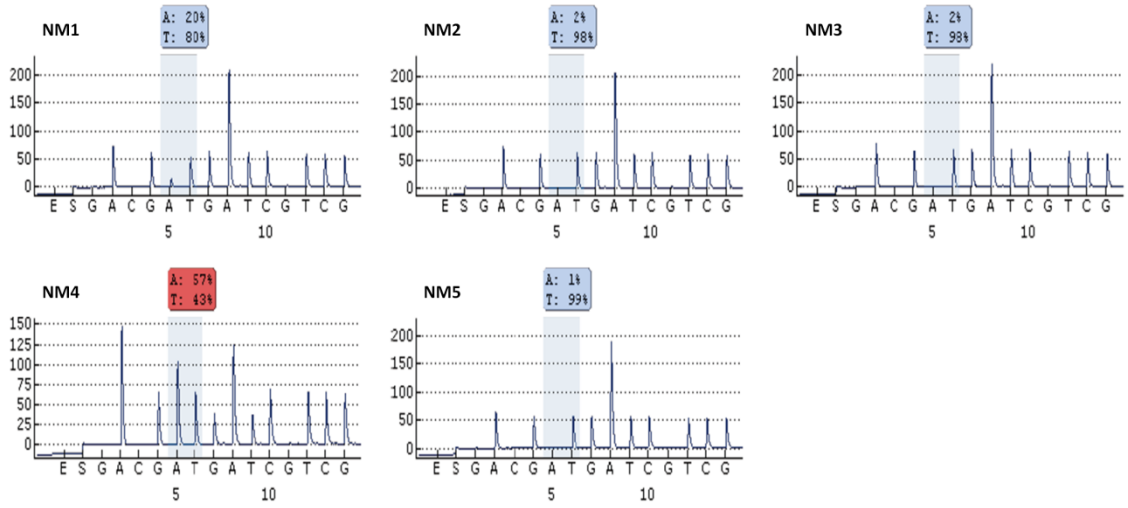

Figure 22: Results from the LS using gDNA and the PM3 assay for Pyrosequencing.

The PM3 assay clearly demonstrated the presence of the *BRAF* V600K mutation in NM4 indicated by the much higher peak at dispensation 2 [A]. The sum of the peaks at dispensation 5 [A] and 6 [T] (the typical *BRAF* V600E mutation site, light blue shaded) is also higher than the normal peaks detecting only one nucleotide (e.g., dispensation 12 [T], 13 [C], and 14 [G]). For details refer to section 3.3.7. Using this strategy NM4 was detected to carry the *BRAF* V600K mutation to an extent of more than 40%.

The adaption of the assays to allow simultaneous detection of the two *BRAF* mutations was done in parallel to DNA isolation from the samples of the TS. The mean DNA yield of 84 ± 69 (median 57 ng; ng ± SD) of the samples of the TS was considerably lower than the one of the LS (826 ± 454; median 712 ng). Therefore, a pre-amplification step was necessary. To check whether the pre-amplification step biases results, we went back to the MS and after that re-analyzed the LS. For HRMA PCR results of the comparison with and without pre-amplification of the MS refer to section 7.2.3 (results for pyrosequencing and AS PCR not shown). Direct comparison of HRMA PCR results of the LS is shown in Figure 23. Pre-amplification showed no adverse effects, neither in HRMA PCR, nor in pyrosequencing, nor in AS PCR (results for pyrosequencing and AS PCR not shown). Re-analysis of the LS using pre-amplification products in combination with the BRAF PM3 primer (this primer allows the detection of the *BRAF* V600K mutation) is shown in Figure 24.

Initially, for pre-amplification primers were used amplifying a 250 bp fragment of the *BRAF* gene, spanning the region around codon 600. Primers were designed to allow subsequent mutational analysis with our assays described in this study. Since considerable DNA fragmentation was observed in the samples of the TS, it was necessary to shorten the length of the pre-amplification fragment later in the project.

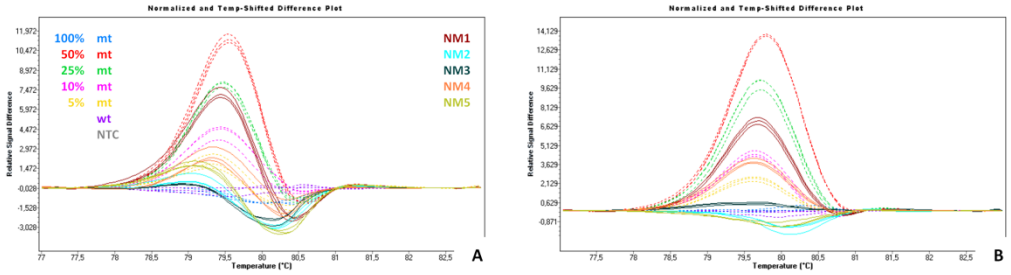

Figure 23: Comparison and reanalysis of the LS with HRMA PCR using BRAF PM1 primer.

Figure 23A shows the difference plot of HRMA PCR using gDNA in comparison to Figure 23B were pre-amplification products served as template. In both plots NM1 clearly carries a *BRAF* mutation; NM4 shows an altered melting behavior in both plots, too. As demonstrated in this figure, no adverse effect could be observed, if gDNA underwent pre-amplification prior to HRMA PCR or not. BRAF PM1 primer was used for this analysis.

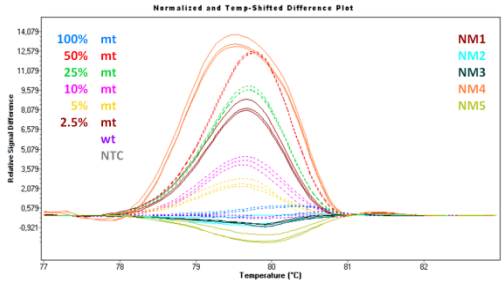

Figure 24: Re-analysis of the LS with HRMA PCR using BRAF PM3 primer and pre-amplification products.

This figure summarizes the re-analysis of the LS with HRMA PCR. DNA blends carrying the *BRAF* V600E mutation are indicated by the dotted lines. This figure vividly demonstrates the improvement of the assay for the detection of the *BRAF* V600K mutation by the example of NM4. This sample shows a completely different melting behavior using the BRAF PM3 primer in comparison to Figure 23 were NM4 has a slightly altered melting behavior only when using BRAF PM1 primer.

Results of the LS using the modified AS PCR assay in combination with the pre-amplification step are presented in Figure 25. NM4 yielded a strong signal for the *BRAF* V600K mutation using the AS PCR which corresponds to 48% mutated DNA in the sample. In NM1 19% mutated DNA carrying the *BRAF* V600E mutation could be detected. NM2 and NM3 gave no signal with mutation specific primers and are thus classified as wt. NM5 was excluded from final analysis due to insufficient DNA quality.

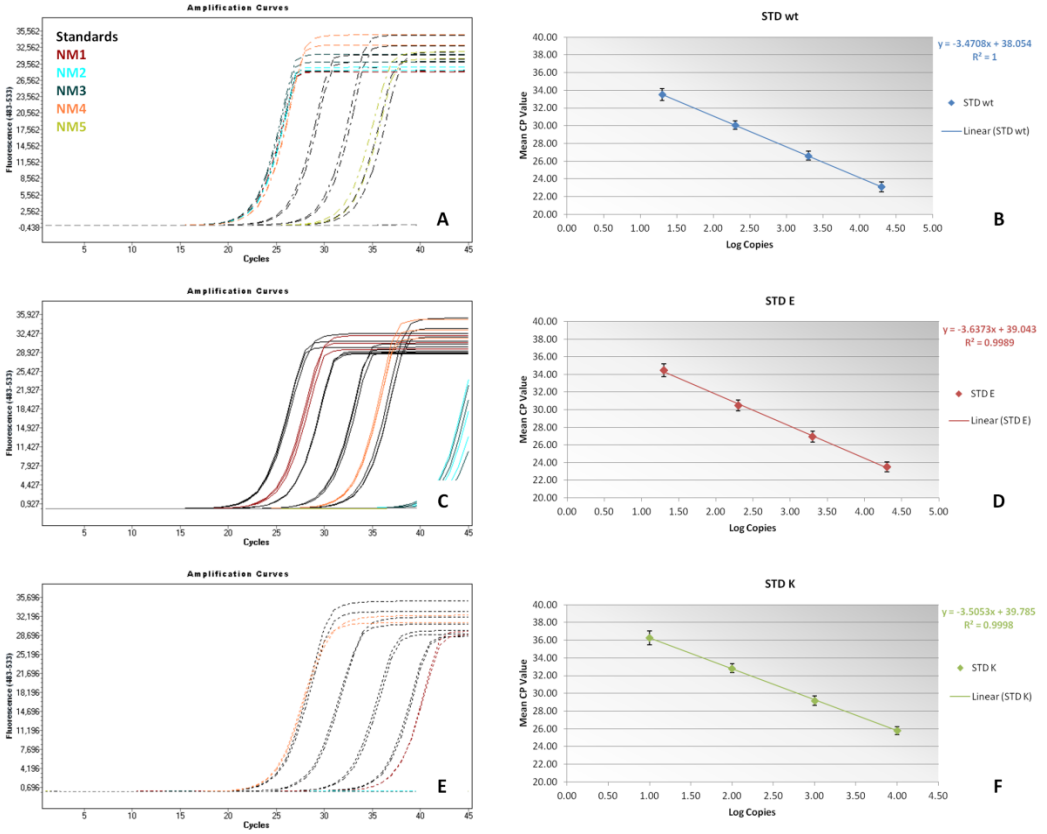

Figure 25: Reanalysis of the LS with AS PCR.

In this figure on the left hand side amplification curves from AS PCR are shown (A: *BRAF* wt, C: *BRAF* V600E, E: *BRAF* V600K). For each mutation and the wt serial dilutions of pre-amplification products from cell line DNA were included to allow quantification (Figure 25B, D, and E). Figure 25A demonstrates once again the poor DNA quality of NM5, since even the pre-amplification product used in this analysis can hardly be amplified. Any Cp values ≥40 were classified as negative signal. For details of calculating the percentage of mutated template in the pre-amplification product refer to section 3.3.6.

4.2.1 Summary Learning Set

The learning set pointed us to the *BRAF* V600K mutation. Therefore, we adapted and optimized all assays, so that they would allow the detection of both mutations, *BRAF* V600E and *BRAF* V600K. In addition, we included a pre-amplification step prior to the mutation analysis assays, because DNA yield was, even in the LS, rather low. Finally, we learned that DNA has to meet a minimum requirement of DNA quality; otherwise any result from downstream analysis is questionable because of increased occurrence of PCR artifacts and errors during amplification. Samples not fulfilling DNA quality requirements were excluded from final analysis (as demonstrated in Table 4: NM5). During this phase of the project, all assays were retested with the MS, whenever a change

was made in the procedure (e.g., pre-amplification step). With the LS we proved the applicability of all of our assays on FFPE material. The results of the LS are summarized in Table 4.

Table 4: Results of the LS.

Sample	DNA Quality[5]	PreAmp.[6]	HRMA PCR	AS PCR	% mt DNA	Pyroseq.	% mt DNA
NM1	✓	✓	mt	E	17.5	E	20.0
NM2	✓	✓	wt	wt		wt	
NM3	✓	✓	wt	wt		wt	
NM4	✓	✓	mt	K	53.1	K	44.2
NM5	×	×	—	—		—	

4.3 Training Set

The low DNA quantity isolated from samples of the TS (as stated in section 4.2) once more demonstrated the importance of the pre-amplification step. For some samples, even the 20 ng gDNA necessary for the pre-amplification were an exclusion criterion. Due to the limited DNA amount, the DNA quality assay had to be changed from a 'single-copy-gene assay' (GAPDH assay) to a 'repetitive sequence assay' (LINE assay) allowing DNA quality assessment with a hundredth of the DNA amount. The LINE assay demonstrated the necessity to shorten the amplicon length used for pre-amplification. The difference in the percentage of amplifiable DNA for the 149 bp LINE fragment and the 249 bp LINE fragment is shown Figure 37 in section 7.2.8. Because of the low percentage of DNA that allowed an amplification of a 249 bp fragments we altered pre-amplification to a 152 bp pre-amplification product. In addition, pre-amplification was further optimized by addition of BSA and $MgCl_2$ (Figure 35), as well as by purification of isolated gDNA with chromatography columns to remove residual melanin. To allow a detection of 1% mt DNA present in a sample we defined quality criteria explained in section 7.2.9. Results of the 'pre-mutation analysis processes' are shown in Figure 26. Results of the mutation analysis of the TS are listed in Table 5.

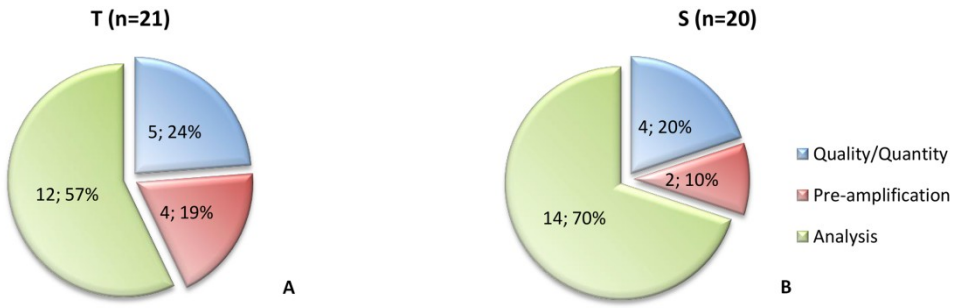

Figure legend on next page.

[5] ✓ 1.0% mt DNA in the sample should be detected with a probability of 0.95.
[6] ✓ PCR product visible on agarose gel.
× Defined requirements failed.
— Analysis not possible.

Figure 26: Drop out TS.

DNA from 12 samples (57%) isolated from the tumor area (T; Figure 26A) and 14 samples isolated from the surrounding area (S; Figure 26B) passed quality criteria and yielded a pre-amplification product. Drop-out because of failing the pre-amplification was more frequent in DNA from tumor area than in DNA from surrounding area.

Table 5: Results of the TS.

Sample	DNA Quality[5]	PreAmp.[6]	HRMA PCR	AS PCR	% mt DNA	Pyroseq.	% mt DNA
LMM1 T[7]/S[8]	✓ / ✓	✓ / ✓	wt / wt	E / wt	0.6	wt / wt	
LMM2 T/S	✗ / ✗	✗ / ✗	— / —	— / —		— / —	
LMM3 T/S	✓ / ✓	✓ / ✗	wt / —	wt / —		wt / —	
LMM4 T/S	✓ / ✓	✓ / ✓	wt / wt	wt / wt		wt / wt	
LMM5 T/S	✓ / ✓	✓ / ✓	wt / wt	wt / wt		wt / wt	
LMM6 T/S	✗ / ✗	✗ / ✗	— / —	— / —		— / —	
LMM7 T/S	✓ / ✓	✗ / ✓	— / wt	— / wt		— / wt	
LMM8 T/S	✓ / ✓	✓ / ✓	wt / wt	wt / wt		wt / wt	
LMM9 T/S	✓ / ✓	✗ / ✓	— / wt	— / wt		— / wt	
LMM10 T/S	✓ / ✓	✓ / ✓	wt / wt	wt / wt		wt / wt	
LMM11 T/S	✗ / ✗	✗ / ✗	— / —	— / —		— / —	
LMM12 /T/S	✓ / ✓ / ✓	✓ / ✓ / ✓	wt / wt / wt	wt / wt / wt		wt / wt / wt	
LMM13 T/S	✓ / ✓	✗ / ✓	— / wt	— / wt		— / wt	
LMM14	✓	✓	wt	wt		wt	
LMM15 /T/S	✓ / ✓ / ✓	✓ / ✓ / ✓	wt / wt / wt	wt / wt / wt		wt / wt / wt	
LMM16 T/S	✗ / ✗	✗ / ✗	— / —	— / —		— / —	
LMM17 T/S	✗ / ✓	✗ / ✓	— / wt	— / wt		— / wt	
LMM18 T/S	✓ / ✓	✓ / ✓	wt / wt	wt / wt		wt / wt	
LMM19 T/S	✓ / ✓	✗ / ✗	— / —	— / —		— / —	
LMM20 /T/S	✓ / ✓ / ✓	✓ / ✓ / ✓	wt / wt / wt	E / wt / wt	0.5	wt / wt / wt	
LMM21 /T/S	✓ / ✓ / ✓	✓ / ✓ / ✓	wt / mt / wt	K / K / wt	2.6 / 3.3	wt / K / wt	5.7
T: 21 S: 20 woD[9]: 4	T: 16 ✓, 5 ✗ S: 16 ✓, 4 ✗ woD: 4 ✓	T: 12 ✓, 9 ✗ S: 14 ✓, 6 ✗ woD: 4 ✓	T: 11 wt, 1 mt S: 14 wt woD: 4 wt	T: 10 wt, 1 E, 1 K S: 14 wt woD: 2 wt, 1 E, 1 K		T: 11 wt, 1 K S: 14 wt woD: 4 wt	

4.3.1 Summary Training Set

In the course of the analysis of the TS we were able to increase the performance of our assays by optimizing the pre-amplification reaction and shortening of the pre-amplification product. Comparing the 3 different assays, AS PCR proved to be the most sensitive assay, which not only detects the mutation like HRMA PCR, but also provides information on the type of mutation (*BRAF* V600E or *BRAF* V600K). Due to the lower sensitivity of HRMA PCR and pyrosequencing, low level mutation could be detected using AS PCR, only. Therefore, we decided to analyze the collective with the AS PCR.

Another question answered by the TS was the necessity of manual dissection. Although *BRAF* V600E mutation was found in LMM20 without manual dissection only, LMM21 showed a higher percentage of mutated DNA in the dissected sample (3.3%; LMM21 T) than without manual dissection (woD; 2.6%; LMM21). Therefore, we decided to manually dissect the samples of the collective. The discrepancy between LMM20 woD and LMM20 T (were no mutation could be detected) can be explained by the different cutting depth of the FFPE tissue sample.

[7] T: DNA isolated from tumor area.
[8] S: DNA isolated from surrounding area.
[9] woD: without manual dissection.

The *BRAF* V600E mutation was detected in the tumor area of LMM1, but not in the corresponding surrounding tissue. The DNA of the tumor area of LMM21 carried the *BRAF* V600K mutation, and again, no mutation could be detected in the corresponding surrounding tissue. Thus, a *BRAF* V600 mutation could be found in 16.7% of the tumor areas (n=2/12) but no mutation at all was found in the corresponding surrounding areas (n=0/14). The frequencies at which the mutations were detected in the TS are shown in Figure 27.

Figure 27: Frequency of the *BRAF* V600 mutations in the TS.

BRAF V600 mutations could be found in DNA from the tumor area of the TS only. No *BRAF* V600 mutation was detected in the DNA of the corresponding surrounding tissue.

Before proceeding with the analysis of the collective, we returned to the MS several times for assay adaption and optimization. An overview of the succession is given in Figure 28.

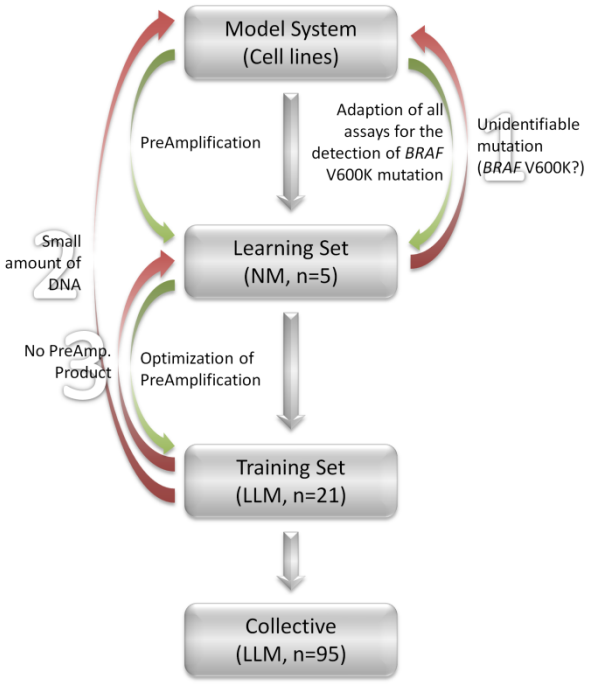

Figure 28: Succession of steps toward the analysis of the collective.

Before analyzing the collective we encountered several challenges. After establishment and optimization of the assays using the MS, we detected a *BRAF* V600K mutation in the learning set (indicated by '1') which led to the adaption of the assays to detect both mutations. The small DNA yield of the samples from the learning set ('2') made a pre-amplification step necessary. Eventually occurring alterations in the performance of the assays were tested using the MS again. In addition, the DNA quality assay was changed from a 'single-copy-gene' assay to a 'repetitive sequence' assay, to reduce the DNA amount necessary for analysis. Finally, pre-amplification itself had to be thoroughly optimized ('3'), since this reaction proved to be more sensitive to melanin and other inhibiting substances than AS PCR or HRMA PCR.

4.4 Collective

DNA isolation from the samples of the collective was done the same way as from samples of the TS. Initially 163 patients with the diagnosis lentigo maligna melanoma were identified from the database for the time period set from 2007 to 2009. Archived tissue sections of those samples were retrieved and examined whether the tumor size was suitable for the investigations of the project. Fourteen samples had to be excluded from analysis because the tissue volume was too small. From the remaining samples sections for DNA isolation and one section for HE staining were prepared. The HE-re-stained sections were examined microscopically for the proportion of LMM tumor cells in the tissue samples. All samples with less than 5% tumor cells present in the HE stain were excluded from further analysis. The remaining 95 samples were manually dissected whenever appropriate and the isolated DNA was checked for its quality. The DNA of the tumor area of 61 and the surrounding area of 39 LMM samples were subject to mutation analysis with AS PCR. The flow chart of sample selection is shown in Figure 29. To minimize drop-out numbers an additional clean-up step was performed before pre-amplification using size-exclusion columns. Thus, the percentage of samples fulfilling the quality requirements, but failing the pre-amplification could be significantly reduced to 1% of the DNA from the tumor area and 4% of the DNA in the surrounding area. In comparison, drop-out in the TS was 19% and 10% of the samples from the tumor and surrounding area, respectively. The summarized results of the collective are given Table 6.

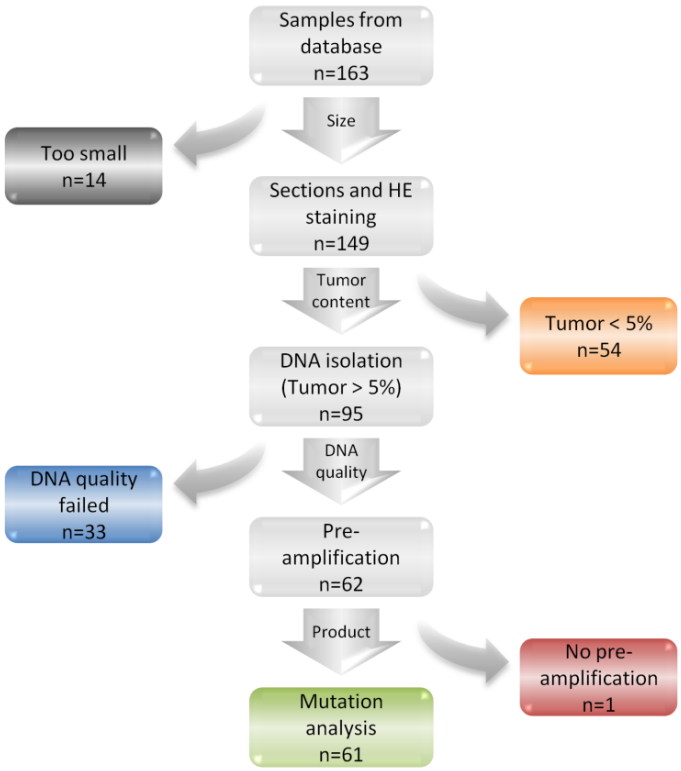

Figure legend on next page.

Figure 29: Drop out collective (I).

Not all of the 163 samples searched from the database were suitable for mutation analysis. 8% of the tissue samples (14 cases) were too small to allow isolation of sufficient DNA. 33% (54 cases) showed too little tumor cell count based on the HE staining and were thus excluded from further analysis leaving 95 samples from which DNA was extracted. Corresponding DNA from the surrounding area was isolated in 51 cases (data for surrounding area not shown in the flow chart; refer to Figure 30B). DNA quality failed in 20% (33 cases). The drop out because of failure of pre-amplification could be reduced to 1% (1 case) due to optimization. Thus, a total of 61 DNA samples from tumor area (37% of the initial 163 cases) and 39 samples from surrounding area underwent mutation analysis.

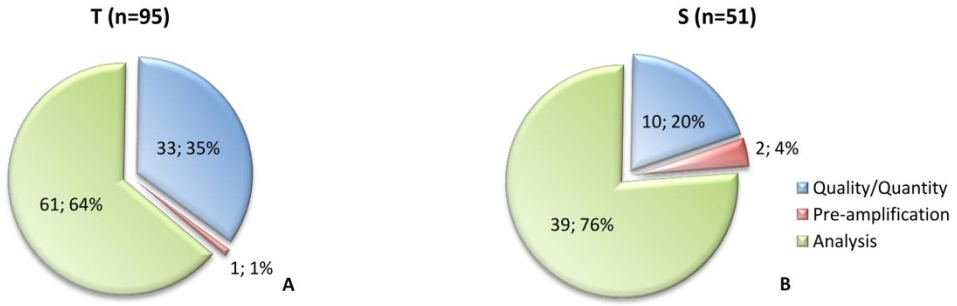

Figure 30: Drop-out collective (II).

These figures focus on the samples from which DNA was isolated, but in contrast to Figure 29 differentiate between tumor area (Figure 30A) and surrounding area (Figure 30B). Although drop-out caused by failing the quality/quantity requirements was more frequent in DNA from the tumor area in the collective compared to surrounding area and the TS, the drop-out due to failing the pre-amplification could be drastically reduced to 1% and 4% in the tumor and surrounding area, respectively.

Although in the model system LOD of the AS PCR was 0.1%, mutations in the samples were detected down to 0.5%. Based on data from Table 10 (please refer to section 7.2.11) most cases allowed the detection of a mutation present at 0.5% (55.5%, 81 DNA samples) what implies a necessary amplifiable DNA quantity of at least 2 ng in the pre-amplification. 13% of the samples (19 DNA samples) had > 1 ng but < 2 ng amplifiable DNA in the pre-amplification resulting in an overall sensitivity of 1%. The remaining 31.5% did not meet the quality requirements.

Table 6: Results of the collective.

Sample ID	DNA Quality[5]	PreAmp.[6]	AS PCR	% mt DNA	P-Seq. PreAmp	% mt DNA	P-Seq. gDNA	% mt DNA
1	✗	✗	—					
2 T / S	✓ / ✓	✓ / ✓	wt / wt					
3	✓	✓	wt					
4 T / S	✗ / ✓	✗ / ✗	— / —					
6 T / S	✓ / ✓	✓ / ✓	K / wt	1.4	? / wt			
8 T / S	✗ / ✗	✗ / ✗	— / —					
11	✓	✓	wt					
12 T / S	✗ / ✗	✗ / ✗	— / —					
13 T / S	✓ / ✓	✓ / ✓	K / wt	2.6	K / wt	2.6		
14	✗	✗	—					
19	✗	✗	—					
21	✗	✗	—					
22 T / S	✓ / ✓	✓ / ✓	K / wt	3.3	K / wt	2.4	?	prob. K 2.6
23	✓	✓	wt					
24	✗	✗	—					
58	✓	✓	wt		wt		wt	
59 T / S	✓ / ✓	✓ / ✓	wt / wt				wt / wt	
60	✓	✓	wt					
63	✗	✗	—					
64 T / S	✓ / ✓	✓ / ✓	K / wt	0.62	wt / wt			
65 T / S	✓ / ✓	✓ / ✓	wt / wt					
67	✓	✓	wt					

Table continued on next page.

Sample ID	DNA Quality[5]	PreAmp.[6]	AS PCR	% mt DNA	P-Seq. PreAmp	% mt DNA	P-Seq. gDNA	% mt DNA
73 T / S	✗ / ✗	✗ / ✗	— / —					
75 T / S	✓ / ✓	✓ / ✓	wt / wt		wt / wt		wt / wt	
76	✓	✓	wt					
77 T / S	✓ / ✓	✓ / ✓	wt / wt					
79	✓	✓	wt					
80 T / S	✓ / ✓	✗ / ✗	— / —					
81	✗	✗	—					
83 T / S	✓ / ✗	✓ / ✗	K / —	0.94	K	1.1		
89 T / S	✓ / ✓	✓ / ✓	wt / wt					
90 T / S	✓ / ✓	✓ / ✓	E / wt	0.64	wt / wt			
94	✗	✗	—					
95 T / S	✗ / ✓	✗ / ✓	— / wt					
96 T / S	✓ / ✓	✓ / ✓	wt / wt					
97 T / S	✓ / ✓	✓ / ✓	wt / wt					
98	✓	✓	wt					
101	✓	✓	wt					
102 T / S	✗ / ✓	✗ / ✓	— / wt					
103 T / S	✓ / ✓	✓ / ✓	wt / wt					
104	✓	✓	wt					
105 T / S	✓ / ✓	✓ / ✓	wt / wt					
107 T / S	✓ / ✓	✓ / ✓	wt / wt					
108 T / S	✓ / ✓	✓ / ✓	wt / wt					
110 T / S	✓ / ✓	✓ / ✓	K / wt	2.76	K / wt	3.4		
111	✓	✓	wt					
112	✗	✗	—					
116 T / S	✓ / ✓	✓ / ✓	wt / wt		wt / wt		wt / wt	
118 T / S	✓ / ✓	✓ / ✓	wt / wt					
121	✗	✗	—					
123 T / S	✗ / ✓	✗ / ✓	— / wt					
124 T / S	✓ / ✓	✓ / ✓	wt / wt					
125 T / S	✗ / ✓	✗ / ✓	— / wt					
129 T / S	✗ / ✗	✗ / ✗	— / —					
132	✗	✗	—					
134 T / S	✓ / ✓	✓ / ✓	wt / wt					
135 T / S	✓ / ✓	✓ / ✓	K / wt	1.56	? / wt	prob. K 1.3		
136 T / S	✓ / ✓	✓ / ✓	wt / wt					
138	✗	✗	—					
139	✓	✓	wt					
140 T / S	✗ / ✗	✗ / ✗	— / —					
142	✗	✗	—					
146	✓	✓	wt					
147	✓	✓	wt					
148 T / S	✗ / ✗	✗ / ✗	— / —					
149-1 T / S	✓ / ✓	✓ / ✓	wt / wt					
149-3 inv / *in situ*	✓ / ✓	✓ / ✓	wt / wt					
149-4 T / S	✓ / ✓	✓ / ✓	wt / wt					
150 T / S	✓ / ✓	✓ / ✓	wt / E	4.57	wt / ?	prob. E 8.1	wt / ?	prob. E 8.8
151 T / S	✓ / ✓	✓ / ✓	wt / wt					
152	✓	✓	K	0.72	wt			
153	✗	✗	—					
156	✓	✓	wt		wt			
158	✓	✓	E	2.22	wt			
159	✗	✗	—					
163 T / S	✓ / ✓	✓ / ✓	wt / wt					
164	✓	✓	wt					

Sample ID	DNA Quality[5]	PreAmp.[6]	AS PCR	% mt DNA	P-Seq. PreAmp	% mt DNA	P-Seq. gDNA	% mt DNA
165	✓	✓	wt					
166-1 T / S	✓ / ✓	✓ / ✓	wt / wt					
166-3 T / S	✓ / ✓	✓ / ✓	wt / **E**	**1.76**	wt / wt			
167	✓	✓	wt					
169 T / S	✓ / ✓	✓ / ✓	wt / wt					
170	✗	✗	—					
173	✓	✓	**K**	**2.98**	**?**	**prob. K 4.3**		
175 T / S	✗ / ✗	✗ / ✗	— / —					
177 T / S	✓ / ✓	✓ / ✓	wt / wt					
178	✓	✓	wt					
180 T / S	✓ / ✗	✓ / ✗	wt / —					
184	✗	✗	—					
187	✗	✗	—					
191 a / b	✗ / ✗	✗ / ✗	— / —					
193	✗	✗	—					
194 T / S	✓ / ✓	✓ / ✓	wt / wt					
196	✗	✗	—					
197 T / S	✓ / ✓	✓ / ✓	wt / wt					
198 T / S	✓ / ✓	✓ / ✓	wt / wt					
199	✓	✓	**K**	**2.43**	**?**	**prob. K 2.9**		
202 T / S	✓ / ✓	✓ / ✓	**E** / wt	**1.93**	wt / wt			
T: 95	**T (95): 62 ✓, 33 ✗**	**T (95): 61 ✓, 34 ✗**	**T (61): 48 wt / 3 E / 10 K**					
S: 51	**S (51): 41 ✓, 10 ✗**	**S (51): 39 ✓, 12 ✗**	**S (39): 37 wt / 2 E**					

A total of 100 DNA samples (61 from tumor area and 39 from surrounding area) were analyzed using AS PCR. The percentage of mutations detected in the tumor area was clearly higher (21%, 13 out of 61 samples analyzed) than in the surrounding area (5%, 2 out of 39). Histopathological reinvestigation of the 2 samples, from which one carried a *BRAF* V600E mutation in the LMM surrounding area, revealed a small melanocytic nevus in the surrounding area. This could easily explain why in that case *BRAF* was found mutated in the DNA of the surrounding area but not in the tumor area.

All samples tested positive for a *BRAF* V600 mutation using AS PCR were re-analyzed with pyrosequencing. In the DNA of the tumor area four *BRAF* V600K mutations were confirmed (LMM13 T, LMM22 T, LMM83 T, and LMM110 T), four *BRAF* V600K mutations were detected as potential low level mutations with uncertain type of mutation (not clear whether *BRAF* V600E or *BRAF* V600K; LMM6 T, LMM135 T, LMM173 T, and LMM199) and five mutations (two *BRAF* V600K and three *BRAF* V600E) could not be detected (LMM64 T, LMM90 T, LMM152, LMM158, and LMM202), most probably due to the lower sensitivity of the assay. One of the two *BRAF* V600E mutations in the DNA of the surrounding area was detected by pyrosequencing as potential low level mutations with uncertain type of mutation (LMM150 S), the other one could not be detected (LMM166 S). As a control 16 DNA samples classified as wt (from the tumor area as well as from the surrounding area) were also re-analyzed using pyrosequencing and the concordance of results from AS PCR and pyrosequencing was 100%. An additional pyrosequencing analysis was done

from gDNA to rule out false positive results caused by pre-amplification and to confirm results for mutated samples. Pyrosequencing results from pre-amplification products were highly concordant to those using gDNA as template. The six samples classified as wt using pre-amplification products showed 100% concordance when using gDNA (LMM58, LMM75 T/S, LMM116 T/S, and LMM150 T). Two *BRAF* V600 mutations detected with AS PCR could be classified as potential low level mutations with uncertain type of mutation (LMM22 T and LMM150 S) using gDNA as template.

The occurrence of the *BRAF* V600 mutations in the collective is summarized in Figure 31. The incidence of the *BRAF* V600K mutation was significantly higher in the DNA from tumor area compared to DNA from the surrounding area (*P*=0.013). In addition, a direct association between the degree of pigmentation and the mutation frequency for *BRAF* V600K in the DNA from the tumor area was observed (Table 7).

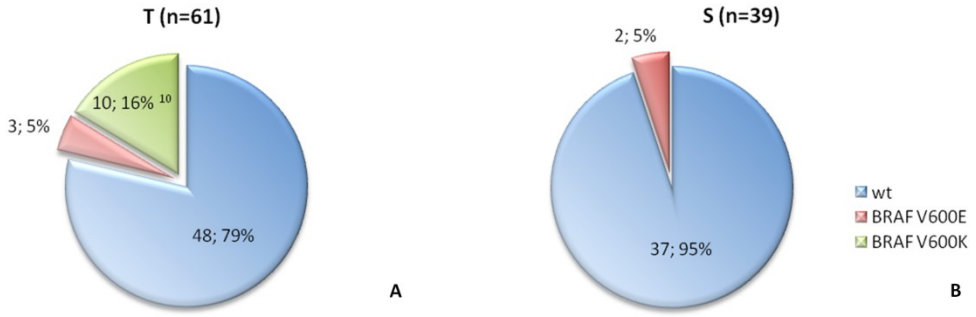

Figure 31: Frequency of the *BRAF* V600 mutations in the collective.

In 3 (5%) of the 61 analyzed samples from the tumor area a *BRAF* V600E was detected in comparison to 10 samples (16%) were a *BRAF* V600K mutation could be found. Taken together, in 21% of the DNA samples from the tumor area a *BRAF* V600 mutation was detected. In the samples from the surrounding area, on the contrary, 95% of the samples were classified as wt and only 2 samples (5%) were found to carry the *BRAF* V600E mutation, whereas in one of the two cases a melanocytic nevus was present. The *BRAF* V600K mutation was not detected at all in the DNA of the surrounding tissue. The occurrence of the *BRAF* V600K mutation was significantly higher in DNA from tumor area compared to DNA from surrounding area (*P*=0.013) [10].

Table 7: Patient characteristics and mutation frequencies.

	wt	*BRAF* V600E	*BRAF* V600K	Total
Age	**76.80 ± 12.05 (n=48)**	**71.77 ± 17.57 (n=3)**	**69.59 ± 10.42 (n=10)**	**75.37 ± 12.18 (n=61)**
male	76.41 ± 10.33 (n=19)	51.52 ± 0.00 (n=1)	65.16 ± 9.05 (n=5)	**73.16 ± 11.61 (n=25)**
female	77.06 ± 13.24 (n=29)	81.90 ± 1.43 (n=2)	74.01 ± 10.65 (n=5)	**76.91 ± 12.48 (n=36)**
Melanoma, LM type (n)				
in situ	46	3	10	**59**
invasive	2			**2**
Sun damage (n)				
CSD	47	3	10	**60**
nonCSD	1			**1**
Pigmentation (n)				
0	2 (100%)			**2**
+	18 (86%)	1 (5%)	2 (9%)	**21**
++	25 (76%)	2 (6%)	6 (18%)	**33**
+++	3 (60%)		2 (40%)	**5**

[10] A comparison of the frequency of the *BRAF* V600K mutation between the DNA from tumor area and surrounding area. Fisher's exact test was used.

5 Discussion

The *BRAF* mutation is gaining more and more importance in the context of MM. It is the most frequently found mutation in MM (in more than 50% of primary melanomas; (Goel et al. 2006)) and it is thought to be an early event in the progression of MM. More recently, studies proved the efficacy of targeted therapies against the mutated form of the BRAF protein in patients with metastatic malignant melanoma; e.g., (Sosman et al. 2012). Only little information is available on the occurrence of *BRAF* V600 mutations in LMM, a subtype of MM. Therefore, we analyzed the prevalence of mutations in codon 600 of the *BRAF* gene in a large cohort of LMM patient samples.

LMM is the most frequent malignant melanoma found in the face (Cohen 1995). The histology of LMM is characterized by atypical melanocytes which are present as single cells or small nests within the dermis. This fact complicates molecular characterization of LMM since tumor cells are found at low percentage within the lesion, requiring highly sensitive methods for mutational analysis.

The objectives of our study were (1) the establishment, optimization, and validation of a highly sensitive method for the detection of *BRAF* V600 mutations in FFPE samples, (2) the analysis of a large, well characterized collective of LMM samples, and (3) the statistical evaluation and interpretation of our results in the context of existing literature.

To our knowledge, this is the first study to analyze the occurrence of the *BRAF* V600E as well as the *BRAF* V600K mutation in a large cohort of well characterized LMM patient samples. In addition, a direct comparison of the occurrence of the *BRAF* mutations between DNA from tumor area and DNA from surrounding area was done.

COLD PCR

One method focusing on the enrichment of low abundance mutations was presented in 2008 by the group of Li, Milbury and Makrigiorgos: They developed an elegant and sophisticated method which, in combination with downstream detection methods like pyrosequencing, allows the detection of low level mutations present in a background of wt DNA (Li et al. 2008). They called their method COLD PCR and demonstrated its usefulness for the detection of mutations found in *KRAS*, *TP53*, and *EGFR*. COLD PCR can replace conventional PCR or real-time PCR used for amplification of gDNA prior to Sanger sequencing and pyrosequencing (Li, Makrigiorgos 2009, Li et al. 2009) or HRMA (Milbury, Li & Makrigiorgos 2009). In their studies the authors found a lower enrichment of mutations carrying a T>A transition compared to C>T exchanges. Nevertheless,

they specified a 5-8 fold increase in sensitivity for mutations retaining the T_m (T>A, C>G) using full COLD PCR (Li et al. 2008).

Being aware of the low tumor cell count in our samples, we thought that this method may be the ideal investigation tool for our purpose and study. Therefore, we tried to adapt COLD PCR for the detection of *BRAF* V600 mutations.

Apparently, temperature profile during COLD amplification favors the formation of primer dimers and considerable effort was necessary to circumvent their formation. In order to amplify a specific PCR product it was necessary to denature primers prior to preparing the master mix and to perform the whole reaction set-up on ice. Although various parameters have been tested (numerous primer pairs, varying $MgCl_2$ and primer concentrations, different hybridization temperatures and critical denaturation temperatures), we retained the same sensitivity of 4% mt DNA in a background of wt DNA using COLD PCR as using our conventional HRMA assay (real-time PCR with subsequent HRMA) established at that time. We also tried to reproduce the authors' results published for the detection of the *TP53* mutation applying COLD PCR in combination with HRMA (Milbury, Li & Makrigiorgos 2009). Using our instrumentation and chemistry, we were not able to increase the sensitivity of the TP53 assay by the application of COLD PCR (Figure 16) compared to the conventional HRMA assay. Therefore, we tested the BRAF assay using the same chemicals as indicated by the authors. Once again, we did not succeed in increasing the sensitivity of our assay.

Our results for adapting COLD PCR for the detection of *BRAF* V600 mutations are in concordance with the data published by Fadhil et al. who also failed to improve the sensitivity of their assay by applying COLD protocols (Fadhil et al. 2010). The authors Mancini et al. on the contrary, were able to increase the sensitivity of their BRAF HRMA assay from a LOD of 12.5% to 6.2% (Mancini et al. 2010). Their sensitivity of 6.2% using COLD PCR is, however, lower than our established sensitivity of 4% using the conventional BRAF HRMA assay. The very complex nature of COLD PCR (multiple parameters that have to be optimized, like temperatures and concentrations) and the fact that one full COLD PCR run takes approximately 6 hours makes COLD PCR a sophisticated method with a limited daily use applicability. Recently, a new application of COLD PCR has been presented by Kristensen et al. (Kristensen et al. 2012). They combined a mutation specific PCR with COLD PCR. A procedure leading to enhanced sensitivity, limiting the potential of mispriming, and allowing the reliable detection of T_m-retaining mutations at the same time. Probably, this approach facilitates the use and adaption of COLD PCR to new target genes.

Unfortunately, in our hands no improvement of sensitivity could be achieved using the COLD protocol prior to HRMA (Figure 17 and Figure 19). Whether the cause was in the instrumentation or in the properties of the sequence to analyze itself is not clear. The chemistry, however, could be ruled out. Thus, we concentrated on other methods, namely conventional HRMA PCR (without COLD PCR), AS PCR and pyrosequencing.

HRMA PCR

The HRMA assay (real time PCR with subsequent HRMA) developed in the course of this study is a new, refined, and adapted protocol of the assay described earlier by our group (Pichler et al. 2009) which now allows the detection of the *BRAF* V600E, as well as of the *BRAF* V600K mutation. The indisputable advantage of HRMA PCR is its easy-to-handle, closed-tube, and cost-effective nature. Our attempt to increase the sensitivity of HRMA PCR by the use of a COLD protocol prior to HRMA failed, as discussed above. Therefore, we used conventional HRMA from now on, only. The LOD of 4% mt DNA in a background of wt DNA of HRMA PCR is comparable to the one of pyrosequencing, whereas the latter has the advantage of providing sequence information of the analyzed samples. As a consequence, HRMA PCR was used for method-comparison in the TS, only, but not for verification of results of the collective.

AS PCR

AS PCR proved to be the method with the highest sensitivity and it was even higher than initially demonstrated by Jarry et al. (Jarry et al. 2004). The LOD was 0.1% mt DNA in a background of wt DNA. The assay proved to have a broad linear dynamic range of at least 3 logs, ranging from 2×10^4 copies to 2×10^1 copies for wt alleles and the *BRAF* V600E mutation, and from 1×10^4 copies to 1×10^1 copies for the *BRAF* V600K mutation. Besides the advantage of the high sensitivity this method also has its drawbacks: Every mutation detected by the assay requires a new, mutation specific primer and has to be validated. In addition, especially in *BRAF*, there is the possibility of cross-reactivity; for example a *BRAF* V600E (c.1799T>A) specific primer may bind to a template carrying the *BRAF* V600K mutation (c.1798_1799GT>AA). The *BRAF* V600K mutation found in NM4 of the learning set was first detected by a cross-reaction of the AS PCR assay for the *BRAF* V600E mutation. This illustrates the second drawback: This type of assay does not provide any sequence information. Thus, samples giving inconclusive results in AS PCR (e.g., the repeatedly detection of minute levels of mutations near the background signal), may indicate a cross-reaction and have to be analyzed with another method, ideally providing sequence information.

Pyrosequencing

Pyrosequencing in its present form was first described in 1998 (Ronaghi, Uhlen & Nyren 1998). It is a fast, reliable and quite sensitive method. In the course of this study 3 different pyrosequencing-assays were designed for the detection of *BRAF* V600 mutations (BRAF PM1, BRAF PM2, and BRAF PM3). BRAF PM3 allows the detection of the *BRAF* V600E as well as the *BRAF* V600K mutation with a LOD of 5.0% and 2.5%, respectively. The PyroMark Q24 software does not support the quantification of complex mutations like the *BRAF* V600K. Therefore, an excel-based semi-automatic procedure was developed for the quantification of the *BRAF* V600K mutation (with consultation of Dr. Narz; QIAGEN, Hilden, Germany). Results from the establishing process with the MS showed an excellent classification and quantification of both mutations (*BRAF* V600E as well as *BRAF* V600K) for DNA blends containing > 5% mt DNA. Blends with ≤ 5% mt DNA were often classified as samples carrying a mutation of an uncertain type (*BRAF* V600E or *BRAF* V600K) or the mutation could not be detected (especially ≤ 2.5%; data not shown).

Pyrosequencing offers unprecedented possibilities and is becoming more and more popular for mutation analysis and for some applications it might even displace Sanger sequencing as the gold standard (Spittle et al. 2007, Tsiatis et al. 2010). Nevertheless, it is up to the investigator to interpret minute deviations in the pyrograms to best exploit the strength of this sequence-based method – its sensitivity.

Learning Set

At the beginning of the study we planned to determine the frequency of the *BRAF* V600E mutation, only. The actual purpose of the learning set was to test the applicability of the assays on FFPE tissue DNA. Discrepant results of HRMA PCR, AS PCR, and pyrosequencing for NM4 (wt, a pretended low level *BRAF* V600E < 1%, and an abundantly 'clear' *BRAF* V600E mutation, respectively) awakened our interest in the *BRAF* V600K mutation. This mutation shares the same nucleotide exchange on position 1799 (T>A) and thus can easily be misinterpreted. The analysis of NM4 with redesigned assays, suitable for the detection of both mutations, confirmed the presence of a prominent V600K mutation (Figure 22 and Figure 24). Thus, the initially low level mutation detected with AS PCR was caused by a cross-reaction, whereas the pyrosequencing assay was unable to distinguish between V600E and V600K mutation. Why no altered melting behavior was detected using HRMA PCR is not clear (Figure 21A).

NM5 showed the importance of checking the DNA quality, especially when working with DNA from FFPE tissue samples. Several authors addressed this concern, but nevertheless it is not necessarily routine (Deichmann et al. 2006, van Beers et al. 2006, van Dongen et al. 2003). The

inconsistent data from NM5 could be interpreted, when the integrity assay showed considerable fragmentation of the DNA (Figure 32). Highly degraded DNA favors the formation of artifacts and increases the probability of synthesis errors of the polymerase during amplification. For this reason results of NM5 were not reliable and the sample was excluded from further analysis.

The initial purpose of the LS to test the applicability of the assays on FFPE derived DNA moved into the background, since the results of the LS led to the development of new assays allowing the simultaneous detection of the *BRAF* V600E and V600K mutation. Thus, an additional focus was added to the study: the *BRAF* V600K mutation.

Results of the LS were unexpected; not the frequency of the *BRAF* V600 mutation (2/5 NM carried a *BRAF* V600 mutation), but rather the occurrence of a *BRAF* V600K mutation in this small sample set. Akslen et al. analyzed 51 cases of NM in their study and found 13 to carry the *BRAF* V600E mutation (25.5%) and 2 to carry the *BRAF* V600K mutation (4%) (Akslen et al. 2005). Current data from the COSMIC database indicates that among all the mutations found in codon 600 of the *BRAF* gene, the *BRAF* V600K mutation accounts for 13% of these mutations found in tissue from NM (Sanger Institute Catalogue Of Somatic Mutations In Cancer). In general, the incidence of the *BRAF* V600K mutation in malignant melanoma is rather low with 6% (Figure 5). Therefore, we did not expect to find any other mutations in codon 600 than the *BRAF* V600E.

In summary, the LS not only fulfilled, but went beyond its purpose. It was thought to be a quick test for the applicability of the assays on FFPE derived DNA, but it turned out to be really informative and led to essential improvements of the project.

Training Set

The small tissue volume of the TS samples and as a consequence the modest DNA yield made a pre-amplification step necessary. Primers for the pre-amplification were chosen considering the pseudogene and the downstream applications, i.e. HRMA PCR, AS PCR and pyrosequencing. Some types of tissue samples, especially when limited in size, require pre-amplification, nested PCR, or multiplex PCR. Several other groups who worked with melanoma samples used these methods to overcome limited amounts of DNA because of, as mentioned above, small tissue volume or dissection of tissue (Edlundh-Rose et al. 2006, Poynter et al. 2006, Houben et al. 2004, Omholt et al. 2003). Unfortunately, primers described in their publications did not span the region around codon 600 of the *BRAF* gene that would have been necessary to allow mutation analysis with the assays developed within this project. Primers used in a study published by Willmore-Payne amplified a product of 250 bp length (Willmore-Payne et al. 2005). These primers were originally designed for HRMA PCR, but adapted to our work, they were used as primers for pre-

amplification, and permitted the application of all of our three assays. Importantly, thorough testing showed, that pre-amplification had no adverse effects on the sensitivity of the assays.

In addition to the pre-amplification step, the assay for determining DNA quality had to be modified. DNA quality assays that amplify highly repetitive DNA sequences like ALU or LINE have mostly been used in the context of circulating DNA from serum (Sunami et al. 2008, Umetani et al. 2006). For this study, the repetitive sequence assay represented the ideal alternative to single-copy-gene assays, because of the limited DNA amount available for analysis. Amplification of a 149 bp and a 249 bp LINE fragment clearly illustrated the moderate quality of FFPE sample derived DNA demonstrated by poorer amplification of the longer fragment. The mean percentage of amplifiable DNA in the TS was 15% ± 8 and 3% ± 3 for the 149 bp and the 249 bp product, respectively (Figure 37). Thus, the amplifiability of the 149 bp product was more than 4-fold higher than the one of the 249 bp product. Based on this data, the length of the pre-amplification product was shortened from 250 bp to 152 bp.

Despite the shorter pre-amplification product, several samples of the TS showed weak or no amplification based on the agarose gel after pre-amplification PCR. Melanin has been identified as potent inhibitor of DNA polymerases (Eckhart et al. 2000) and several authors add BSA to PCR reactions in order to reduce negative effects of melanin, when working with melanin-containing samples (Edlundh-Rose et al. 2006, Cruz et al. 2003, Kusters-Vandevelde et al. 2009). Melanin not only reversibly binds the DNA polymerase, but also reduces freely available Mg^{2+} ions in the PCR reaction (Pötsch, Bender 2001). The combination of adding 0.2 µg/µl BSA and increasing final $MgCl_2$ concentration from 1.5 mM to 4.5 mM led to an average 4-fold increase in the yield of PCR products (Figure 35). In general, DNA from the surrounding area seemed to be amplified easier and to a higher extent, than DNA from the tumor area.

Modifications made in the course of the analysis of the TS were a prerequisite for the analysis of the collective. The TS allowed the thorough evaluation of samples and methods. The minimal quality and quantity requirements were defined as a product of DNA quantity used for the pre-amplification and percentage of amplifiable DNA as defined by the surrogate parameter LINE 149bp. Samples had to have at least 1 ng amplifiable DNA in the pre-amplification reaction to allow the detection of up to 1% mt DNA in the background of wt DNA (for details refer to 7.2.9). From the 21 tumor DNA samples 24% (5 samples) did not fulfill this criterion. Four samples (19%) from the remaining 16 samples did not give any pre-amplification product, despite all of supplements added to the reaction. Thus, a total of 12 samples (57% from the initial 21 samples)

could be analyzed. If the length of the pre-amplification product had not been changed from 250 bp to 152 bp, the majority of 86% (18/21 samples) would have failed quality requirements.

All, except one, samples of the TS underwent manual dissection. The necessity of manual dissection was tested in small set of 4 not dissected samples of the TS (LMM12, LMM15, LMM20, and LMM21) that were analyzed in parallel to the dissected samples. Although the eschewal of the dissection simplified the DNA isolation and increased the DNA yield, it was not the method of choice for two reasons: (1) it would have been impossible to compare mutation frequencies between DNA from tumor area and surrounding area, and (2) the volume of the tissue samples was very variable, thus manual dissection made samples, with respect to tumor cell count, more comparable. As expected and demonstrated by sample LMM21, the dissected sample (LMM21 T) showed a higher percentage of mutated DNA than the sample without dissection (LMM21; Table 5). The increase in mutated DNA found in the dissected sample was most probably due to the enrichment of tumor cells and the omittance of non tumor tissue, respectively, thus reducing the wt background. Unexpectedly, LMM20 carried a mutation in the sample without dissection, but not in the dissected one. One reason for this discrepancy could be the process of DNA isolation. Sections of the FFPE tissue blocks were first prepared for the DNA where the samples had been dissected. Subsequently, sections for the DNA isolation without dissection were cut, because the question of comparing DNA from dissected vs. not dissected samples evolved at a later time point. Therefore, the sections for the two DNA preparations originated from different depths of the tissue block and therefore might contain different amounts of tumor cells.

Even though the sample size of the TS was limited, the results of mutation analysis were informative. None of the two *BRAF* mutations was found in the DNA of the surrounding area, whereas DNA from the tumor area of one sample was positive for the *BRAF* V600E and one for the *BRAF* V600K mutation. Thus, *BRAF* V600 mutations were exclusively found in 17% of the samples from the tumor area. In addition, the percentages of mutated DNA within these samples were rather low (< 5%), making a sensitive method a prerequisite for their detection. Table 5 reflects results of the comparison of the 3 methods established within this study. Only AS PCR is able to detect low abundance mutations in both samples (LMM1 T and LMM21 T), whereas HRMA PCR and pyrosequencing were able to detect the more prominent mutation in LMM21 T, only.

Besides the substantial additional gain of information the TS provided, the TS served its primary purpose: The analysis of the TS demonstrated the necessity of a highly sensitive method, since the percentages of mt DNA within the samples were rather low. Therefore, AS PCR was the method of choice for the analysis of the collective. Results of the comparison of DNA from tumor area and

surrounding area demonstrated the absence of *BRAF* V600 mutations in the skin adjacent to the lesion in this limited set of samples. The conclusions drawn from the TS with respect to the analysis of the collective were: (1) manual dissection of the samples is essential; (2) AS PCR is the only method that is able to detect low level mutations; (3) pyrosequencing is used for verification of mutations found in samples of the collective since it is as sensitive as HRMA PCR, but in addition, provides sequence information.

Collective

Tissue volume in the samples of the collective varied considerably and thus, manual dissection proved to be a valuable tool to make samples more comparable with respect to tumor cell count. Microscopic evaluation of the HE stained sections showed, that tumor cell count was sometimes insufficient for further analysis. Therefore, more than one third of the samples were excluded from further analysis. Pre-amplification turned out to be necessary since DNA quantity would not have allowed direct analysis of gDNA.

In order to decrease the drop out probability of the remaining samples, another clean up step was introduced prior to pre-amplification. In their study Dörrie et al. discussed the adverse effects of melanin in nucleic acids and how to purify nucleic acid solutions from samples containing melanin (Dorrie et al. 2006). The additional purification of DNA samples from the collective led to a decrease in drop-out, mainly due to a better pre-amplification (Figure 30).

The limiting criterion for sensitivity in mutation analysis proved to be the DNA and not the assay. Although LOD of the AS PCR was 0.1%, mutations in the samples were detected only down to 0.5%. Thus, in the described study set-up the quality of the DNA, and not the analysis method limited the sensitivity. The necessity of sensitivity and dissection was supported by the low abundance mutations found in the samples. All mutations detected were present at < 5% in the sample DNA.

Mutation analysis of the collective substantiated the data from the TS. Comparable to the TS, mutations were predominantly detected in DNA from tumor area, especially the *BRAF* V600K mutation, which was detected exclusively in this area. Taken together, a *BRAF* V600 mutation was detected in 21% of DNA samples from tumor area and in 5% of DNA samples from surrounding area. Thus, the frequency of *BRAF* V600 mutation is substantially higher in DNA from tumor area, especially when taking into account that one sample with a *BRAF* V600 mutation in DNA from surrounding area, revealed a melanocytic nevus adjacent to the melanoma *in situ*. Benign nevi are known to frequently harbor *BRAF* V600 mutations. In some studies the *BRAF* V600E mutation was found in up to 80% of the nevi (Poynter et al. 2006, Ichii-Nakato et al. 2006, Pollock et al. 2003,

Taube et al. 2009, Uribe, Wistuba & Gonzalez 2003). In general, the *BRAF* V600E mutation seems to play an important role in nevi development. In their study Patton et al. demonstrated the effect of activated $BRAF^{V600E}$ by generating transgenic zebrafishes (Patton et al. 2005). The expression of mutated $BRAF^{V600E}$ led to the formation of distinct pigmentation with no evidence of tissue invasion. Activated $BRAF^{V600E}$ in the presence of germline *p53* mutation, however, led to the formation of invasive melanomas. This finding supports the hypothesis that *BRAF* mutation is an early event in melanoma development, but this mutation alone will not cause melanoma. To our knowledge, until now the *BRAF* V600K mutation, on the contrary, has never been detected in benign nevi.

Generally, the *BRAF* V600K mutation has been rarely described in literature, but is gaining more and more attention recently (Willmore-Payne et al. 2005, Halait et al. 2012, Rubinstein et al. 2010). Probably, the prevalence of the *BRAF* V600K mutation has been underestimated in the past because of cross reactivity with *BRAF* V600E specific assays and the previous focus on the *BRAF* V600E mutation (Rubinstein et al. 2010). Cross-reactivity per se is critical in *BRAF* since 7 different mutations have been described for codon 600, 3 of them with a T>A exchange at nucleotide position 1799. The authors Anderson and Halait presented a new, FDA approved, PCR based method primarily for the detection of the *BRAF* V600E mutation in melanoma patients (Halait et al. 2012, Anderson et al. 2012). They broached the issue cross-reactivity in their manuscript, too. The AS PCR assays for the *BRAF* V600E and the *BRAF* V600K mutation described in their study showed cross-reactivity with *BRAF* V600K of 0.4% and *BRAF* V600E of 0.1%, respectively. No cross-reactivity was observed between the mutation specific assays and *BRAF* wt DNA. Furthermore, no cross-reactivity was determined for the other *BRAF* V600 mutations like: *BRAF* V600E complex (c.1799_1800TG>AA), *BRAF* V600R (c.1798_1799GT>AG), *BRAF* V600D (c.1799_1800TG>AT), *BRAF* V600M (c.1798G>A), and *BRAF* V600G (c.1799T>G).

This demonstrates the predicament between sensitivity and selectivity of assays for mutation analysis. AS PCR was the assay most suitable for the analysis of the samples. While it provides the necessary sensitivity, there is the disadvantage of eventually missing rare mutations like the ones indicated above or detecting cross-reactivity. Unfortunately, Sanger sequencing as well as pyrosequencing are not sensitive enough to detect the low level mutations found in this collective, but would provide sequence information. In their work Lassacher et al. and Pollock et al. demonstrated the value of a sensitive method for mutation detection (Pollock et al. 2003, Lassacher et al. 2006) in lesions of the skin. Both groups showed several cases where the mutation was detected by the more sensitive method, only.

In general, results of the study at hand are interesting but unexpected. On average, 90% of melanomas show a constitutive activation of ERK which is downstream of NRAS and BRAF in the MAPK pathway (Figure 3, (Cohen et al. 2002)). While *NRAS* mutations are found in 15-30% of melanomas, *BRAF* mutations can be detected in 50-70% (Gray-Schopfer, Wellbrock & Marais 2007). *BRAF* and *NRAS* mutations seem to be mutually exclusive, only rare exceptions have been described (Edlundh-Rose et al. 2006, Omholt et al. 2003). The *BRAF* V600E mutation accounts for more than 90% within the *BRAF* V600 mutations found in malignant melanoma. Data for the presence and frequency of *BRAF* mutations in LMM is controversial. Taking into account, that different methods were used for sample preparation like manual or laser capture microdissection and for mutation analysis like Sanger sequencing or allele specific PCR, the divergent results in literature can easily be explained. What has been repeatedly demonstrated is that *BRAF* mutations are more frequent in MM lesions of nonCSD skin compared to CSD skin (Maldonado et al. 2003, Platz et al. 2008). This is consistent with the results of our study finding *BRAF* mutated in a relatively low portion of the LMM lesions examined, most of them located on CSD skin.

Our results demonstrate the presence of *BRAF* V600 mutations in LMM, with the majority of mutations being low abundance *BRAF* V600K mutations (10/13, 76.9%). The *BRAF* V600K mutation was exclusively found in DNA from tumor area and not in DNA from surrounding area. One can speculate if the different type of mutation (V600K and not V600E) found in LMM results from a divergent progression of the lesion and it would be interesting, if the *BRAF* V600K mutation is generally more likely to occur on CSD skin than the *BRAF* V600E mutation. Due to the aforementioned reasons it is complicated to put data from this study in context to nowadays available literature. Nevertheless, it is noteworthy that Akslen et al. found 15% of their LMM samples to carry a *BRAF* mutation, whereas none of the detected mutation was a *BRAF* V600E mutation, but a V600K, L597L, and an E586K mutation (Akslen et al. 2008). There might be a correlation between the slow progression of LMM, its preferential occurrence on CSD skin in elderly persons, and the increased presence of the *BRAF* V600K mutation. Maybe the role of UV induced DNA damage has to be reconsidered for LMM. It is also noticeable, that in our study the occurrence of the *BRAF* V600K mutation is directly correlated to the degree of pigmentation. A similar association has been described for KIT alterations and hyperpigmentation (Wu et al. 2009).

Currently, no conclusions can be drawn for the usefulness of the *BRAF* V600 mutation for discriminating LMM from SL or PAK. Two studies that analyzed SL and actinic keratosis proved the absence of the *BRAF* V600E mutation by using AS PCR for detection (Hafner et al. 2009, Zaravinos et al. 2009). Unfortunately, from their studies no data is available on the *BRAF* V600K mutation. Due to the moderate occurrence of the *BRAF* V600K mutation in LMM (*BRAF* V600K mutation was

found in 16% of DNA from tumor area) in our study, this mutation does not seem to play a solely, essential role in the development of LMM and therefore most likely will not be of major help for diagnostic differentiation of SL or PAK from LMM. However, the knowledge of the predominant existence of the *BRAF* V600K mutation in a subset of MM lesions may contribute to the better understanding of the underlying mechanisms in melanoma development.

6 Conclusion

The objective of the study at hand was the analysis of a large, well characterized sample set of LMM with a highly sensitive method. During the course of the project, three PCR based assays for mutation analysis (namely HRMA PCR, AS PCR and pyrosequencing) were established, optimized and tested for their applicability and suitability. Due to its unexcelled LOD of 0.1%, AS PCR proved to be the method of choice. The low abundance mutations found in the FFPE samples (<5% mt DNA in a background of wt DNA) not only proved the necessity of a highly sensitive method, but also emphasized the importance of manual dissection and quality requirements applied in this study.

While, based on the data available from literature, we concentrated on the detection of the *BRAF* V600E mutation at the beginning, it turned out that the *BRAF* V600K mutation should be taken into account, too. 163 FFPE tissue blocks were identified through the database search and retrieved from the archive of the Department of Dermatology, Medical University of Graz. DNA from only 37% of the samples (61 cases) fulfilled the requirements to allow a reliable mutation analysis, where at least 1% mt DNA in a background of wt DNA can be detected. This demonstrates the necessity of careful and thorough sample preparation, archiving and analysis. If the quality requirements had not been applied, the samples size would have been larger, but the overall percentage of samples carrying a mutation would be much lower, because low level mutations most likely would have been lost.

The *BRAF* V600K mutation was found exclusively in the DNA from tumor area (16%, 10/61). *BRAF* V600E mutation was found to a significant smaller extend in the tumor area (5%, 3/61) and in the DNA of the surrounding area (5%; 2/39). All mutations found in this sample set were low-abundance mutations and more information is necessary to determine the clinical significance of low level mutations. In addition, the *BRAF* V600K might have been underestimated in its frequency in the past, because most studies concentrated on the *BRAF* V600E mutation. New and refined technologies offer the opportunity to take a closer look on rare and low-abundance mutations like the *BRAF* V600K mutation.

Taken together, the relatively low portion of LMM lesions we found mutated at the *BRAF* gene indicates that *BRAF* mutation plays a role at best in a subset of LMM lesions. At this time point no conclusion can be drawn if there is any correlation between the presence of a *BRAF* mutation in a LMM *in situ* and the probability of its progression to an invasive form. The samples were retrieved from patients who had their primary tumor excision between 2007 and 2009 and the time period

elapsed by now is simply too short to make any long-term analysis on the impact of *BRAF* mutation on tumor progression.

To better understand the nature of melanoma progression and to define an improved classification system, more information is necessary from well characterized sample sets. It might be a coincidence, but it is striking that the *BRAF* V600K mutation, which is found only rarely in MM in general, was more frequent in LMM. This subtype of MM is the only one occurring nearly exclusively on CSD skin and has an unusual slow progression compared to NM, SSM, or ALM.

In MM several other genes besides *BRAF* have been identified to harbor alterations like *KIT*, *NRAS*, or *PTEN* (reviewed in, e.g., (Ko, Fisher 2011, Kong, Kumar & Xu 2010)). None of the aforementioned molecules reaches the significance *BRAF* has attained over the last few years in MM. Nevertheless, for the basic understanding more information is necessary about cumulating alterations besides *BRAF*. Therefore, more in-depth studies are warranted to determine possible alterations of second molecules, like *NRAS* or *PTEN* in the collective of this study.

7 Appendices

7.1 Appendix A – Bibliography

Akslen, L.A., Angelini, S., Straume, O., Bachmann, I.M., Molven, A., Hemminki, K. & Kumar, R. 2005, "BRAF and NRAS mutations are frequent in nodular melanoma but are not associated with tumor cell proliferation or patient survival", *J Invest Dermatol,* vol. 125, no. 2, pp. 312-317.

Akslen, L.A., Puntervoll, H., Bachmann, I.M., Straume, O., Vuhahula, E., Kumar, R. & Molven, A. 2008, "Mutation analysis of the EGFR-NRAS-BRAF pathway in melanomas from black Africans and other subgroups of cutaneous melanoma", *Melanoma Res,* vol. 18, no. 1, pp. 29-35.

Alsina, J., Gorsk, D.H., Germino, F.J., Shih, W., Lu, S.E., Zhang, Z.G., Yang, J.M., Hait, W.N. & Goydos, J.S. 2003, "Detection of mutations in the mitogen-activated protein kinase pathway in human melanoma", *Clin Cancer Res,* vol. 9, no. 17, pp. 6419-6425.

Anderson, S., Bloom, K.J., Vallera, D.U., Rueschoff, J., Meldrum, C., Schilling, R., Kovach, B., Lee, J.R., Ochoa, P., Langland, R., Halait, H., Lawrence, H.J. & Dugan, M.C. 2012, "Multisite Analytic Performance Studies of a Real-Time Polymerase Chain Reaction Assay for the Detection of BRAF V600E Mutations in Formalin-Fixed Paraffin-Embedded Tissue Specimens of Malignant Melanoma", *Archives of Pathology & Laboratory Medicine,* .

Arkenau, H.T., Kefford, R. & Long, G.V. 2011, "Targeting BRAF for patients with melanoma", *British journal of cancer,* vol. 104, no. 3, pp. 392-398.

Avruch, J., Khokhlatchev, A., Kyriakis, J.M., Luo, Z., Tzivion, G., Vavvas, D. & Zhang, X.F. 2001, "Ras activation of the Raf kinase: tyrosine kinase recruitment of the MAP kinase cascade", *Recent progress in hormone research,* vol. 56, pp. 127-155.

Broekaert, S.M., Roy, R., Okamoto, I., van den Oord, J., Bauer, J., Garbe, C., Barnhill, R.L., Busam, K.J., Cochran, A.J., Cook, M.G., Elder, D.E., McCarthy, S.W., Mihm, M.C., Schadendorf, D., Scolyer, R.A., Spatz, A. & Bastian, B.C. 2010, "Genetic and morphologic features for melanoma classification", *Pigment cell & melanoma research,* vol. 23, no. 6, pp. 763-770.

Brummer, T., Martin, P., Herzog, S., Misawa, Y., Daly, R.J. & Reth, M. 2006, "Functional analysis of the regulatory requirements of B-Raf and the B-Raf(V600E) oncoprotein", *Oncogene,* vol. 25, no. 47, pp. 6262-6276.

Bustin, S.A., Benes, V., Garson, J.A., Hellemans, J., Huggett, J., Kubista, M., Mueller, R., Nolan, T., Pfaffl, M.W., Shipley, G.L., Vandesompele, J. & Wittwer, C.T. 2009, "The MIQE guidelines: minimum information for publication of quantitative real-time PCR experiments", *Clinical chemistry,* vol. 55, no. 4, pp. 611-622.

Chudnovsky, Y., Khavari, P.A. & Adams, A.E. 2005, "Melanoma genetics and the development of rational therapeutics", *J Clin Invest,* vol. 115, no. 4, pp. 813-824.

Clark, W.H. (ed) 1979, *Human malignant melanoma*, Grune & Stratton, New York.

Clark, W.H.,Jr, Elder, D.E., Guerry, D.,4th, Epstein, M.N., Greene, M.H. & Van Horn, M. 1984, "A study of tumor progression: the precursor lesions of superficial spreading and nodular melanoma", *Human pathology,* vol. 15, no. 12, pp. 1147-1165.

Clark, W.H.,Jr & Mihm, M.C.,Jr 1969, "Lentigo maligna and lentigo-maligna melanoma", *The American journal of pathology,* vol. 55, no. 1, pp. 39-67.

Cohen, C., Zavala-Pompa, A., Sequeira, J.H., Shoji, M., Sexton, D.G., Cotsonis, G., Cerimele, F., Govindarajan, B., Macaron, N. & Arbiser, J.L. 2002, "Mitogen-actived protein kinase activation is an early event in melanoma progression", *Clinical cancer research : an official journal of the American Association for Cancer Research,* vol. 8, no. 12, pp. 3728-3733.

Cohen, L.M. 1995, "Lentigo maligna and lentigo maligna melanoma", *Journal of the American Academy of Dermatology,* vol. 33, no. 6, pp. 923-36; quiz 937-40.

Cruz, F.,3rd, Rubin, B.P., Wilson, D., Town, A., Schroeder, A., Haley, A., Bainbridge, T., Heinrich, M.C. & Corless, C.L. 2003, "Absence of BRAF and NRAS mutations in uveal melanoma", *Cancer Res,* vol. 63, no. 18, pp. 5761-5766.

Curtin, J.A., Fridlyand, J., Kageshita, T., Patel, H.N., Busam, K.J., Kutzner, H., Cho, K.H., Aiba, S., Brocker, E.B., LeBoit, P.E., Pinkel, D. & Bastian, B.C. 2005, "Distinct sets of genetic alterations in melanoma", *N Engl J Med,* vol. 353, no. 20, pp. 2135-2147.

Dandachi, N. & Wolf, P. 2010, *Detection of the BRAF V600E Mutation in Lentigo Maligna Melanoma Lesions: Potential Diagnostic and Clinical Relevance*, Proposal submitted to the Austrian National Bank.

Davies, H., Bignell, G.R., Cox, C., Stephens, P., Edkins, S., Clegg, S., Teague, J., Woffendin, H., Garnett, M.J., Bottomley, W., Davis, N., Dicks, E., Ewing, R., Floyd, Y., Gray, K., Hall, S., Hawes, R., Hughes, J., Kosmidou, V., Menzies, A., Mould, C., Parker, A., Stevens, C., Watt, S., Hooper, S., Wilson, R., Jayatilake, H., Gusterson, B.A., Cooper, C., Shipley, J., Hargrave, D., Pritchard-Jones, K., Maitland, N., Chenevix-Trench, G., Riggins, G.J., Bigner, D.D., Palmieri, G., Cossu, A., Flanagan, A., Nicholson, A., Ho, J.W., Leung, S.Y., Yuen, S.T., Weber, B.L., Seigler, H.F., Darrow, T.L., Paterson, H., Marais, R., Marshall, C.J., Wooster, R., Stratton, M.R. & Futreal, P.A. 2002, "Mutations of the BRAF gene in human cancer", *Nature,* vol. 417, no. 6892, pp. 949-954.

Davies, M.A., Stemke-Hale, K., Lin, E., Tellez, C., Deng, W., Gopal, Y.N., Woodman, S.E., Calderone, T.C., Ju, Z., Lazar, A.J., Prieto, V.G., Aldape, K., Mills, G.B. & Gershenwald, J.E. 2009, "Integrated Molecular and Clinical Analysis of AKT Activation in Metastatic Melanoma", *Clin Cancer Res,* vol. 15, no. 24, pp. 7538-7546.

Deichmann, M., Krahl, D., Thome, M., Wust, K., Hassanzadeh, J. & Helmke, B. 2006, "The oncogenic B-raf V599E mutation occurs more frequently in melanomas at sun-protected body sites", *Int J Oncol,* vol. 29, no. 1, pp. 139-145.

Deichmann, M., Thome, M., Benner, A. & Naher, H. 2004, "B-raf exon 15 mutations are common in primary melanoma resection specimens but not associated with clinical outcome", *Oncology,* vol. 66, no. 5, pp. 411-419.

Dorrie, J., Wellner, V., Kampgen, E., Schuler, G. & Schaft, N. 2006, "An improved method for RNA isolation and removal of melanin contamination from melanoma tissue: implications for tumor antigen detection and amplification", *Journal of immunological methods,* vol. 313, no. 1-2, pp. 119-128.

Eckhart, L., Bach, J., Ban, J. & Tschachler, E. 2000, "Melanin binds reversibly to thermostable DNA polymerase and inhibits its activity", *Biochemical and biophysical research communications,* vol. 271, no. 3, pp. 726-730.

Edlundh-Rose, E., Egyhazi, S., Omholt, K., Mansson-Brahme, E., Platz, A., Hansson, J. & Lundeberg, J. 2006, "NRAS and BRAF mutations in melanoma tumours in relation to clinical characteristics: a study based on mutation screening by pyrosequencing", *Melanoma Res,* vol. 16, no. 6, pp. 471-478.

Fadhil, W., Ibrahem, S., Seth, R. & Ilyas, M. 2010, "Quick-multiplex-consensus (QMC)-PCR followed by high-resolution melting: a simple and robust method for mutation detection in formalin-fixed paraffin-embedded tissue", *Journal of clinical pathology,* vol. 63, no. 2, pp. 134-140.

Fargnoli, M.C., Pike, K., Pfeiffer, R.M., Tsang, S., Rozenblum, E., Munroe, D.J., Golubeva, Y., Calista, D., Seidenari, S., Massi, D., Carli, P., Bauer, J., Elder, D.E., Bastian, B.C., Peris, K. & Landi, M.T. 2008, "MC1R variants increase risk of melanomas harboring BRAF mutations", *J Invest Dermatol,* vol. 128, no. 10, pp. 2485-2490.

Fecher, L.A., Cummings, S.D., Keefe, M.J. & Alani, R.M. 2007, "Toward a molecular classification of melanoma", *J Clin Oncol,* vol. 25, no. 12, pp. 1606-1620.

Galabova-Kovacs, G., Kolbus, A., Matzen, D., Meissl, K., Piazzolla, D., Rubiolo, C., Steinitz, K. & Baccarini, M. 2006, "ERK and beyond: insights from B-Raf and Raf-1 conditional knockouts", *Cell cycle (Georgetown, Tex.),* vol. 5, no. 14, pp. 1514-1518.

Goel, V.K., Lazar, A.J., Warneke, C.L., Redston, M.S. & Haluska, F.G. 2006, "Examination of mutations in BRAF, NRAS, and PTEN in primary cutaneous melanoma", *J Invest Dermatol,* vol. 126, no. 1, pp. 154-160.

Gorden, A., Osman, I., Gai, W., He, D., Huang, W., Davidson, A., Houghton, A.N., Busam, K. & Polsky, D. 2003, "Analysis of BRAF and N-RAS mutations in metastatic melanoma tissues", *Cancer Res,* vol. 63, no. 14, pp. 3955-3957.

Gray-Schopfer, V., Wellbrock, C. & Marais, R. 2007, "Melanoma biology and new targeted therapy", *Nature,* vol. 445, no. 7130, pp. 851-857.

Hacker, E., Hayward, N.K., Dumenil, T., James, M.R. & Whiteman, D.C. 2010, "The association between MC1R genotype and BRAF mutation status in cutaneous melanoma: findings from an Australian population", *The Journal of investigative dermatology,* vol. 130, no. 1, pp. 241-248.

Hafner, C., Stoehr, R., van Oers, J.M., Zwarthoff, E.C., Hofstaedter, F., Landthaler, M., Hartmann, A. & Vogt, T. 2009, "FGFR3 and PIK3CA mutations are involved in the molecular pathogenesis of solar lentigo", *The British journal of dermatology,* vol. 160, no. 3, pp. 546-551.

Halait, H., Demartin, K., Shah, S., Soviero, S., Langland, R., Cheng, S., Hillman, G., Wu, L. & Lawrence, H.J. 2012, "Analytical performance of a real-time PCR-based assay for V600 mutations in the BRAF gene, used as the companion diagnostic test for the novel BRAF inhibitor vemurafenib in metastatic melanoma", *Diagnostic molecular pathology : the American journal of surgical pathology, part B,* vol. 21, no. 1, pp. 1-8.

Houben, R., Becker, J.C., Kappel, A., Terheyden, P., Brocker, E.B., Goetz, R. & Rapp, U.R. 2004, "Constitutive activation of the Ras-Raf signaling pathway in metastatic melanoma is associated with poor prognosis", *J Carcinog,* vol. 3, no. 1, pp. 6.

Ichii-Nakato, N., Takata, M., Takayanagi, S., Takashima, S., Lin, J., Murata, H., Fujimoto, A., Hatta, N. & Saida, T. 2006, "High frequency of BRAFV600E mutation in acquired nevi and small congenital nevi, but low frequency of mutation in medium-sized congenital nevi", *J Invest Dermatol,* vol. 126, no. 9, pp. 2111-2118.

Inamdar, G.S., Madhunapantula, S.V. & Robertson, G.P. 2010, "Targeting the MAPK pathway in melanoma: why some approaches succeed and other fail", *Biochemical pharmacology,* vol. 80, no. 5, pp. 624-637.

Jarry, A., Masson, D., Cassagnau, E., Parois, S., Laboisse, C. & Denis, M.G. 2004, "Real-time allele-specific amplification for sensitive detection of the BRAF mutation V600E", *Molecular and cellular probes,* vol. 18, no. 5, pp. 349-352.

Jo, Y.S., Huang, S., Kim, Y.J., Lee, I.S., Kim, S.S., Kim, J.R., Oh, T., Moon, Y., An, S., Ro, H.K., Kim, J.M. & Shong, M. 2009, "Diagnostic value of pyrosequencing for the BRAF V600E mutation in ultrasound-guided fine-needle aspiration biopsy samples of thyroid incidentalomas", *Clin Endocrinol (Oxf),* vol. 70, no. 1, pp. 139-144.

Kibbe, W.A. 2007, "OligoCalc: an online oligonucleotide properties calculator", *Nucleic acids research,* vol. 35, no. Web Server issue, pp. W43-6.

Ko, J.M. & Fisher, D.E. 2011, "A new era: melanoma genetics and therapeutics", *The Journal of pathology,* vol. 223, no. 2, pp. 241-250.

Kong, Y., Kumar, S.M. & Xu, X. 2010, "Molecular pathogenesis of sporadic melanoma and melanoma-initiating cells", *Archives of Pathology & Laboratory Medicine,* vol. 134, no. 12, pp. 1740-1749.

Kristensen, L.S., Andersen, G.B., Hager, H. & Hansen, L.L. 2012, "Competitive amplification of differentially melting amplicons (CADMA) enables sensitive and direct detection of all mutation types by high-resolution melting analysis", *Human mutation,* vol. 33, no. 1, pp. 264-271.

Kumar, R., Angelini, S., Czene, K., Sauroja, I., Hahka-Kemppinen, M., Pyrhonen, S. & Hemminki, K. 2003, "BRAF mutations in metastatic melanoma: a possible association with clinical outcome", *Clin Cancer Res,* vol. 9, no. 9, pp. 3362-3368.

Kusters-Vandevelde, H.V., Klaasen, A., Kusters, B., Groenen, P.J., van Engen-van Grunsven, I. A., van Dijk, M.R., Reifenberger, G., Wesseling, P. & Blokx, W.A. 2009, "Activating mutations of the GNAQ gene: a frequent event in primary melanocytic neoplasms of the central nervous system", *Acta Neuropathol,* .

Lassacher, A., Worda, M., Kaddu, S., Heitzer, E., Legat, F., Massone, C., Cerroni, L., Kerl, H., Ananthaswamy, H.N. & Wolf, P. 2006, "T1799A BRAF mutation is common in PUVA lentigines", *J Invest Dermatol,* vol. 126, no. 8, pp. 1915-1917.

Li, J. & Makrigiorgos, G.M. 2009, "COLD-PCR: a new platform for highly improved mutation detection in cancer and genetic testing", *Biochemical Society transactions,* vol. 37, no. Pt 2, pp. 427-432.

Li, J., Milbury, C.A., Li, C. & Makrigiorgos, G.M. 2009, "Two-round coamplification at lower denaturation temperature-PCR (COLD-PCR)-based sanger sequencing identifies a novel spectrum of low-level mutations in lung adenocarcinoma", *Hum Mutat,* vol. 30, no. 11, pp. 1583-1590.

Li, J., Wang, L., Mamon, H., Kulke, M.H., Berbeco, R. & Makrigiorgos, G.M. 2008, "Replacing PCR with COLD-PCR enriches variant DNA sequences and redefines the sensitivity of genetic testing", *Nature medicine,* vol. 14, no. 5, pp. 579-584.

Maldonado, J.L., Fridlyand, J., Patel, H., Jain, A.N., Busam, K., Kageshita, T., Ono, T., Albertson, D.G., Pinkel, D. & Bastian, B.C. 2003, "Determinants of BRAF mutations in primary melanomas", *J Natl Cancer Inst,* vol. 95, no. 24, pp. 1878-1890.

Mancini, I., Santucci, C., Sestini, R., Simi, L., Pratesi, N., Cianchi, F., Valanzano, R., Pinzani, P. & Orlando, C. 2010, "The Use of COLD-PCR and High-Resolution Melting Analysis Improves the Limit of Detection of KRAS and BRAF Mutations in Colorectal Cancer", *The Journal of molecular diagnostics : JMD,* .

McKenna, J.K., Florell, S.R., Goldman, G.D. & Bowen, G.M. 2006, "Lentigo maligna/lentigo maligna melanoma: current state of diagnosis and treatment", *Dermatologic surgery : official publication for American Society for Dermatologic Surgery [et al.],* vol. 32, no. 4, pp. 493-504.

Milbury, C.A., Li, J. & Makrigiorgos, G.M. 2009, "COLD-PCR-enhanced high-resolution melting enables rapid and selective identification of low-level unknown mutations", *Clin Chem,* vol. 55, no. 12, pp. 2130-2143.

Miller, A.J. & Mihm, M.C.,Jr 2006, "Melanoma", *The New England journal of medicine,* vol. 355, no. 1, pp. 51-65.

Moelling, K., Heimann, B., Beimling, P., Rapp, U.R. & Sander, T. 1984, "Serine- and threonine-specific protein kinase activities of purified gag-mil and gag-raf proteins", *Nature,* vol. 312, no. 5994, pp. 558-561.

Omholt, K., Platz, A., Kanter, L., Ringborg, U. & Hansson, J. 2003, "NRAS and BRAF mutations arise early during melanoma pathogenesis and are preserved throughout tumor progression", *Clin Cancer Res,* vol. 9, no. 17, pp. 6483-6488.

Patton, E.E., Widlund, H.R., Kutok, J.L., Kopani, K.R., Amatruda, J.F., Murphey, R.D., Berghmans, S., Mayhall, E.A., Traver, D., Fletcher, C.D., Aster, J.C., Granter, S.R., Look, A.T., Lee, C., Fisher, D.E. & Zon, L.I. 2005, "BRAF mutations are sufficient to promote nevi formation and cooperate with p53 in the genesis of melanoma", *Curr Biol,* vol. 15, no. 3, pp. 249-254.

Pichler, M., Balic, M., Stadelmeyer, E., Ausch, C., Wild, M., Guelly, C., Bauernhofer, T., Samonigg, H., Hoefler, G. & Dandachi, N. 2009, "Evaluation of high-resolution melting analysis as a diagnostic tool to detect the BRAF V600E mutation in colorectal tumors", *The Journal of molecular diagnostics : JMD,* vol. 11, no. 2, pp. 140-147.

Platz, A., Egyhazi, S., Ringborg, U. & Hansson, J. 2008, "Human cutaneous melanoma; a review of NRAS and BRAF mutation frequencies in relation to histogenetic subclass and body site", *Mol Oncol,* vol. 1, no. 4, pp. 395-405.

Pollock, P.M., Harper, U.L., Hansen, K.S., Yudt, L.M., Stark, M., Robbins, C.M., Moses, T.Y., Hostetter, G., Wagner, U., Kakareka, J., Salem, G., Pohida, T., Heenan, P., Duray, P., Kallioniemi, O., Hayward, N.K., Trent, J.M. & Meltzer, P.S. 2003, "High frequency of BRAF mutations in nevi", *Nat Genet,* vol. 33, no. 1, pp. 19-20.

Pötsch, L. & Bender, K. 2001, "Untersuchungen zu möglichen Mechanismen einer PCR-Hemmung in Haarextrakten durch Melanine", *Rechtsmedizin,* vol. 11, no. 2, pp. 42-45.

Poynter, J.N., Elder, J.T., Fullen, D.R., Nair, R.P., Soengas, M.S., Johnson, T.M., Redman, B., Thomas, N.E. & Gruber, S.B. 2006, "BRAF and NRAS mutations in melanoma and melanocytic nevi", *Melanoma Res,* vol. 16, no. 4, pp. 267-273.

Rapp, U.R., Goldsborough, M.D., Mark, G.E., Bonner, T.I., Groffen, J., Reynolds, F.H.,Jr & Stephenson, J.R. 1983, "Structure and biological activity of v-raf, a unique oncogene transduced by a retrovirus", *Proceedings of the National Academy of Sciences of the United States of America,* vol. 80, no. 14, pp. 4218-4222.

Reed, J.A. & Shea, C.R. 2011, "Lentigo maligna: melanoma in situ on chronically sun-damaged skin", *Archives of Pathology & Laboratory Medicine,* vol. 135, no. 7, pp. 838-841.

Ronaghi, M., Uhlen, M. & Nyren, P. 1998, "A sequencing method based on real-time pyrophosphate", *Science (New York, N.Y.),* vol. 281, no. 5375, pp. 363, 365.

Rubinstein, J.C., Sznol, M., Pavlick, A.C., Ariyan, S., Cheng, E., Bacchiocchi, A., Kluger, H.M., Narayan, D. & Halaban, R. 2010, "Incidence of the V600K mutation among melanoma patients with BRAF mutations, and potential therapeutic response to the specific BRAF inhibitor PLX4032", *Journal of translational medicine,* vol. 8, pp. 67.

Sanger Institute Catalogue Of Somatic Mutations In Cancer *, The mutation data was obtained from the Sanger Institute Catalogue Of Somatic Mutations In Cancer web site, http://www.sanger.ac.uk/cosmic Bamford et al (2004) The COSMIC (Catalogue of Somatic Mutations in Cancer) database and website. Br J Cancer, 91,355-358.* Available: http://www.sanger.ac.uk/perl/genetics/

CGP/cosmic?action=bycancer&coords=AA%3AAA&start=1&end=767&ln=BRAF&hn=malignant_melanoma&sn=skin&ss=NS&ss=axilla&ss=upper_leg&sh=nodular&samps=1001&display=Apply [2012, 03].

Sebolt-Leopold, J.S. & Herrera, R. 2004, "Targeting the mitogen-activated protein kinase cascade to treat cancer", *Nature reviews.Cancer,* vol. 4, no. 12, pp. 937-947.

Sosman, J.A., Kim, K.B., Schuchter, L., Gonzalez, R., Pavlick, A.C., Weber, J.S., McArthur, G.A., Hutson, T.E., Moschos, S.J., Flaherty, K.T., Hersey, P., Kefford, R., Lawrence, D., Puzanov, I., Lewis, K.D., Amaravadi, R.K., Chmielowski, B., Lawrence, H.J., Shyr, Y., Ye, F., Li, J., Nolop, K.B., Lee, R.J., Joe, A.K. & Ribas, A. 2012, "Survival in BRAF V600-mutant advanced melanoma treated with vemurafenib", *The New England journal of medicine,* vol. 366, no. 8, pp. 707-714.

Spittle, C., Ward, M.R., Nathanson, K.L., Gimotty, P.A., Rappaport, E., Brose, M.S., Medina, A., Letrero, R., Herlyn, M. & Edwards, R.H. 2007, "Application of a BRAF pyrosequencing assay for mutation detection and copy number analysis in malignant melanoma", *J Mol Diagn,* vol. 9, no. 4, pp. 464-471.

Statistik Austria 2011, 13.09.2011-last update*, Malignes Melanom; Krebsinzidenz und Krebsmortalität, Österreich ab 1983* [Homepage of STATISTIK AUSTRIA], [Online]. Available: http://www.statistik.at/web_de/statistiken/gesundheit/krebserkrankungen/haut/index.html [02.04.2012].

Sunami, E., Vu, A.T., Nguyen, S.L., Giuliano, A.E. & Hoon, D.S. 2008, "Quantification of LINE1 in circulating DNA as a molecular biomarker of breast cancer", *Annals of the New York Academy of Sciences,* vol. 1137, pp. 171-174.

Swetter, S.M., Boldrick, J.C., Jung, S.Y., Egbert, B.M. & Harvell, J.D. 2005, "Increasing incidence of lentigo maligna melanoma subtypes: northern California and national trends 1990-2000", *The Journal of investigative dermatology,* vol. 125, no. 4, pp. 685-691.

Takata, M., Murata, H. & Saida, T. 2009, "Molecular pathogenesis of malignant melanoma: a different perspective from the studies of melanocytic nevus and acral melanoma", *Pigment Cell Melanoma Res,* .

Taube, J.M., Begum, S., Shi, C., Eshleman, J.R. & Westra, W.H. 2009, "Benign nodal nevi frequently harbor the activating V600E BRAF mutation", *Am J Surg Pathol,* vol. 33, no. 4, pp. 568-571.

Thomas, N.E., Edmiston, S.N., Alexander, A., Millikan, R.C., Groben, P.A., Hao, H., Tolbert, D., Berwick, M., Busam, K., Begg, C.B., Mattingly, D., Ollila, D.W., Tse, C.K., Hummer, A., Lee-Taylor, J. & Conway, K. 2007, "Number of nevi and early-life ambient UV exposure are associated with BRAF-mutant melanoma", *Cancer Epidemiol Biomarkers Prev,* vol. 16, no. 5, pp. 991-997.

Tsiatis, A.C., Norris-Kirby, A., Rich, R.G., Hafez, M.J., Gocke, C.D., Eshleman, J.R. & Murphy, K.M. 2010, "Comparison of Sanger sequencing, pyrosequencing, and melting curve analysis for the detection of KRAS mutations: diagnostic and clinical implications", *The Journal of molecular diagnostics : JMD,* vol. 12, no. 4, pp. 425-432.

Umetani, N., Kim, J., Hiramatsu, S., Reber, H.A., Hines, O.J., Bilchik, A.J. & Hoon, D.S. 2006, "Increased integrity of free circulating DNA in sera of patients with colorectal or periampullary cancer: direct quantitative PCR for ALU repeats", *Clinical chemistry,* vol. 52, no. 6, pp. 1062-1069.

Uribe, P., Wistuba, I. & Gonzalez, S. 2003, "BRAF mutation: a frequent event in benign, atypical, and malignant melanocytic lesions of the skin", *Am J Dermatopathol,* vol. 25, no. 5, pp. 365-370.

van Beers, E.H., Joosse, S.A., Ligtenberg, M.J., Fles, R., Hogervorst, F.B., Verhoef, S. & Nederlof, P.M. 2006, "A multiplex PCR predictor for aCGH success of FFPE samples", *British journal of cancer,* vol. 94, no. 2, pp. 333-337.

van Dongen, J.J., Langerak, A.W., Brüggemann, M., Evans, P.A., Hummel, M., Lavender, F.L., Delabesse, E., Davi, F., Schuuring, E., Garcia-Sanz, R., van Krieken, J.H., Droese, J., Gonzalez, D., Bastard, C., White, H.E., Spaargaren, M., Gonzalez, M., Parreira, A., Smith, J.L., Morgan, G.J., Kneba, M. & Macintyre, E.A. 2003, "Design and standardization of PCR primers and protocols for detection of clonal immunoglobulin and T-cell receptor gene recombinations in suspect lymphoproliferations: report of the BIOMED-2 Concerted Action BMH4-CT98-3936", *Leukemia : official journal of the Leukemia Society of America, Leukemia Research Fund, U.K,* vol. 17, no. 12, pp. 2257-2317.

Viros, A., Fridlyand, J., Bauer, J., Lasithiotakis, K., Garbe, C., Pinkel, D. & Bastian, B.C. 2008, "Improving melanoma classification by integrating genetic and morphologic features", *PLoS Med,* vol. 5, no. 6, pp. e120.

Wan, P.T., Garnett, M.J., Roe, S.M., Lee, S., Niculescu-Duvaz, D., Good, V.M., Jones, C.M., Marshall, C.J., Springer, C.J., Barford, D., Marais, R. & Cancer Genome Project 2004, "Mechanism of activation of the RAF-ERK signaling pathway by oncogenic mutations of B-RAF", *Cell,* vol. 116, no. 6, pp. 855-867.

Willmore-Payne, C., Holden, J.A., Tripp, S. & Layfield, L.J. 2005, "Human malignant melanoma: detection of BRAF- and c-kit-activating mutations by high-resolution amplicon melting analysis", *Hum Pathol,* vol. 36, no. 5, pp. 486-493.

Wu, J.M., Alvarez, H., Garcia, P., Rojas, P.L., Wong, G., Maitra, A., Antonescu, C. & Montgomery, E.A. 2009, "Melanoma hyperpigmentation is strongly associated with KIT alterations", *Am J Dermatopathol,* vol. 31, no. 7, pp. 619-625.

Zaidi, M.R., Day, C.P. & Merlino, G. 2008, "From UVs to metastases: modeling melanoma initiation and progression in the mouse", *The Journal of investigative dermatology,* vol. 128, no. 10, pp. 2381-2391.

Zaravinos, A., Kanellou, P., Baritaki, S., Bonavida, B. & Spandidos, D.A. 2009, "BRAF and RKIP are significantly decreased in cutaneous squamous cell carcinoma", *Cell Cycle,* vol. 8, no. 9, pp. 1402-1408.

Zhang, J.H., Chung, T.D. & Oldenburg, K.R. 1999, "A Simple Statistical Parameter for Use in Evaluation and Validation of High Throughput Screening Assays", *Journal of biomolecular screening,* vol. 4, no. 2, pp. 67-73.

7.2 Appendix B – Supplementary Data

7.2.1 Additional Primers Used

Primers that were used during this work, but early in the process excluded from further optimization are listed in Table 8.

Table 8: Additional primers used in this work.

	fwd (5'-3')	rev (5'-3')	Amplicon
Pre-Amplification			
BRAF_Pre [11]	CTCTTCATAATGCTTGCTCTGATAGG	TAGTAACTCAGCAGCATCTCAGG	250 bp
HRMA PCR – COLD PCR			
BRAF 147	GGTGATTTTGGTCTAGCTACAG	AGTAACTCAGCAGCATCTCAGG	147 bp
BRAF 1	GGTGATTTTGGTCTAGCTAC	GGATCCAGACAACTGTTC	72 bp
BRAF 2	CATGAAGACCTCACAGTA	GATCCAGACAACTGTTCA	95 bp
BRAF 3	ATAGGTGATTTTGGTCTAGC	TCCAGACAACTGTTCAAACT	72 bp
BRAF 4	AGGTGATTTTGGTCTAGC	CTGTTCAAACTGATGGGA	61 bp
BRAF 6	GATTTTGGTCTAGCTACAG	GTGGAAAAATAGCCTCAA	106 bp
BRAF 7	TCCTTTACTTACTACACCTCAG	TTCAAACTGATGGGACCCAC	114 bp
TP 53	GCCTCTGATTCCTCACTGATTG	TAGGGCACCACCACACTATG	129 bp

7.2.2 DNA Quality of the LS

DNA from the LS (NM n=5) was isolated and the integrity checked with an assay described by van Beers et al. (van Beers et al. 2006). The assay is based on a multiplex PCR amplifying 4 DNA fragments of the *GAPDH* gene in different lengths (from 100 bp to 400 bp). In addition FFPE DNA isolation was done with and without deparaffinization. Results are shown in Figure 32.

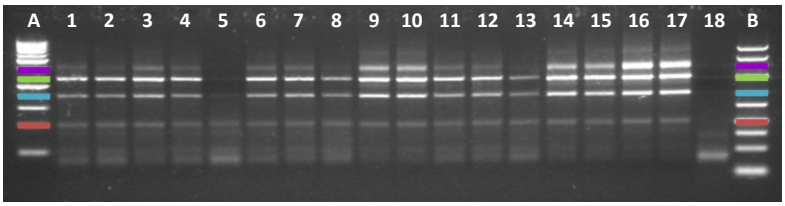

Figure 32: DNA integrity of LS.

Lane A and B size marker with 100 bp indicated in red, 200 bp in blue, 300 bp in green and 400 bp in purple, lane 1 to 5 NM1 to NM5, lane 6 to 10 'young' FFPE material with deparaffinization prior to DNA isolation, lane 11 to 15 'young' FFPE material without deparaffinization prior to DNA isolation, lane 16 and 17 cell line DNA, lane 18 no template control. This figure demonstrates the influence of the archival period as samples displayed in lanes 6 to 15 showed much higher integrity than those in lane 1 to 5 where archival period is up to 6 years compared to less than one year in 'young' samples. Especially NM5 shows low quality.

7.2.3 Pre-Amplification MS

Pre-amplification had no adverse effect on HRMA PCR in the MS as demonstrated in Figure 33.

[11] Primers from (Willmore-Payne et al. 2005)

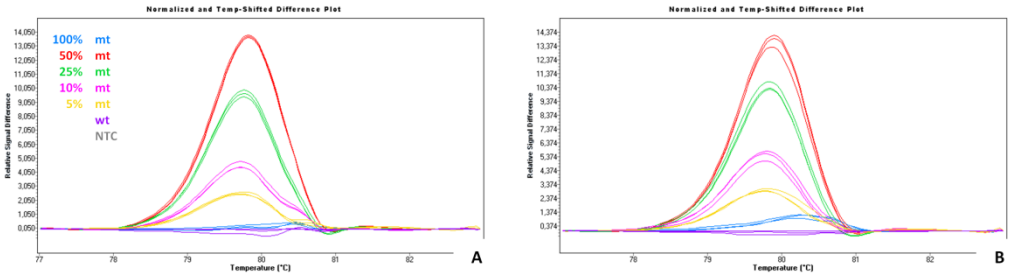

Figure 33: Comparison of HRMA PCR of the MS with and without pre-amplification.

Figure 33A shows the difference plot after HRMA PCR using gDNA as template, in comparison to Figure 33B where pre-amplification product served as template. No difference in sensitivity was observed. BRAF PM1 primer was used for amplification, but this primer did not allow analysis of the *BRAF* V600K mutation.

7.2.4 Adaption of HRMA PCR

To allow the detection of the *BRAF* V600E as well as the V600K mutation with HRMA PCR the newly designed BRAF PM3 primer was used. Figure 34 shows difference plots generated after HMRA PCR using pre-amplification products of the MS (DNA blends of SK-MEL-30 and SK-MEL-28 for *BRAF* V600E and SK-MEL-30 and IGR-1 for *BRAF* V600K). Please note, that reactions labeled 100% mt in Figure 34B contain 50% mt copies of the *BRAF* V600K amplicon since IGR-1 cell line is heterozygous.

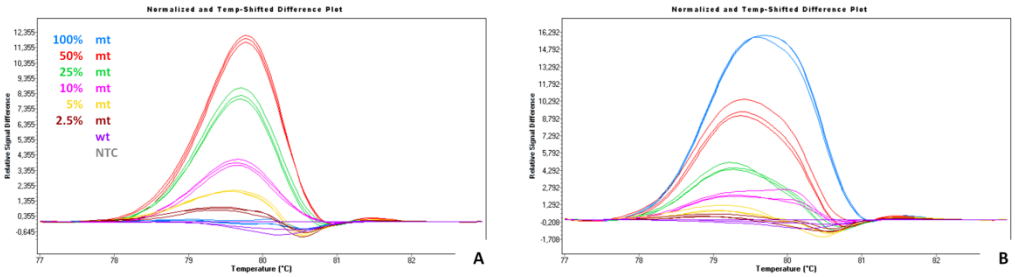

Figure 34: Difference plots after HRMA PCR using PM3 primer.

Figure 34A depicts the difference plot of DNA blends carrying the *BRAF* V600E mutation. Since SK-MEL-28 are homozygous for the *BRAF* V600E mutation and this mutation is a T>A exchange, the melting behavior of 100% mt and wt are very similar. Figure 34B shows the difference plot of DNA blends carrying the *BRAF* V600K mutation. IGR-1 cell line, which was used in this MS, is heterozygous for the *BRAF* V600K mutation. Therefore, and because the *BRAF* V600K mutation is more complex (GT>AA), the 100% sample (heterozygote) shows a completely different melting behavior than the wt sample.

7.2.5 Optimizing Pre-Amplification

Some samples of the TS could not be amplified despite good DNA quantity and quality. The modification of the PCR reaction with respect to BSA and $MgCl_2$ concentration resulted in an up to 4-fold better amplification of the gDNA (Figure 35). Ranges tested were 0.0 µg/µl to 1.2 µg/µl BSA and 1.5 mM to 6.0 mM $MgCl_2$ final concentrations in the PCR reaction.

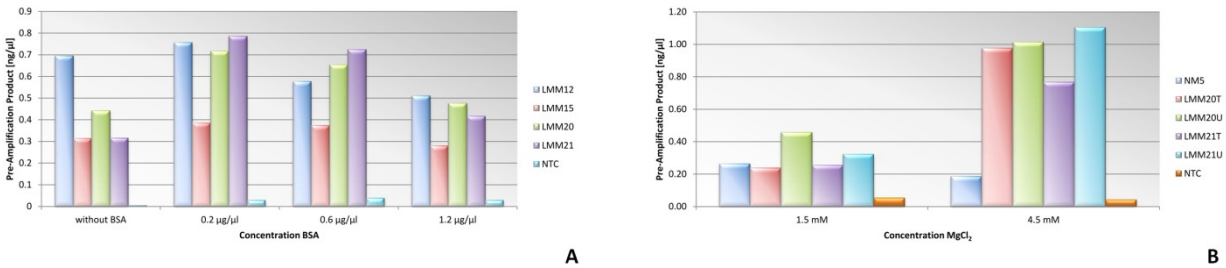

Figure 35: Influence of BSA and $MgCl_2$ concentration on pre-amplification.

The yield of pre-amplification product was remarkably increased by the addition of BSA and by the raise of $MgCl_2$ concentration. For the pre-amplification a final concentration of 0.2 µg/µl BSA and 4.5 mM $MgCl_2$ was from now on used.

7.2.6 Z-Factor AS PCR for Pre-Amplification Products

Z-factor for AS PCR was (re-) calculated for the *BRAF* V600E and *BRAF* V600K mutation using pre-amplification products of the serial DNA blends as template. The Z-factor is 0.7 for 0.1% *BRAF* V600E mt DNA (calculated 20 copies mt DNA) and 0.9 for 0.5% *BRAF* V600K mt DNA (calculated 50 copies mt DNA). Every sample carrying a mutation was checked for initial copy count to be detected in the pre-amplification product. Samples carrying a lower copy count than 3 copies mt DNA in the pre-amplification product were assessed as wt.

7.2.7 Z-Factor Pyrosequencing for Pre-Amplification Products

Also for the pyrosequencing BRAF PM3 assay the Z-factor was (re-) calculated. The Z-factor for the *BRAF* V600E mutation is 0.3 for 5% mt DNA, for the *BRAF* V600K mutation 0.6 for 2.5% mt DNA (data not shown).

7.2.8 DNA Quality of the TS

In order to overcome limited amounts of DNA the LINE assay was used instead of the GAPDH assay for samples of the TS as well as the collective. It was used as a surrogate parameter to determine the percentages of amplifiable DNA in the samples since FFPE DNA tends to considerably fragment. The percentage amplifiable DNA in the samples was calculated with the use of a standard curve generated from high molecular gDNA. A LINE assay was chosen, because DNA quantity proved to be a limiting criterion and it would have been impossible to do a DNA quality assay using a single copy gene. Results of the TS are summarized in Figure 36 and Figure 37.

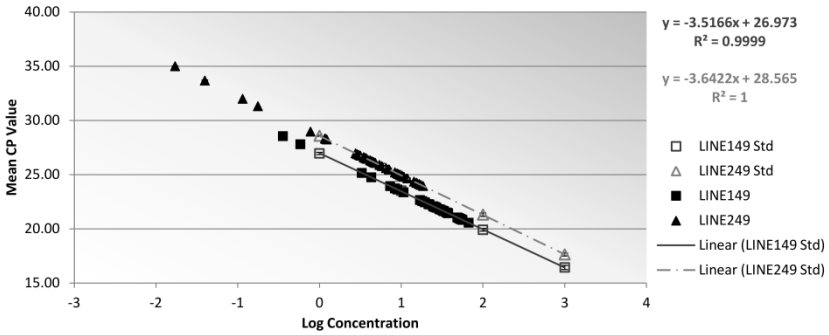

Figure 36: Standard curves of LINE of the TS.

For the analysis of the TS standard curves were included in each run for LINE 149 bp as well as for LINE 249 bp. The diagram shows the mean values of all standard curves of the TS, including data from the samples of the TS.

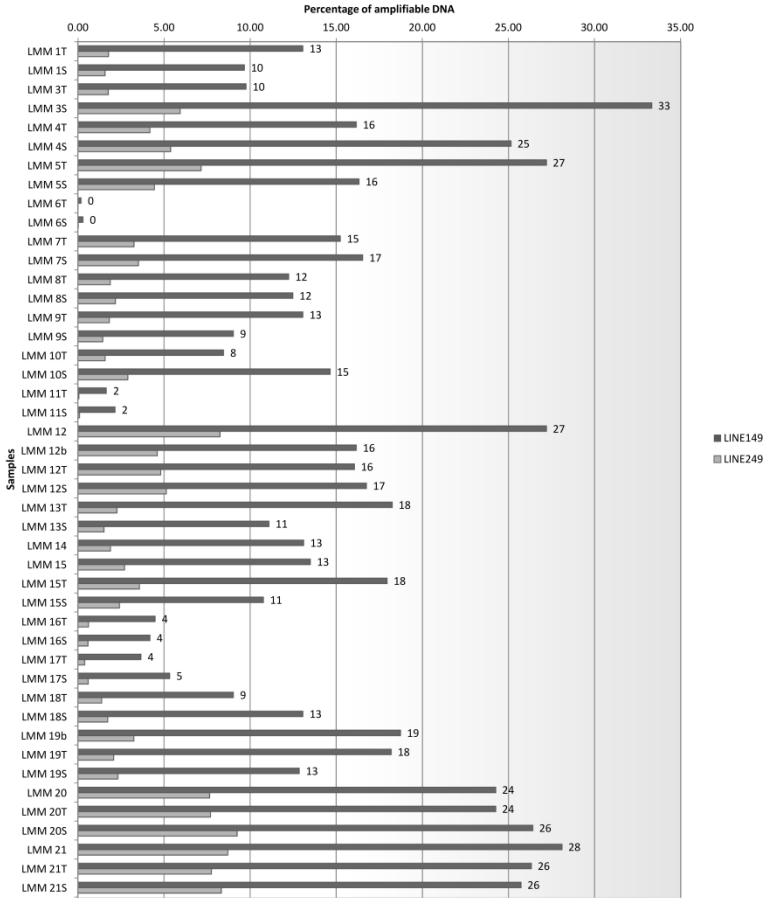

Figure 37: DNA quality of the TS.

Amplifiability of the samples was very heterogeneous. Some samples seem to be completely fragmented, since no product at all could be amplified (e.g., LMM 6T and LMM 6S).

7.2.9 Calculation of Copies per Reaction for the TS

The resulting percentage of amplifiable DNA for the LINE 149 bp fragment was used as surrogate parameter for the amplifiability of the 152 bp pre-amplification product. Percentages from LINE 149 bp were multiplied with the DNA quantity used for pre-amplification (in most of the cases 20 ng unless indicated otherwise). The minimal requirement for further analysis was a calculated template count of 303 copies. Under these circumstances 1.0% mt DNA (i.e. 3 copies) in a background of wt DNA should be detected with a probability of 0.95. In Table 9 PCR data of the TS is summarized.

Table 9: Calculation of copies per reaction for the TS.

Samples	% amplif. LINE 149bp	ng DNA PreAmp	Amplifiable DNA [ng]	Copies PreAmp	Amplicons in AS PCR	Mu. DNA E % AS PCR	Copies E in PreAmp	Amplicons E in AS PCR	Mu. DNA K % AS PCR	Copies K in PreAmp	Amplicons K in AS PCR
LMM 1T	13.06	20	2.61	791.76	28174.55	0.63	5.01	178.28	0.00	0.03	1.08
LMM 1S	9.67	20	1.93	585.85	26717.43	0.00	0.01	0.55	0.00	0.00	0.04
LMM 2T		9.71	0.00	0.00			0.00	0.00		0.00	0.00
LMM 2S		1.82	0.00	0.00			0.00	0.00		0.00	0.00
LMM 3T	9.76	20	1.95	591.63	17714.25	0.00	0.02	0.55	0.00	0.00	0.04
LMM 3S	33.32	15.2	5.06	1534.79			0.00	0.00		0.00	0.00
LMM 4T	16.16	20	3.23	979.52	27903.44	0.00	0.02	0.55	0.00	0.00	0.04
LMM 4S	25.14	13	3.27	990.54	31052.01	0.00	0.02	0.55	0.00	0.00	0.04
LMM 5T	27.20	20	5.44	1648.48	22456.55	0.00	0.04	0.55	0.00	0.00	0.04
LMM 5S	16.32	20	3.26	989.18	24088.73	0.00	0.02	0.55	0.00	0.00	0.04
LMM 6T	0.18	20	0.04	10.79			0.00	0.00		0.00	0.00
LMM 6S	0.29	20	0.06	17.64			0.00	0.00		0.00	0.00
LMM 7T	15.24	20	3.05	923.46			0.00	0.00		0.00	0.00
LMM 7S	16.54	20	3.31	1002.22	24907.13	0.00	0.02	0.55	0.00	0.00	0.04
LMM 8T	12.24	20	2.45	741.58	20247.07	0.00	0.02	0.55	0.00	0.00	0.04
LMM 8S	12.48	20	2.50	756.29	22531.70	0.00	0.02	0.55	0.00	0.00	0.04
LMM 9T	13.06	20	2.61	791.76			0.00	0.00		0.00	0.00
LMM 9S	9.02	20	1.80	546.92	21145.85	0.00	0.01	0.55	0.00	0.00	0.04
LMM 10T	8.45	20	1.69	512.26	25926.01	0.00	0.01	0.55	0.00	0.00	0.04
LMM 10S	14.65	20	2.93	887.89	21216.62	0.00	0.02	0.55	0.00	0.00	0.04
LMM 11T	1.64	20	0.33	99.67			0.00	0.00		0.00	0.00
LMM 11S	2.15	20	0.43	130.37			0.00	0.00		0.00	0.00
LMM 12	27.20	20	5.44	1648.48	21075.32	0.00	0.04	0.55	0.00	0.00	0.04
LMM 12b	16.16	20	3.23	979.52	23453.40	0.00	0.02	0.55	0.00	0.00	0.04
LMM 12T	16.06	20	3.21	973.12	21216.62	0.00	0.03	0.55	0.00	0.00	0.04
LMM 12S	16.75	20	3.35	1015.43	21791.34	0.00	0.03	0.55	0.00	0.00	0.04
LMM 13T	18.24	20	3.65	1105.65			0.00	0.00		0.00	0.00
LMM 13S	11.09	20	2.22	672.20	23453.40	0.00	0.02	0.55	0.00	0.00	0.04
LMM 14	13.11	20	2.62	794.36	17420.79	0.00	0.03	0.55	0.00	0.00	0.04
LMM 15	13.50	20	2.70	818.11	23064.86	0.00	0.02	0.55	0.00	0.00	0.04
LMM 15T	17.95	20	3.59	1087.70	20588.14	0.00	0.03	0.55	0.00	0.00	0.04
LMM 15S	10.77	20	2.15	652.69	26628.32	0.00	0.01	0.55	0.00	0.00	0.04
LMM 16T	4.48	20	0.90	271.43	18316.09	0.00	0.01	0.55	0.00	0.00	0.04
LMM 16S	4.18	20	0.84	253.39	11942.85	0.00	0.01	0.55	0.00	0.00	0.04
LMM 17T	3.66	20	0.73	221.57	15971.38	0.00	0.01	0.55	0.00	0.00	0.04
LMM 17S	5.33	20	1.07	322.86	19845.24	0.00	0.01	0.55	0.00	0.00	0.04
LMM 18T	9.02	20	1.80	546.92	24990.49	0.00	0.01	0.55	0.00	0.00	0.04
LMM 18S	13.06	20	2.61	791.76	21718.66	0.00	0.02	0.55	0.00	0.00	0.04
LMM 19b	18.73	20	3.75	1135.00			0.00	0.00		0.00	0.00
LMM 19T	18.18	20	3.64	1102.04			0.00	0.00		0.00	0.00
LMM 19S	12.85	20	2.57	778.90			0.00	0.00		0.00	0.00
LMM 20	24.26	20	4.85	1470.00	23803.75	0.48	7.08	114.64	0.00	0.07	1.07
LMM 20T	24.26	20	4.85	1470.00	23610.65	0.00	0.03	0.55	0.00	0.00	0.04
LMM 20T	24.26	20	4.85	1470.00	24008.38	0.00	0.03	0.55	0.00	0.00	0.04
LMM 20S	26.41	20	5.28	1600.61	27258.42	0.00	0.03	0.55	0.00	0.00	0.04
LMM 20S	26.41	20	5.28	1600.61	28659.31	0.00	0.03	0.55	0.00	0.00	0.04
LMM 21	28.11	20	5.62	1703.34	24494.82	0.00	0.06	0.86	2.61	44.41	638.65
LMM 21T	26.32	20	5.26	1595.38	20248.89	0.01	0.19	2.37	3.26	52.00	659.95
LMM 21S	25.73	20	5.15	1559.23	26450.98	0.00	0.03	0.55	0.37	5.78	98.07
LMM 21S	25.73	20	5.15	1559.23	22456.55	0.00	0.04	0.55	0.14	2.17	31.22

< 5% < 20ng

< 303 c (>1.0%) < 1000 Amp.
303-606 c bis 1.0%
> 606 c bis 0.5%

> 0,1% > 3 copies > 20 Amp.

> 0,5% > 3 copies > 50 Amp.

7.2.10 DNA Quality of the Collective

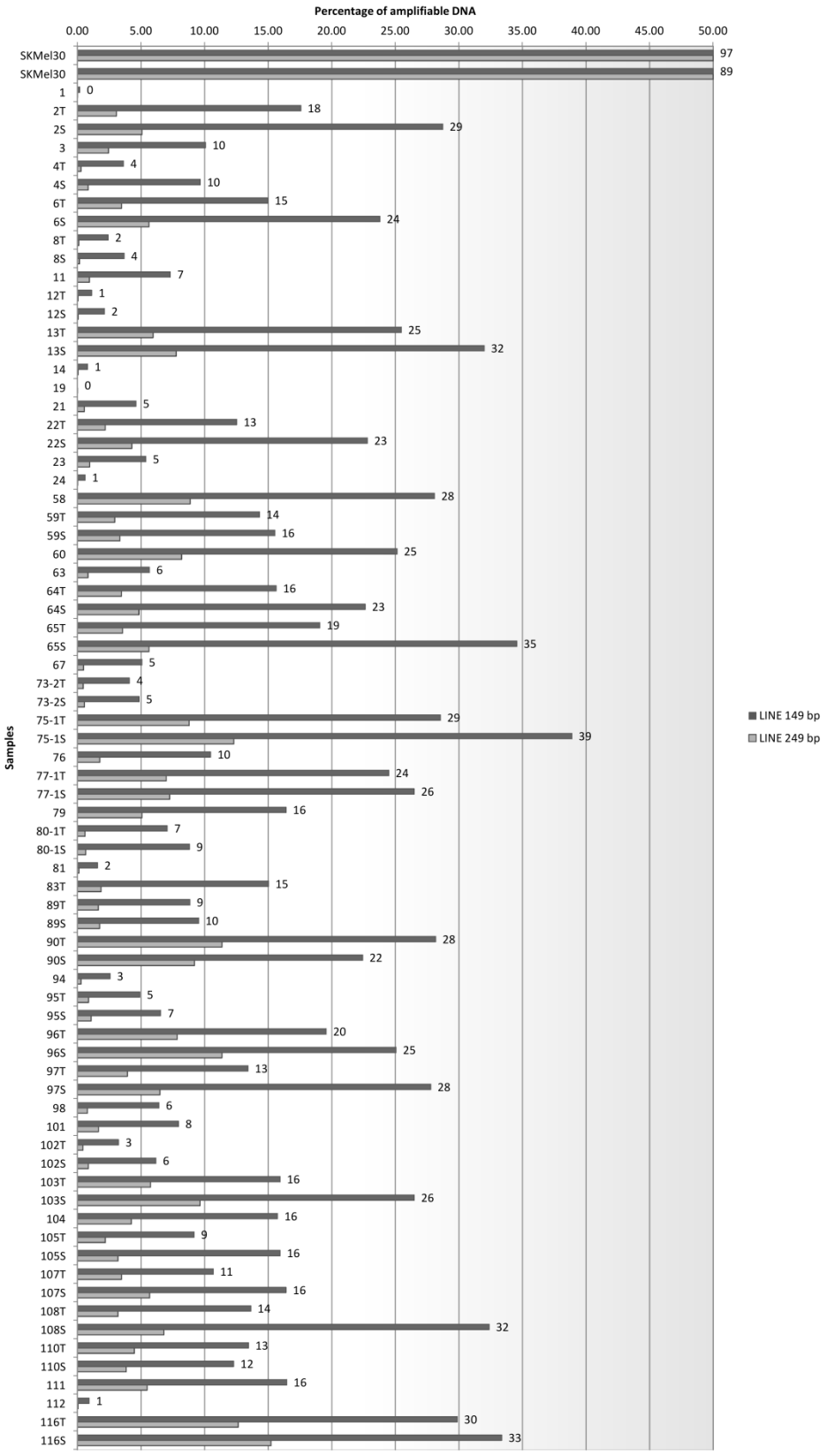

Figure continued on next page.

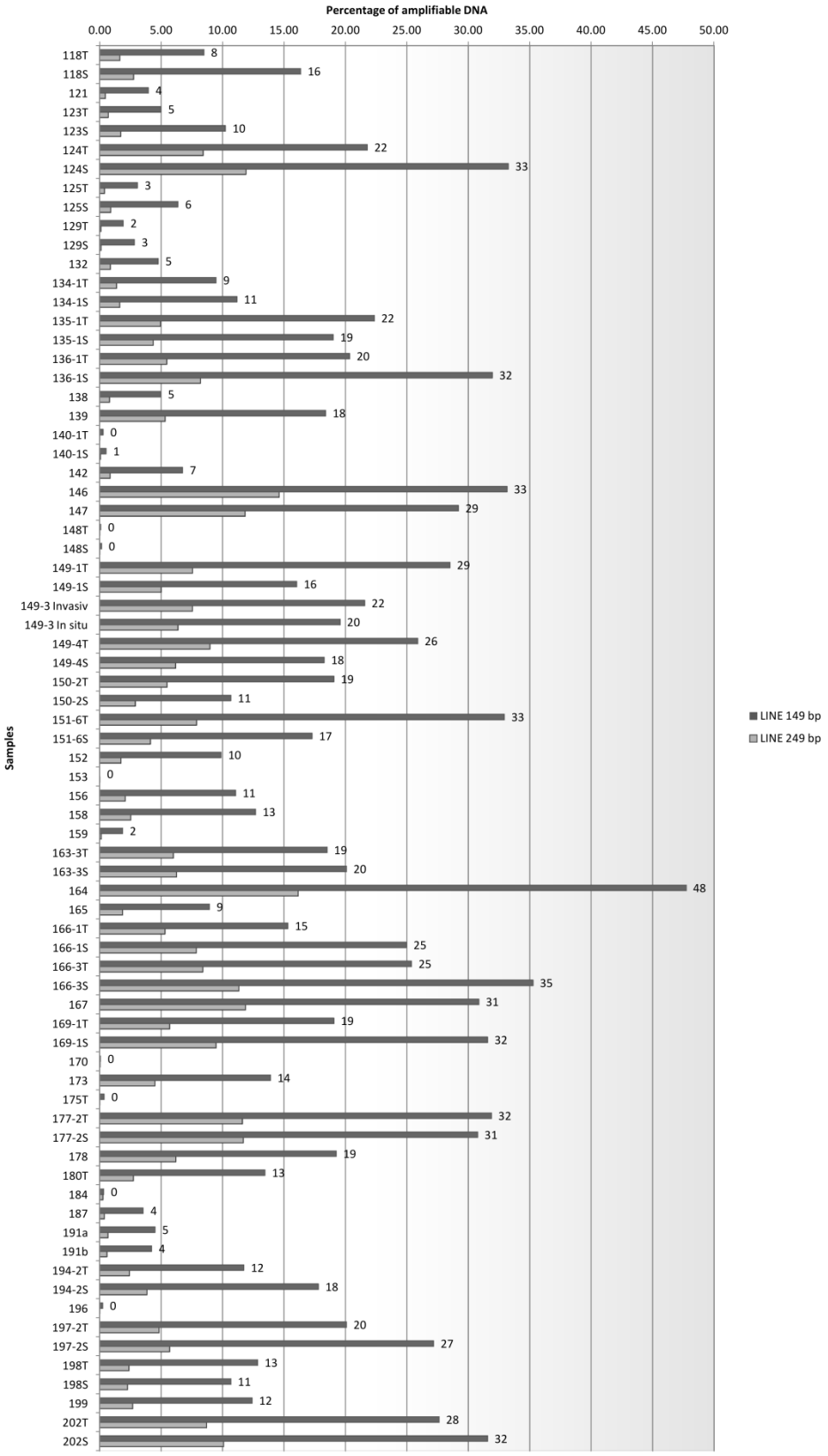

Figure 38: **DNA quality of the collective.**

7.2.11 Calculation of Copies per Reaction in the Collective

Table 10: Calculation of copies per reaction for the collective.

Samples	% amplif. LINE 149bp	ng DNA PreAmp	Amplifiable DNA [ng]	Copies PreAmp	Amplicons in AS PCR	Mu. DNA E % AS PCR	Copies E in PreAmp	Amplicons E in AS PCR	Mu. DNA K % AS PCR	Copies K in PreAmp	Amplicons K in AS PCR
1	0.17	6.6	0.01	3.42	0.02	57.56	1.97	0.01	57.56	1.98	0.01
2T	17.57	20	3.51	1064.66	24260.19	0.00	0.01	0.33	0.00	0.00	0.07
2S	28.72	19.1	5.49	1662.49	29182.87	0.00	0.02	0.33	0.00	0.00	0.01
3	10.07	20	2.01	610.07	18794.56	0.00	0.01	0.33	0.00	0.01	0.41
4T	3.61	20	0.72	218.73	727.61	1.00	2.39	7.95	0.00	0.00	0.01
4S	9.65	20	1.93	584.79	0.06	57.56	42.74	0.01	20.45	119.61	0.01
6T	14.98	20	3.00	907.64	31014.55	0.00	0.04	1.30	1.38	12.48	426.53
6S	23.78	20	4.76	1441.23	27277.50	0.00	0.02	0.33	0.30	4.35	82.27
8T	2.41	20	0.48	146.07	0.44	57.56	4.38	0.01	3.03	4.43	0.01
8S	3.67	20	0.73	222.32	0.02	57.56	42.74	0.01	57.56	128.87	0.01
11	7.29	20	1.46	441.95	20372.05	0.00	0.01	0.33	0.00	0.00	0.01
12T	1.11	20	0.22	67.51	7387.08	0.00	0.00	0.04	0.00	0.00	0.01
12S	2.11	20	0.42	127.81	0.06	20.45	25.77	0.01	20.45	26.14	0.01
13T	25.46	20	5.09	1543.23	26293.00	0.00	0.06	0.99	2.64	40.70	693.35
13S	31.98	20	6.40	1938.32	25313.68	0.00	0.02	0.33	0.22	4.26	55.70
14	0.79	20	0.16	47.65	8007.26	0.00	0.00	0.01	0.00	0.00	0.01
19	0.00	20	0.00	0.18	0.02	57.56	0.10	0.01	57.56	0.11	0.01
21	4.59	20	0.92	278.33	13659.53	0.00	0.01	0.33	0.00	0.00	0.01
22T	12.52	20	2.50	758.81	24753.44	0.00	0.03	0.90	3.30	25.05	817.11
22S	22.79	20	4.56	1381.49	27935.95	0.00	0.02	0.33	0.00	0.00	0.01
23	5.37	20	1.07	325.42	21209.99	0.00	0.00	0.33	0.00	0.00	0.01
24	0.59	20	0.12	35.78	0.12	57.56	3.84	0.01	10.97	3.92	0.01
58	28.08	20	5.62	1701.60	26208.73	0.00	0.02	0.33	0.00	0.00	0.01
59T	14.31	20	2.86	867.19	25858.94	0.00	0.01	0.33	0.00	0.00	0.01
59S	15.52	20	3.10	940.74	24671.03	0.00	0.01	0.33	0.00	0.00	0.01
60	25.13	20	5.03	1523.26	23458.76	0.00	0.02	0.33	0.00	0.00	0.01
63	5.65	3.6	0.20	61.66	25858.94	0.00	0.00	0.33	0.00	0.00	0.01
64T	15.62	20	3.12	946.89	24494.04	0.00	0.02	0.43	0.62	5.89	152.30
64S	22.63	8.5	1.92	582.85	23856.08	0.00	0.01	0.33	0.00	0.00	0.01
65T	19.06	20	3.81	1154.96	28029.95	0.00	0.01	0.33	0.00	0.00	0.01
65S	34.55	15.2	5.25	1591.58	20235.65	0.00	0.03	0.33	0.00	0.00	0.01
67	5.06	20	1.01	306.89	16266.50	0.00	0.00	0.04	0.00	0.00	0.01
73-2T	4.08	20	0.82	247.54	17338.56	0.00	0.00	0.15	0.00	0.00	0.07
73-2S	4.84	20	0.97	293.22	25004.75	0.00	0.00	0.33	0.00	0.00	0.01
75-1T	28.54	20	5.71	1729.53	25685.80	0.00	0.02	0.33	0.00	0.00	0.01
75-1S	38.88	20	7.78	2356.56	24754.10	0.00	0.03	0.33	0.00	0.01	0.07
76	10.47	20	2.09	634.39	24920.90	0.00	0.01	0.33	0.00	0.00	0.01
77-1T	24.49	20	4.90	1484.09	25342.99	0.00	0.02	0.33	0.00	0.00	0.01
77-1S	26.48	20	5.30	1604.73	26652.63	0.00	0.02	0.33	0.00	0.00	0.01
79	16.41	20	3.28	994.29	28890.27	0.00	0.01	0.33	0.00	0.00	0.01
80-1T	7.06	20	1.41	427.73	3074.13	0.00	0.00	0.01	0.00	0.00	0.01
80-1S	8.81	20	1.76	533.83	2.70	57.56	2.58	0.01	0.49	2.63	0.01
81	1.57	7.6	0.12	36.08	0.86	1.00	0.54	0.01	1.54	0.55	0.01
83T	15.02	13.9	2.09	632.87	22216.98	0.03	0.17	5.86	0.94	5.94	208.64
83S		1.3	0.00	0.00	18605.73	0.00	0.00	0.33	0.00	0.00	0.01
89T	8.84	20	1.77	535.57	15312.12	0.00	0.01	0.33	0.00	0.00	0.01
89S	9.52	20	1.90	577.22	18605.73	0.00	0.01	0.33	0.00	0.00	0.01
90T	28.17	20	5.63	1707.15	22684.25	0.64	10.95	145.44	0.00	0.03	0.41
90S	22.43	20	4.49	1359.18	21641.80	0.00	0.02	0.33	0.00	0.00	0.01
94	2.56	20	0.51	154.88	14576.53	0.02	0.03	2.73	8.75	13.59	1279.16
95T	4.90	20	0.98	297.06	17691.49	0.00	0.01	0.33	0.00	0.00	0.01
95S	6.53	20	1.31	395.63	17751.02	0.00	0.01	0.33	0.00	0.00	0.01
96T	19.56	20	3.91	1185.44	19699.11	0.00	0.02	0.33	0.00	0.00	0.01
96S	25.05	20	5.01	1518.31	25342.99	0.00	0.02	0.33	0.00	0.00	0.01
97T	13.41	20	2.68	812.52	21138.87	0.00	0.01	0.33	0.00	0.00	0.01
97S	27.78	4.3	1.19	361.99	26474.17	0.00	0.00	0.33	0.00	0.00	0.01
98	6.40	20	1.28	387.98	22381.17	0.00	0.01	0.33	0.00	0.00	0.07
101	7.94	20	1.59	481.00	16376.15	0.00	0.01	0.33	0.00	0.00	0.01
102T	3.22	20	0.64	195.17	15729.17	0.00	0.00	0.33	0.00	0.00	0.01
102S	6.16	20	1.23	373.11	16765.77	0.00	0.01	0.33	0.00	0.00	0.01
103T	15.93	20	3.19	965.57	20647.62	0.00	0.02	0.33	0.00	0.00	0.01
103S	26.48	20	5.30	1604.73	25513.82	0.00	0.02	0.33	0.00	0.00	0.01
104	15.73	20	3.15	953.08	19436.20	0.00	0.02	0.33	0.00	0.00	0.01
105T	9.16	20	1.83	555.10	16431.25	0.00	0.01	0.33	0.00	0.00	0.01
105S	15.93	20	3.19	965.57	24016.89	0.07	0.72	18.01	0.00	0.00	0.01
107T	10.67	20	2.13	646.90	20578.38	0.00	0.00	0.11	0.00	0.00	0.01
107S	16.41	20	3.28	994.29	20440.66	0.00	0.02	0.33	0.00	0.00	0.07
108T	13.63	20	2.73	825.85	18668.39	0.00	0.01	0.33	0.00	0.00	0.07
108S	32.38	6.3	2.04	618.08	31106.10	0.00	0.01	0.33	0.00	0.00	0.01
110T	13.45	20	2.69	815.17	25117.00	0.01	0.07	2.09	2.76	22.50	693.35
110S	12.28	20	2.46	744.13	23383.73	0.00	0.01	0.33	0.02	0.12	3.66
111	16.46	20	3.29	997.53	22531.97	0.00	0.01	0.33	0.00	0.00	0.01
112	0.90	20	0.18	54.81	99.16	1.00	0.08	0.14	18.99	10.41	18.83
116T	29.87	20	5.97	1810.20	19898.73	0.00	0.03	0.33	0.00	0.01	0.12
116S	33.37	20	6.67	2022.13	17870.67	0.01	0.11	0.94	0.00	0.00	0.01
118T	8.47	20	1.69	513.37	22306.06	0.00	0.01	0.37	0.00	0.00	0.01
118S	16.35	12.6	2.06	624.37	28600.66	0.00	0.01	0.33	0.00	0.00	0.07
121	3.95	20	0.79	239.61	14756.67	0.00	0.01	0.33	0.00	0.00	0.01
123T	4.98	20	1.00	301.94	12814.99	0.00	0.00	0.04	0.00	0.00	0.01
123S	10.23	20	2.05	620.09	16709.54	0.00	0.01	0.33	0.00	0.00	0.01
124T	21.78	20	4.36	1319.92	21641.80	0.00	0.02	0.33	0.00	0.00	0.01
124S	33.26	16.7	5.55	1682.99	31106.10	0.00	0.02	0.33	0.00	0.00	0.01
125T	3.08	20	0.62	186.47	15312.12	0.00	0.00	0.33	0.00	0.00	0.01
125S	6.36	20	1.27	385.46	20997.33	0.00	0.01	0.33	0.00	0.00	0.01
129T	1.91	20	0.38	115.91	0.06	20.45	23.71	0.01	20.45	23.71	0.01
129S	2.83	20	0.57	171.33	0.02	57.56	42.74	0.01	57.56	99.31	0.01
132	4.76	20	0.95	288.48	21209.99	0.00	0.00	0.33	0.00	0.00	0.01
134-1T	9.46	20	1.89	573.47	20235.65	0.00	0.01	0.33	0.00	0.00	0.01
134-1S	11.17	20	2.23	677.08	18357.41	0.00	0.01	0.33	0.00	0.00	0.01
135-1T	22.35	20	4.47	1354.76	18840.11	0.00	0.02	0.33	1.58	21.34	296.79
135-1S	18.99	20	3.80	1151.20	19129.24	0.00	0.02	0.33	0.09	1.01	16.76
136-1T	20.34	20	4.07	1232.68	26922.57	0.00	0.01	0.33	0.00	0.00	0.01
136-1S	31.96	4.2	1.34	406.72	30898.22	0.27	1.12	84.82	0.00	0.01	0.41
138	4.97	20	0.99	300.95	17107.10	0.00	0.01	0.33	0.00	0.00	0.01
139	18.39	20	3.68	1114.32	24178.78	0.00	0.02	0.33	0.00	0.00	0.01

Table continued on next page.

Samples	% amplif. LINE 149bp	ng DNA PreAmp	Amplifiable DNA [ng]	Copies PreAmp	Amplicons in AS PCR	Mu. DNA E % AS PCR	Copies E in PreAmp	Amplicons E in AS PCR	Mu. DNA K % AS PCR	Copies K in PreAmp	Amplicons K in AS PCR
140-1T	0.27	20	0.05	16.54	0.29	1.58	0.74	0.01	4.58	0.76	0.01
140-1S	0.51	20	0.10	31.10	0.29	1.58	1.40	0.01	4.58	1.42	0.01
142	6.74	11.3	0.76	230.75	13844.30	0.00	0.01	0.33	0.00	0.00	0.01
146	33.15	20	6.63	2009.01	22531.97	0.00	0.03	0.33	0.00	0.00	0.01
147	29.20	20	5.84	1769.41	20856.74	0.05	0.93	10.99	0.00	0.00	0.01
148T	0.08	20	0.02	4.92	0.29	1.58	0.22	0.01	4.58	0.23	0.01
148S	0.14	7	0.01	2.99	0.29	1.58	0.13	0.01	4.58	0.14	0.01
149-1T	28.51	5.5	1.57	475.24	21934.55	0.00	0.01	0.33	0.00	0.00	0.01
149-1S	16.04	20	3.21	971.88	21569.29	0.00	0.01	0.33	0.00	0.00	0.07
149-3 Invasiv	21.57	20	4.31	1307.09	27842.27	0.00	0.02	0.33	0.00	0.00	0.01
149-3 In situ	19.56	20	3.91	1185.44	21569.23	0.00	0.02	0.33	0.00	0.00	0.01
149-4T	25.88	20	5.18	1568.56	27013.15	0.00	0.02	0.33	0.00	0.00	0.01
149-4S	18.27	20	3.65	1107.09	23696.35	0.00	0.02	0.38	0.00	0.00	0.01
150-2T	19.06	20	3.81	1154.96	26120.84	0.04	0.49	11.00	0.00	0.00	0.01
150-2S	10.67	20	2.13	646.90	21497.29	4.57	29.57	982.73	0.00	0.01	0.41
151-6T	32.93	20	6.59	1995.97	24097.76	0.00	0.03	0.33	0.00	0.01	0.07
151-6S	17.28	20	3.46	1047.47	24505.84	0.00	0.01	0.33	0.00	0.00	0.01
152	9.87	20	1.97	598.27	23469.86	0.00	0.01	0.33	0.72	4.29	168.18
153	0.01	20	0.00	0.32	454.64	0.00	0.00	0.01	0.00	0.00	0.01
156	11.05	10.4	1.15	348.37	23458.82	0.46	1.60	107.43	0.00	0.00	0.07
158	12.68	20	2.54	768.76	20578.77	2.22	17.08	457.08	0.00	0.02	0.41
159	1.86	20	0.37	112.57	4145.31	0.00	0.00	0.04	0.00	0.00	0.01
163-3T	18.51	20	3.70	1121.60	27286.75	0.00	0.01	0.33	0.00	0.00	0.01
163-3S	20.08	20	4.02	1216.73	26652.63	0.00	0.01	0.33	0.00	0.00	0.01
164	47.74	20	9.55	2893.16	30078.65	0.00	0.03	0.33	0.00	0.01	0.07
165	8.92	20	1.78	540.83	19831.90	0.00	0.01	0.33	0.00	0.00	0.01
166-1T	15.32	20	3.06	928.57	30078.59	0.00	0.01	0.33	0.00	0.00	0.01
166-1S	24.97	20	4.99	1513.37	31953.33	0.00	0.02	0.36	0.00	0.00	0.01
166-3T	25.38	20	5.08	1538.21	30794.21	0.00	0.02	0.33	0.00	0.00	0.01
166-3S	35.26	20	7.05	2137.23	26922.96	1.76	37.57	473.25	0.00	0.03	0.41
167	30.86	20	6.17	1870.12	31315.78	0.00	0.02	0.33	0.00	0.00	0.01
169-1T	19.06	20	3.81	1154.96	25945.95	0.00	0.01	0.33	0.00	0.00	0.01
169-1S	31.57	20	6.31	1913.24	17164.66	0.00	0.04	0.33	0.00	0.00	0.01
170	0.05	20	0.01	3.33	0.29	1.58	0.15	0.01	4.58	0.15	0.01
173	13.90	20	2.78	842.15	27288.48	0.00	0.01	0.43	2.98	25.13	814.32
175T	0.35	20	0.07	21.46	0.06	20.17	4.34	0.01	20.45	4.39	0.01
175S		2.1	0.00	0.00	1448.60	0.00	0.00	0.01	0.00	0.00	0.01
177-2T	31.88	20	6.38	1932.02	32823.63	0.00	0.01	0.11	0.00	0.00	0.01
177-2S	30.76	20	6.15	1864.04	30690.95	0.00	0.02	0.33	0.00	0.00	0.01
178	19.24	20	3.85	1166.30	25258.00	0.00	0.02	0.33	0.00	0.00	0.01
180T	13.45	20	2.69	815.17	22683.85	0.00	0.01	0.33	0.00	0.00	0.01
180S		2.1	0.00	0.00	22231.25	0.00	0.00	0.33	0.00	0.00	0.01
184	0.32	4.3	0.01	4.17	7769.21	1.58	0.14	58.58	0.01	0.00	0.41
187	3.54	9	0.32	96.45	11054.67	9.49	4.34	893.93	0.00	0.00	0.41
191a	4.50	20	0.90	272.94	19965.58	0.00	0.00	0.33	0.00	0.00	0.01
191b	4.22	20	0.84	255.73	19241.32	0.00	0.00	0.33	0.00	0.00	0.01
193			0.00	0.00	4710.07	22.21	0.00	0.01	0.01	0.00	0.41
194-2T	11.73	20	2.35	710.97	29182.87	0.00	0.01	0.33	0.00	0.00	0.01
194-2S	17.80	20	3.56	1078.62	28029.95	0.00	0.02	0.57	0.00	0.00	0.01
196	0.24	20	0.05	14.47	0.06	20.17	2.91	0.01	20.45	2.96	0.01
197-2T	20.08	20	4.02	1216.73	26652.63	0.05	0.62	13.60	0.00	0.00	0.01
197-2S	27.18	20	5.44	1647.08	18234.50	0.00	0.03	0.33	0.00	0.00	0.01
198T	12.85	20	2.57	778.84	18173.35	0.00	0.01	0.33	0.00	0.00	0.01
198S	10.67	20	2.13	646.90	23776.08	0.00	0.01	0.49	0.00	0.00	0.01
199	12.40	20	2.48	751.44	18562.93	0.00	0.03	0.73	2.43	18.24	450.53
202T	27.62	20	5.52	1674.12	29085.41	1.93	32.35	562.11	0.00	0.02	0.41
202S	31.57	20	6.31	1913.24	28124.26	0.03	0.62	9.05	0.00	0.00	0.01

< 5% < 20ng

< 303 c (Limit >1.0%) < 1000 Amplicons
303-606 c Limit 1.0%
> 606 c Limit 0.5%

> 0,1% > 3 copies > 20 Amplicons

> 0,5% > 3 copies > 50 Amplicons

7.2.12 Progressive Steps of the Project

Figure 39 illustrates the work flow of the project. Like Figure 28 it is thought to explain the complex progression of this study. Unlike Figure 28 Figure 39 concentrates on the progression of adaption of individual assays. Several adjustments had to be made in the course of the project and some of the adjustments were made in parallel (e.g., adaption of the assays for the simultaneous detection of the *BRAF* V600E and V600K mutation because of the results of the LS and the DNA isolation of the samples of the TS). Time progression is indicated vertically.

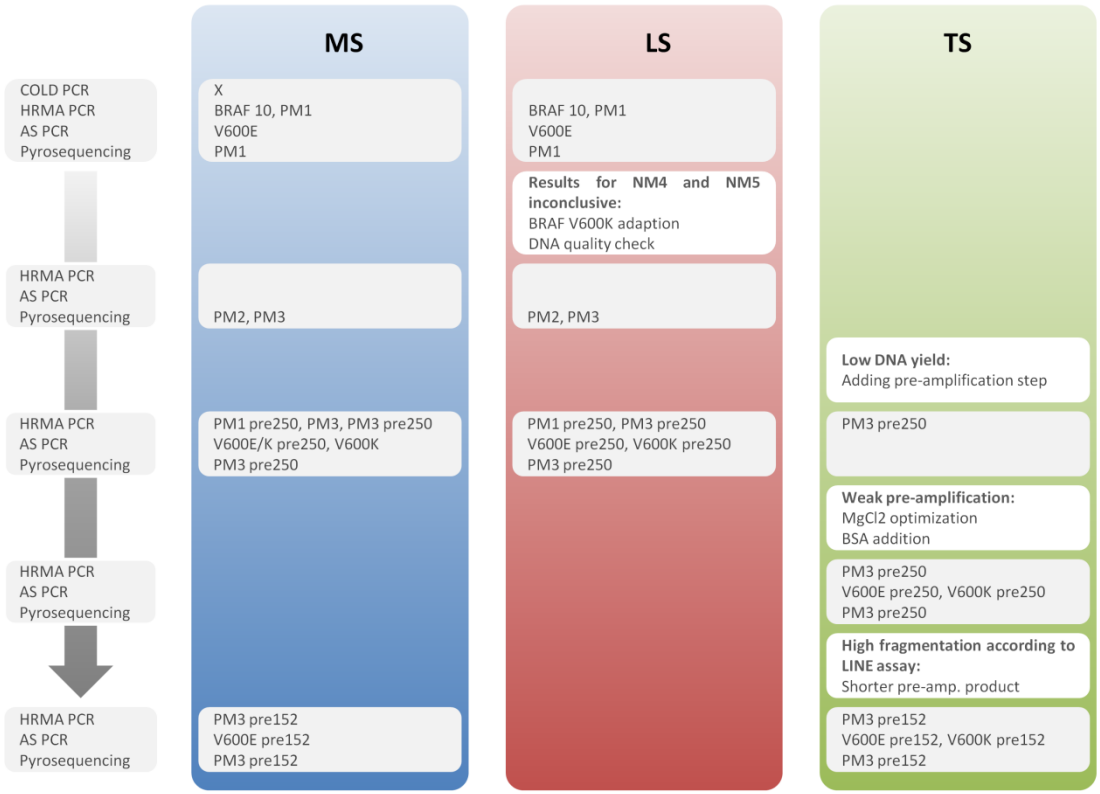

Figure 39: Illustration of the work flow of the project.

In order to rule out changes in the sensitivities of the assays, most of the amendments made while analyzing the LS have been tested on the MS as well. To best evaluate optimization of the pre-amplification step it was mainly tested on samples of the TS.

Funding of the Project

This project was supported by the Austrian National Bank Fund grant Nr. 14209 to Dr. Dandachi.

Curriculum Vitae

PERSONAL INFORMATION

Name	Elke Stadelmeyer
Date of Birth	02. Dec. 1973
Place of Birth	Linz
Marital Status	Single
Address	8020 Graz, Falkenhofgasse 33
E-mail Address	elke.stadelmeyer@medunigraz.at

SCIENTIFIC EXPERIENCE

Since Oct. 2007	Medical University Graz, Department of Internal Medicine, Division of Oncology *Research assistant*
Nov. 2005 – Sep. 2007	Medical University Graz, Department of Orthopedic Surgery *Research assistant*
June 2003 – Sep. 2005	EccoCell, Graz; Medical University Graz, Institute of Molecular Biology and Biochemistry *Research assistant in a joint venture*
Feb. 2001 – Dec. 2002	Medical University Graz, Department of Internal Medicine, Division of Hematology *Master thesis*

EDUCATION

Since Oct. 2009	**Doctoral studies (O790 202):** Doctoral School of General and Clinical Pathophysiology, Medical University Graz. **Doctoral thesis:** 'Detection of *BRAF* mutations in Lentigo maligna melanoma using a highly sensitive method' at the Med. Univ. Graz, Division of Oncology.
Mar. 2003	Final examination
Oct. 1994 – Mar. 2003	**Diploma studies (B440):** Biology at the Karl-Franzens University Graz; branch of study: Microbiology. **Master thesis:** 'Analysis of Antigen-Uptake in Dendritic Cells of B-Cell Chronic Lymphocytic Leukemia Patients' at the University Hospital Graz, Division of Hematology.
Oct. 1993 – Sep. 1994	Chemistry and Physics with emphasis on molecular biology at the Johannes Kepler University Linz.
June 1993	University entrance diploma

LANGUAGE ABILITY

German, English